VS2DRT: Variably Saturated Two Dimensional Reactive Transport Modeling in the Vadose Zone

To the Faculty of Geosciences, Geo-Engineering and Mining

of the Technische Universität Bergakademie Freiberg

Approved

PhD THESIS

To attain the academic degree of Doctor rerum naturalium

(Dr. rer. nat.)

Submitted by

Sosina Shimeles Haile

(M.Tech)

Born on the 19th of July 1978 in Addis Ababa, Ethiopia

Reviewers:

Prof. Dr. Border J. Merkel, TU Bergakademie Freiberg

Prof. Dr. Helmut Geistlinger, Helmholtz Center for Environmental Research-UFZ

Date of the award: 22nd of February 2013, Freiberg, Germany

Dedicated to my beloved parents Wude Mekonne and Atnafu Mengiste

& the soul of my father Shimeles Haile

Declaration

I hereby declare that I completed this work without any improper help from a third party and without using any aids other than those cited. All ideas derived directly or indirectly from other sources are identified as such.

I did not seek the help of a professional doctorate-consultant. This thesis has not previously been submitted to another examination authority in the same or similar form in Germany or abroad.

Abstract

Contaminate transport in vadose is a huge concern since the vadose zone is the main passage way for ground water recharge. Understanding this process is crucial in order to prevent contamination, protect and rehabilitate ground water resources. Reactive transport models are instrumental for such purposes and there are numerous solute transport simulation programs for both ground water and vadose zone but most of this models are limited to simple Linear, Langmuir and Freundlich sorption models and first order decay and fail to simulate more complex geochemical reactions that are common in the vadose zone such as cation exchange, surface complexation, redox reaction and biodegradation. So it is necessary to enhance capabilities of solute transport models by incorporating well tested hydrogeochemical models like PHREEQC in to them to be able closely approximate the geochemical transport process in the subsurface.

In this PhD research a new reactive transport model called VS2DRT was created by coupling existing public domain solute and heat transport models VS2DT, VS2DH with hydrochemical model PHREEQC using non-iterative operator splitting technique. VS2DRT was compiled using MinGW compiler using tools like autotools and automake. A graphical user interface was also created using QT creator and Argus ONE numerical development tools. The new model was tested for one dimensional conservative Cl transport, surface complexation, cation exchange, dissolution of calcite and gypsum, heat and solute transport as well as for two dimensional cation exchange cases. Their results were compared with VS2DT, VS2DH, HP1 and HP2 models and the results are in good agreement.

Kurzfassung (German)

Der Transport von Kontaminationen in der ungesättigten Zone ist von großer Bedeutung, da diese den Hauptweg für Grundwasserneubildung darstellt. Das Prozessverständnis in diesem Bereich ist zwingend, um Kontaminationen zu verhindern bzw. Grundwasser-Ressourcen zu schützen oder zu rehabilitieren. Reaktive Transportmodelle werden zur Lösung dieser Aufgabenstellungen genutzt, wobei es eine Anzahl an Transportmodellen für die gesättigte und die ungesättigte Zone gibt. Allerdings sind die meisten dieser Modelle auf einfache Sorption-Modelle (Lineare Isotherme, Langmuir-Isotherme, bzw. Freundlich-Isotherme) sowie Zerfall erster Ordnung beschränkt. Dies hat zur Folge, dass komplexere geochemische Reaktionen, wie sie in der ungesättigten Zone vorkommen (Kationenaustausch, Oberflächenkomplexierung, Redoxreaktionen und Biodegradation), nicht modelliert werden können. Folglich ist es notwendig, die Einsatzmöglichkeiten von Transportmodellen zu verbessern, indem hydrogeochemische Modelle wie PHREEQC in diese integriert werden, um geochemische Transportprozesse im Untergrund abzubilden. Im Rahmen dieser Dissertation wurde ein neues reaktives Transportmodell (VS2DRT) entwickelt, durch die Kopplung der schon existierenden, frei verfügbaren Stoff- und Wärmetransportmodelle VS2DT und VS2DH mit dem hydrogeochemischen Code PHREEQC. VS2DRT wurde mit Hilfe des MinGW Kompilers unter Nutzung der Funktionen autotools und automake erstellt. Eine graphische Benutzeroberfläche wurde mit Hilfe des Programms QT creator und Argus ONE (numerisches Entwicklungs-Werkzeug) entwickelt. Das neue Modell wurde für verschiedene Szenarien getestet: eindimensionalen, konservativen Transport von Chlorid, Oberflächenkomplexierung, Kationenaustausch, Lösungsmechanismen von Calcit und Gips, Wärme- und Stofftransport, sowie für zweidimensionale Kationenaustauschprozesse. Die Ergebnisse wurden mit den Ergebnissen der VS2DT, VS2DH, HP1 und HP2 Modellierungen verglichen und zeigten eine gute Übereinstimmung.

Acknowledgement

It has been a long journey glory to the Almighty God who has made everything possible.

I would like to take this opportunity to express my heartfelt gratitude to my supervisor Prof. Dr. habil Border J. Merkel, Head of Geology Department and Chair of Hydrogeology, for giving me the opportunity to do this research and for his guidance, valuable discussions, comments, suggestions and support I received at every stage of my work. I am also very grateful to Dr. Volkmar Dunger for his constructive supervision.

I am deeply indebted to German Academic Exchange Service (DAAD) and TU Bergakademie Freiberg (TUBAF) for financing my study.

I am very thankful to Mrs. Manuela Junghans, Cornelia Magnus, Cornelia Kneip, Sabine Schrenk, Petra Kräher, Heike Beyer and Stefanie Lindner from TUBAF and Studentenwerk Freiberg. I would like to thank also Jürgen Gelke and Joachim Scharfe.

Special thanks go to Mr. Tino Beier for always being there to fix computer related problems and to all my colleagues at the Institute of Hydrogeology TUBAF, specially Dr. Eyad Aboshindi, Dr. Samer Bachmaf, Raghid Sabri, Wondem Gezahegne, Dr. Sameh Wisam, Dr. Nair Sreejesh, Dr. Mandy Schipek, Ramadan Aziz, Mustafa Almukhtar, Alireza Arab, Mohammed Omer, Omed Mustafa, Iwona Woloszyn and Zheenbek Kulenbekov.

Last but not least, I am deeply obliged to my beloved mother Wude Mekonne and my father Atnafu Mengiste, my brothers, friends and my husband Kehulu Ylikal for their love, support and understanding during my study. My dear daughter, Bethel, you are my angel, inspiration and courage we did it together thank God.

Table of content

List of figures

Figures **Page No.**

List of tables

Tables **Page No.**

List of abbreviations

1D	one dimensional
2D	two dimensional
L	length unit
T	time unit
-	dimensionless
°C	degree centigrade
J	joule
W	watt
m	meter
cm	centimeter
g	gram
cm/h	centimeter per hour
mmol	milmole
mol/kg	mole per kilogram
mmol/kg	milmole per kilogram
m^2/g	meter square per gram
Cl	chloride
Ca	calcium
Na	sodium
C	carbon

Chapter One: Introduction

1.1 Background

Vadose zone lays between the earth's surface and the water table playing a crucial role in earth's ecosystem. It provides nutrients and water for plants and act as a source of contaminate and recharge water for the ground water system. It is a complex system (Healy & Ronan, 1996) where all three phases gas, liquid and solid coexist and various physical, chemical and biological activities take part. Human activities such as the use of fertilizers, pesticides and unsafe disposal of waste greatly affect the quality of ground water. Clear understanding of the vadose zone processes is important from agricultural, hydrogeological and environmental perspective. The present study is focused on modeling hydrogeological and environmental aspects of vadose zone processes.

The vadose zone processes of interest in this study are water flow, heat transport, solute transport and reactive transport. These processes affect both quality as well as quantity of the ground water by affecting the chemistry and amount of recharge water. Hence, modeling of such processes could be instrumental in predicting and estimating quality and quantity of ground water recharge. Such prediction could be used for planning and implementing sustainable ground water utilization and management as well as to take proper remedial measures.

Although there are numerous analytical and numerical models to simulate vadose zone processes none of them has the capacity to fully simulate this complex system. Many of the models are focused on water flow and solute transport or heat transport. HP1 (Jacques & Simunek, 2005), HYDROGEOCHEM (Yeh & Tripathi, 1990), TOUGHREACT (Xu, E.I., Spycher, & Pruess, 2004) and UNSATCHEM2D (Simunek & Suarez, 1994) are few reac-

tive transport models available to do 1D and multi-dimensional reactive transport simulation in vadose zone.

This PhD research focuses on development of 2D reactive transport model with abilities to simulate water flow, heat transport, multi-solute transport and reactive transport in the vadose zone by coupling the latest versions of VS2DT (Healy, 1990), VS2DH (Healy & Ronan, 1996) with PHREEQC (Parkhurst & Appelo, 1999). Such model could have applications in the study of contaminate transport, acid mine drainage, nuclear repository both in one and two dimension.

VS2DT is a computer program written in FORTRAN90 programming language and simulates advective dispersive solute transport in variably saturated porous media in one and two dimension. It is based on VS2D (Lappala, Healy, & Weeks, 1987) which simulates flow of water in variably saturated porous media based on Richard's equation. The model is a single solute transport with fixed head, fixed flux, evaporation, evapotranspiration and seepage face flow boundary conditions and fixed concentration and flux concentration transport boundary conditions. It considers various source/sink terms like root water uptake, first order decay, Linear, Freundlich and Langmuir isotherm adsorptions.

VS2DH is a computer program written in FORTRAN90 programming language and simulates advective dispersive heat transport in variably saturated porous media in one and two dimension. It is based on the VS2DT model taking advantage of the similarity in the advective dispersive transport processes of solute and heat transport. The major difference between the two programs is the difference in parameters presented in solute and heat transport governing equations. VS2DH is not applicable for vapor phase flow and variable density

conditions. It can have fixed heat flux and fixed temperature boundary conditions. The source and sink term can be due the flow of water into or out of the domain. It assumes that saturated hydraulic conductivity is a function of temperature.

PHREEQC is based on either ion-association aqueous model or Specific Interaction Theory (SIT, PITZER) with capabilities for speciation and saturation index calculation, batch reaction, kinetic reactions, one dimensional transport and inverse modeling (Parkhurst & Appelo, 1999). PHREEQC has been used as geochemical module for reactive transport models. Some of the reactive transport models that include PHREEQC in their models are PHT3D (Appelo & Rolle, 2010), TACK (Källvenius & Ekberg, 2003), PHAST (Parkhurst, Kipp, Engesgaard, & Charlton, 2004), PHWAT (Mao, Prommer, Barry, Langevin, Panteleit, & Li, 2006) and HP1 (Jacques & Simunek, 2005) for ground water and vadose zone respectively.

The main task of this PhD research was to prepare a new two dimensional multi-component reactive transport model called VS2DRT (Variably Saturated 2 Dimensional Reactive Transport) for vadose zone by coupling VS2DT, VS2DH and PHREEQC models. The model has capabilities to simulate water flow, heat transport and multi-component reactive transport as well as equilibrium and kinetic reactions in the vadose zone.

1.2 Literature review

Vadose zone hydrology is rather a young field of study which involves multidisciplinary fields of soil physics, hydrogeology, geochemistry and deals with physical, chemical and biological processes in the subsurface. The first graduate courses in this field were offered only in early 1980s (U.S. Department of Energy, 2001). The vadose zone is considered as neglected component of nature (Ronen & Sorek, 2005). Most of the papers before 1980s are

on soil physics and groundwater hydrogeology aspect of the subsurface. The main milestones studies that paved the road for vadose studies are in 1856 Darcy Law concerning flow in porous medium, in 1855 Fick's law for solute transport and in 1822 for heat transport. In 1899 Slichter published "Theoretical investigation of groundwater", which provided exact solutions for flow and pressure field around a pumped wells (Tindall & Kunkel, 1999; Selker, Keller, & McCord, 1999). In 1907 Buckingham extended Darcy's law to flow in unsaturated systems and proposed that hydraulic conductivity must be a function of moisture content and hydraulic potential must include capillary pressure (Selker, Keller, & McCord, 1999; Tindall & Kunkel, 1999; Nimmo & Landa, 2005; Raats & van Genuchten, 2006). In 1911 Green and Ampt made significant contribution on the infiltration of water in soil (Selker, Keller, & McCord, 1999; Tindall & Kunkel, 1999). In 1931 Richards derived Richard's equation, which is a governing equation in unsaturated zone hydrology (Richards, 1931). In 1930 Haines introduced hysteresis (Selker, Keller, & McCord, 1999; Raats & van Genuchten, 2006). In 1915 Bouyoucous demonstrated that temperature affected pressure gradients in soil columns under isothermal conditions and in 1940 Moore showed that temperature has a considerable effect on the soil hydraulic properties (Nielsen, van Genuchten, & Biggar, 1986). The evolution of soil physics and solute transport studies in the subsurface is presented in figure 1.2. Further comprehensive works on soil physics aspect of vadose zone could be referred to (Philip, 1974; Raats & van Genuchten, 2006).

Many models of varying degree of complexity and dimensionality have been developed during the past several decades to quantify the basic physical and chemical processes affecting the flow and contaminate transport in the unsaturated zone (Simunek & Bradford, 2008). Compilation of many analytical solutions for convection-dispersion equation of solute

transport in one and multi-dimension is presented in public domain software package STANMOD (Studio of Analytical MODels) (Simunek, van Genuchten, Sejna, Toride, & Leij, 1999). It incorporates CFITM (van Genuchten, 1980), CFITIM (van Genuchten, 1981), and CHAIN (van Genuchten, 1985) one-dimensional models and 3DADE (Leij & Bradford, 1994) and N3DADE (Leij and Toride, 1997) two- and three-dimensional models. Analytical models are only applicable to very simplified problems and simple geometries.

Analytical solutions can usually be derived only for simplified transport systems involving linearized governing equations, homogeneous soils, simplified geometries of the transport domain, and constant or highly simplified initial and boundary conditions (Simunek J., 2005). To obtain more realistically solution to the non-linear Richards equation numerical solutions are essential. Numerical models are preferable in majority of the cases due to their unique ability to handle complex geometry, heterogeneous soils, more realistic initial and boundary conditions as well as non-linear relationships. VS2DTI (Healy,1990), DAISY (Abrahamsen & Hansen, 2000), TOUGH2 (Pruess, Oldenburg, & Moridis, 1999), MACRO 5 (Larsbo, 2003), SHAW (Flerchinger, 2000), SWAP (Kroes, van Dam, Huygen, & Vervoort, 1999), HYDRUS-1D (Simunek, Sejna, Saito, Sakai, & van Genuchten, 2009), HYDRUS-2D (Sejna, Simunek, & and van Genuchten, 2011) and UNSATH (Fayer,2000) are some of the widely used numerical models for simulating variably-saturated water flow and solute transport in the vadose zone.

Some of currently available biogeochemical models are UNSATCHEM2D (Simunek & Suarez 1994), PHREEQC (Parkhurst and Appelo, 1999), 3DHYDROGEOCHEM (Yeh & Cheng, 1999), HBG123D (Gwo, et al., 2001), CrunchFlow (Steefel, 2009) and HP1 (Jacques and Simunek, 2005). A comprehensive literature review on transport of reactive solutes in

soil is presented in the book “Advances In Porous Media volume 2” (Corapcioglu, 1994). Table 1.2a and 1.2b presents selected public domain and commercial reactive transport models respectively.

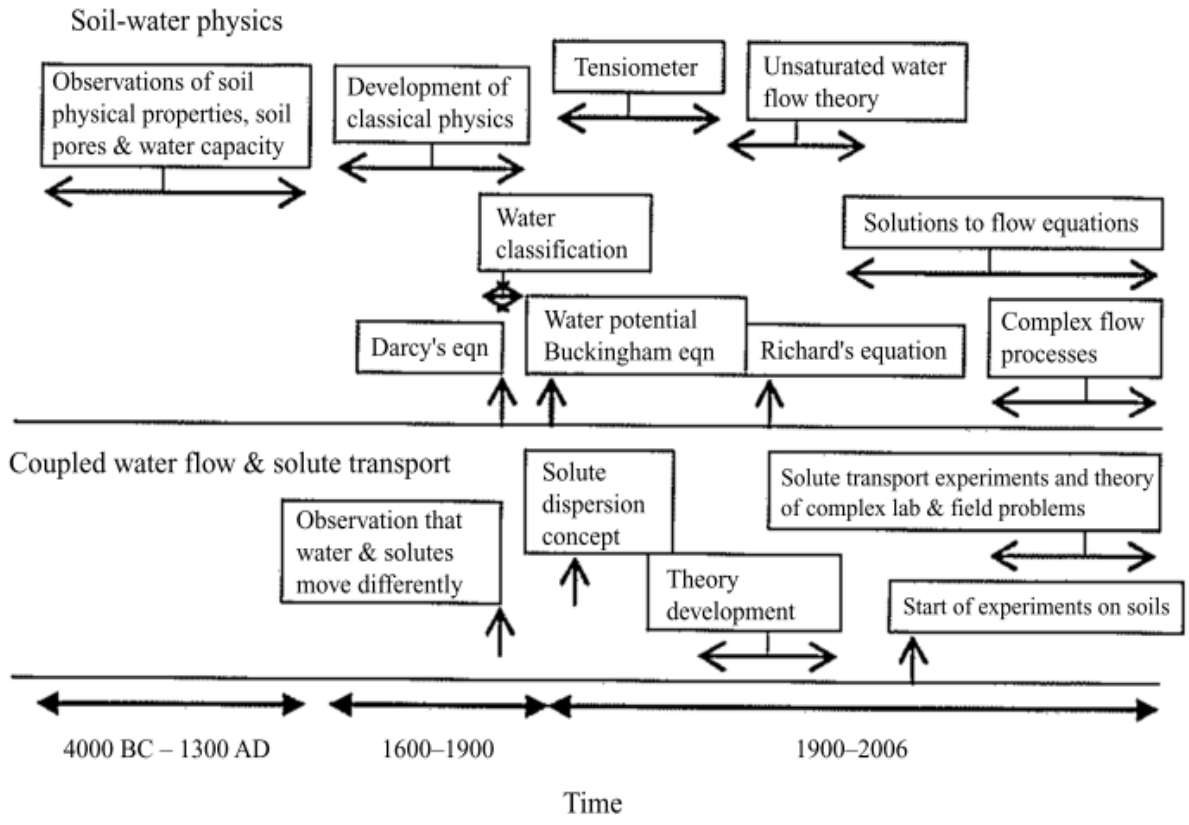

Figure 1.2 Evolution of the science of soil-water physics and solute transport (Rolston, 2007)

Table 1.2a Public domain reactive transport models

Models	General capabilities
2DFATMIC	1D/2D variably saturated flow and transport of microbes and chemicals with simple chemical reactions like decay kinetics, linear/non-linear adsorption
3DFATMIC	1D/2D/3D variably saturated flow and transport of microbes and chemicals with simple chemical reactions like decay kinetics ,linear/non-linear adsorption
CHEMFLO	1D variably saturated flow and solute transport
CHAIN_2D	2D water flow, heat and multiple solute transport in variably saturated porous media
FEHM	1D/2D/3D multiphase, multicomponent, non-isothermal, reactive flow through variably saturated porous and fractured media
HydroBioGeoChem123	1D/2D/3D solute transport, heat transport, mixed, heterogeneous, chemical kinetics and equilibrium and coupled reactive transport in variably saturated porous media
PESTAN	1D analytical simulation of organic solute transport in the vadose zone
RITZ	1D analytical simulation of unsaturated zone flow and transport of oily wastes during land treatment.
SUTRA	variably saturated, variable-density ground-water flow with solute or energy transport
UNSATCHEM	1D simulation of variably saturated water flow, heat transport, CO_2 production and transport ,multicomponent transport with major ion equilibrium and kinetic chemistry
UNSATCHEM-2D	2D simulation of variably saturated water flow, heat transport, CO_2 production and transport ,multicomponent transport with major ion equilibrium and kinetic chemistry
VLEACH	1D simulation of liquid-phase advection, solid-phase sorption, vapor-phase diffusion, and three-phase equilibration in vadose zone.
HYDRUS1D	1D simulation of flow water, heat and multiple solutes in variably saturated media
PHREEQC	chemical reaction and 1D reactive transport
VS2DI	1D/2D heat or solute transport in variably saturated porous media
HP1	1D simulation of flow water, heat and multiple solutes reactive transport in variably saturated media
SWMS_2D	1D/2D water flow and solute transport in variably saturated porous media
SWMS_3D	1D/2D/3D water flow and solute transport in variably saturated porous media
RETRASO	1D/2D multiphase flow, heat and reactive transport in variably saturated porous media
SHAW	1D simulation of water flow, heat and solute transport in variably saturated media

Table 1.2b Commercial reactive transport models

Models	General capabilities
3DFEMFAT	3D flow and solute transport in variably saturated porous media including salt water intrusions
AIRFLOW-SVE	simulation of vapor flow and multi-component vapor transport in unsaturated, heterogeneous and anisotropic soil
BIOF&T2D/3D	2D/3D simulation of biodegradation, flow and solute transport in variably saturated media as well as fractured media
CTRAN/W	1D/2D water flow and solute transport in variably saturated porous media
FEFLOW	2D/3D simulation of water flow, heat and solute transport in variably saturated media
FRAC3DVS	1D/2D/3D simulation of water flow and solute transport in variably saturated porous fractured media
HYDROGEOCHEM	1D coupled simulation of water flow, chemical reactions and reactive solute transport in variably saturated porous media zone
HYDROGEOCHEM2	2D coupled simulation of water flow, chemical reactions and reactive solute transport in variably saturated porous media zone
HYDRUS2D/3D	2D/3D simulation of flow water, heat and multiple solutes in variably saturated media
KYSPILL	1D/2D/3D simulation of water flow and solute transport in variably saturated porous media
MIGRATE	1D/2D water flow and solute transport in variably saturated porous media
MODFLOW-SURFACT	1D/2D/3D MODFLOW based simulation of water flow and solute transport in variably saturated porous media
MOFAT	1D/2D multiphase flow and transport of up to five non-inert chemical species.
POLLUTE	1D simulation of water flow and solute transport in variably saturated porous media zone
TOUGHREACT	1D /2D/3D simulation chemical reaction and multiphase fluids ,heat and reactive transport in variably saturated porous and fractured media

1.3 Objective

The main objective of this PhD work was to develop two dimensional reactive transport model for unsaturated zone by coupling public domain flow, heat and solute transport models VS2DT and VS2DH with PHREEQC. The specific objectives are:

- To modify the solute transport model VS2DT for multi-solute transport.
- To couple the heat and multi-solute transport.
- To couple the heat, multi-solute transport models with chemical reaction code PHREEQC.
- To run and test the VS2DRT model with various published literature data.
- To create a graphical user interface for VS2DRT using QT creator and Argus ONE numerical development software.

1.4 Methodology and materials used

The methodology used to achieve the above mentioned objectives are:

1. Literature review: - which involves collecting and reviewing various articles on the topic and relevant codes as well as source codes of VS2DT, VS2DH, PHREEQC and PHAST.
2. Get acquainted with FORTRAN90, C/C++ programming languages, Autotools, QT Creator and Argus ONE development environment.
3. Compiling, running and testing each program using freely available compilers like MinGW which has a capability to compile FORTRAN and C/C++ programs.
4. Develop interface functions between FORTRAN90 heat and multi-solute transport programs and C/C++ geochemical program by adapting such functions from PHAST.
5. Writing a configure script which would help to create Makefile for VS2DRT.

6. Develop pre-processor graphical GUI for non-spatial input data using public domain Qt Creator.

7. Develop pre-processor and post-processor GUI using Argus ONE.

Materials used:

- Various published journals, reports and books
- Argus ONE software
- MinGW compiler
- QT Creator
- Source codes of VS2DH, VS2DT, PHREEQC and some functions from PHAST source code

1.5 Features and limitations

The following features are applicable for VS2DRT model:

- Constant density liquid phase flow in the porous media
- The flow equation is based on Richards equation
- The solute transport is based on advection dispersion transport equation
- The heat transport is based on advection dispersion transport equation
- Viscosity and saturated hydraulic conductivity are functions of temperature
- Multi-solute transport
- Various chemical equilibrium and kinetic reactions

- Root water uptake
- Heterogeneous porous media
- Effect of temperature on thermodynamics constants and rate parameters
- Same molecular diffusion coefficient is used for all solute

The main limitations of VS2DRT model are:

- Inherited limitations from PHREEQC model for various geochemical computations as explained by (Parkhurst & Appelo, 1999)
- Gaseous flow is neglected
- Change of porosity and hydraulic conductivity and density due to chemical reaction are not considered

Chapter Two: Unsaturated water flow

2.1 Unsaturated water flow equation

The flow of water in the unsaturated zone is described by Richards' equation neglecting effects of vapor phase flow, thermal or solution density gradients is given in equation 2.1 for 1D flow (Suarez & Simunek, 1996).

$$\frac{\partial \theta}{\partial t} = \frac{\partial}{\partial z}\left[K\left(\frac{\partial h}{\partial z} + 1\right)\right] - S \tag{2.1}$$

The terms h, θ, t, z, K and S in equation 2.1 refer pressure head [L], water content [L^3 L^{-3}], time [T], spatial coordinate [L], hydraulic conductivity [LT^{-1}] and source/sink term [T^{-1}] respectively. VS2DRT uses modified form of Richards' equation for two dimensional unsaturated flows given in equation 2.2 (Lappala, Healy, & Weeks, 1987).

$$v\rho\left[C_m + sS_s\right]\frac{\partial H}{\partial t} - \rho A_x KK_r(h)\frac{\partial H}{\partial x} - \rho A_z KK_r(h)\frac{\partial H}{\partial z} - \rho q v = 0 \tag{2.2}$$

The terms v, ρ, C_m, s, S_s, H, t, KK_r , q, A_x and A_z refer to volume [L^3], liquid density [ML^{-3}], specific moisture capacity [L^{-1}], liquid saturation [L^0], specific storage [L^{-1}], total pressure head, time [T], effective hydraulic conductivity [LT^{-1}], volumetric source/sink term, area [L^2] in x and z faces respectively.

2.2 Temperature dependence of saturated hydraulic conductivity in soil

In case of heat transport or heat and solute transport simulation saturated hydraulic conductivity is computed in VS2DRT as function of temperature. Equation 2.3 shows that saturated hydraulic conductivity depends on viscosity and temperature.

$$K = \frac{\rho g k}{\mu(T)} \tag{2.3}$$

where the terms K, ρ, g, k, T and μ refer to saturated hydraulic conductivity [LT^{-1}], density [ML^{-3}], gravity [MT^{-2}], intrinsic permeability [L^2], temperature [°C] and viscosity [$MLT^{-1}L^{-2}$] respectively. Viscosity could be approximated using empirical equation 2.4 (Kipp, 1987).

$$\mu(T) = 0.00002414 \times 10^{\frac{247.8}{T+133.18}} \tag{2.4}$$

VS2DRT adapts VS2DTH's assumption that temperature has much less effect on density of water than that of viscosity over the range of pore-water pressures and temperatures typically encountered under variably saturated field conditions (Healy & Ronan, 1996).

2.3 Unsaturated soil hydraulic properties

The flow of water in the vadose is highly controlled by its hydraulic properties. These hydraulic properties include porosity, residual moisture content, volumetric moisture content, specific storage and hydraulic conductivity. In VS2DRT moisture content, specific moisture capacity and relative hydraulic conductivity could be computed using Brooks and Corey (Brooks & Corey, 1964), Haverkamp, Van Genuchten (van Genuchten, 1980) or Rossi-Nimmo (Rossi & Nimmo, 1994) equations.

Brooks and Corey's (Brooks & Corey, 1964) equations of volumetric moisture content, specific moisture capacity and relative hydraulic conductivity can be computed using equations 2.5, 2.6 and 2.7 respectively.

$$s_e = \frac{\theta - \theta_r}{\phi - \theta_r} = \left(\frac{h_b}{h}\right)^{\lambda}, \quad h > h_b; \tag{2.5}$$

$$s_e = 1.0 \quad , h \le h_b ;$$

$$c_m(h) = -(\phi - \theta_r)\left(\frac{\lambda}{h_b}\right)\left(\frac{h}{h_b}\right)^{-(\lambda+1)} \quad , h < h_b \tag{2.6}$$

$$c_m(h) = 0 \quad , h \ge h_b$$

$$K_r(h) = \left(\frac{h_b}{h}\right)^{2+3\lambda} \quad , h < h_b \tag{2.7}$$

$$K_r(h) = 0 \quad , h \ge h_b$$

where the terms S_e, θ, θ_r, ϕ, h_b, λ, $K_r(h)$ and $C_m(h)$ refer to effective saturation [-], volumetric moisture content [-], residual moisture content [-], porosity [-], bubbling pressure or air-entry pressure potential [L], pore size distribution index which is a function of soil texture [-], relative hydraulic conductivity [LT^{-1}] and specific moisture capacity [L^{-1}] respectively.

Haverkamp's equations of volumetric moisture content, specific moisture capacity and relative hydraulic conductivity can be computed using equations 2.8, 2.9 and 2.10 respectively.

$$s_e = \frac{1}{1+\left(\frac{h}{\alpha}\right)^{\beta}} \tag{2.8}$$

$$c_m(h) = \frac{(\phi - \theta_r)\left(\frac{\beta}{\alpha}\right)\left(\frac{h}{\alpha}\right)^{\beta-1}}{\left[1+\left(\frac{h}{\alpha^{\beta}}\right)\right]^2} \quad , h < 0 \tag{2.9}$$

$$c_m(h) = 0 \quad , h > 0$$

$$K_r(h) = \frac{1}{1+\left(\frac{h}{A'}\right)^{B'}} \tag{2.10}$$

where the terms S_e, θ_r, ϕ, α, β, A' and B' refer to effective saturation [-], residual moisture content [-], porosity [-], pressure potential at which $S_e=0.5$ [L], slope of a log-log plot of $(1/S_e - 1)$ versus h [-], pressure potential at which $S_e=0.5$ [L], slope of a log-log plot of $(1/K_r - 1)$ versus h [-] respectively.

Van Genuchten's (van Genuchten, 1980) equations of volumetric moisture content, specific moisture capacity and relative hydraulic conductivity can be computed using equations 2.11, 2.12 and 2.13 respectively.

$$s_e = \left[\frac{1}{\left[1 + \left(\frac{h}{\alpha'} \right) \right]^{\beta'}} \right]^{\gamma} \tag{2.11}$$

$$c_m(h) = \frac{-\gamma\beta'(\phi - \theta_r)\left(\frac{h}{\alpha'}\right)^{\beta'-1}}{\alpha'\left[1 + \left(\frac{h}{\alpha'}\right)\beta'\right]^{\gamma+1}} \quad , h \le 0 \tag{2.12}$$

$$c_m(h) = 0 \quad , h > 0$$

$$K_r(h) = \frac{\left\{ 1 - \left(\frac{h}{\alpha'} \right)^{\beta'-1} \left[1 + \left(\frac{h}{\alpha'} \right)^{\beta'} \right]^{-\gamma} \right\}^2}{\left[1 + \left(\frac{h}{\alpha'} \right)^{\beta'} \right]^{\frac{\gamma}{2}}} \tag{2.13}$$

where the terms S_e, θ_r, ϕ, α', β', γ, $K_r(h)$ and $C_m(h)$ refer to effective saturation [-], residual moisture content [-], porosity [-], reciprocal of α van Genuchten parameter [-], $((1-\gamma)^{-1})$ [-], $(1-\beta'^{-1})$ [-], relative hydraulic conductivity $[LT^{-1}]$ and specific moisture capacity$[L^{-1}]$ respectively.

Rossi Nimmo model (Rossi & Nimmo, 1994) can be used to estimate volumetric moisture content and relative hydraulic conductivity over the entire range of saturation using equations 2.14 to 2.17.

$$\frac{\theta}{\theta_s} = \theta_I = 1 - c\left(\frac{\psi}{\psi_0}\right)^2 \qquad 0 <= \psi <= \psi_i$$

$$\frac{\theta}{\theta_s} = \theta_{II} = \left(\frac{\psi_0}{\psi}\right)^{\lambda} \qquad \psi_i <= \psi <= \psi_j \tag{2.14}$$

$$\frac{\theta}{\theta_s} = \theta_{III} = \alpha \ln\left(\frac{\psi_d}{\psi}\right) \qquad \psi_j <= \psi <= \psi_d$$

$$K_r(\theta) = \sqrt{\frac{\theta}{\theta_s}} \frac{I^2(\theta)}{I^2(\theta_s)} \tag{2.15}$$

$$I(\theta) = I_{III}(\theta) \qquad 0 <= \theta <= \theta\, j$$

$$I(\theta) = I_{II}(\theta) \qquad \theta j <= \theta <= \theta i \tag{2.16}$$

$$I(\theta) = I_{I}(\theta) \qquad \theta i <= \theta <= \theta\, s$$

$$I_{III}(\theta) = \frac{\alpha}{\psi_d}\left[\exp\left(\frac{1}{\alpha}\frac{\theta}{\theta_s}\right) - 1\right]$$

$$I_{II}(\theta) = I_{III}(\theta_j) + \frac{1}{\psi_0}\frac{\lambda}{\lambda+1}\left[\left(\frac{\theta}{\theta_s}\right)^{\left(\frac{\lambda+1}{\lambda}\right)} - \left(\frac{\theta_j}{\theta_s}\right)^{\left(\frac{\lambda+1}{\lambda}\right)}\right] \tag{2.17}$$

$$I_{I}(\theta) = I_{II}(\theta_i) + \frac{2C^{1/2}}{\psi_0}\left[\left(1 - \frac{\theta_i}{\theta_s}\right)^{1/2} - \left(1 - \frac{\theta}{\theta_s}\right)^{1/2}\right]$$

$\theta i = \theta(\psi)$, $\theta j = \theta(\psi j)$

where θ, θ_s, ψ, ψ_0 and ψ_d represents volumetric water content [-], saturated water content [-], matrix suction [L], air entry value [L] and matrix suction [L] at zero volumetric moisture content respectively and c , λ and α parameters.

2.4 Initial and boundary conditions for water flow

In order to simulate the flow water in a certain domain of unsaturated porous media over a period of time it is necessary to know the spatial distribution of pressure head in the porous media at the beginning of the simulation and how it would be affected by external forces acting at the boundaries of the domain of interest and source or sink points in the domain of interest. In VS2DRT initial condition for unsaturated water flow could be pressure head or volumetric moisture in the domain of interest at the beginning of a simulation.

Initial condition for water flow could be mathematically expressed in equation 2.18:

$$h(x,z,t)=h_0(x,z) \quad or \quad \theta(x,z,t)=\theta_0(x,z) \qquad \text{at } t=0 \tag{2.18}$$

where h_0 and θ_0 is spatial initial pressure head [L] and volumetric moisture content [-] in the domain of interest.

Boundary conditions for unsaturated water flow refer to physical situations like impermeable boundaries, water table and seepage face and external forces like infiltration, evaporation and evapotranspiration acting at the boundaries of the domain of interest during the simulation period.

In VS2DRT the flow boundary conditions can be set as specified flux across the boundary, specified total pressure potential along the boundary or a combination of the two boundary conditions. Specified flux boundary (Neumann boundary type) can be mathematically expressed in equation 2.19 as:

$$-\sum_{k=1}^{m} \rho K K_r(h) \frac{\partial H}{\partial n_k} = f_1(x,z,t,\nabla H,h) \tag{2.19}$$

where the term f_1 refers to a general function which depends on spatial, temporal variables as well as on gradient of total hydraulic potential across the boundary face and pressure head at the boundary face.

Specified head boundary (Dirichlet boundary type) can be mathematically expressed in equation 2.20 as:

$$h(x,z,t) = f_2(x,z,t,\nabla H,h) \tag{2.20}$$

where the term f_2 refers to a general temporal variable function.

Combination of flux and head boundary (Cauchy boundary type) can be mathematically expressed in equation 2.21 as:

$$\begin{aligned} -\sum_{k=1}^{m} \rho K K_r(h) \frac{\partial H}{\partial n_k} &= f_1(x,z,t,\nabla H,h) && \text{if flux} < IC \\ h(x,z,t) &= f_2(x,z,t,\nabla H,h) && \text{if flux} > IC \end{aligned} \tag{2.21}$$

where the term *IC* refers to the infiltration capacity of the soil.

2.5 Evaporation

Evaporation normally occurs at surface of the soil where liquid water leaves the unsaturated zone in the form of vapor gas. Evaporation from soil surface depends mainly on soil moisture content, solar radiation, wind and vapor-pressure gradient. Moreover, evaporation is determined by potential evaporative demand of the atmosphere and the ability of the soil transmits water upward to the land surface. Normally evaporation rate decreases with time in soils where moisture content is due to rainfall and irrigation. In presence of shallow groundwater evaporation may occur more or less at constant rate depending on climatic

condition. In cases of wet surface soil evaporation occurs at atmospheric evaporation demand rate. In case of dry surface soil evaporation depends mainly on the ability of the dry soil to transmit water to surface and it normally decreases and eventually cease. Two boundary conditions that may occur at the land surface due to evaporation are:

1. Specified liquid flux which equals to atmospheric evaporation demand, until the soil cannot any longer satisfy the atmospheric evaporative demand.

2. Specified flux caused by pressure potential gradient between the soil and the atmosphere.

2.6 Evapotranspiration

Evapotranspiration occurs at the earth surface through evaporation from soil surface and transpiration from vegetation. Evapotranspiration depends on air temperature, relative humidity, soil moisture content, wind, solar radiation, and type of vegetation cover and the ability of the soil to transmit water to roots. In VS2DRT plant root extraction is expressed as the ratio of pressure-potential difference between the plant root and soils to combined resistance to flow imposed by the soil and roots. Evapotranspiration represents the sink term in the unsaturated flow equation and in the model mathematically it is expressed in equation 2.22 (Lappala, Healy and Weeks, 1987) as:

$$\begin{aligned} (v\rho q)_m &= v\frac{\rho(h_{root}-h_m)}{R_m + R_{root_m}}, && \text{if } h_m > h_{root} \\ (v\rho q)_m &= 0, && \text{if } h_m <= h_{root}; \end{aligned} \qquad (2.22)$$

where the terms h_m, h_{root}, R_m and R_{rootm} refer to pressure potential in the soil in volume m [L], pressure potential in the plant roots [L], resistance to flow in the soil towards the roots in volume m [LT], and resistance to flow in the roots occurring in volume m [LT] respec-

tively. In VS2DRT the resistance term is computed using equation 2.23 (Lappala, Healy and Weeks, 1987) as:

$$R_m + R_{root_m} = \frac{1}{KK_r(h)r(z,t)} \tag{2.23}$$

Evapotranspiration due to plant root extraction is computed in VS2DRT using empirical expression (Lappala, Healy and Weeks, 1987) using equation 2.24:

$$q_m = KK_r(h)r(z,t)(h_{root} - h) \tag{2.24}$$

Where the terms $r(z,t)$ and h_{root} refer to the root activity function as a function of depth and time and the pressure head in the root for the entire system. The total plant root extraction for a given column of cells is given by using equation 2.25 (Lappala, Healy, & Weeks, 1987):

$$Q = \rho \sum_{m=1}^{m} (cq)_m \tag{2.25}$$

To simulate evapotranspiration using VS2DRT periodically variable potential evapotranspiration, minimum pressure in the roots, and depth of rooting, root activity at the bottom of the root and root activity at the land surface are required. The detail implementation of evapotranspiration computation can be referred from VS2D documentation (Lappala, Healy, & Weeks, 1987).

Chapter Three: Heat transport in unsaturated zone

Heat transport in unsaturated zone involves the transfer of heat in soil through thermal conduction, thermo-mechanical dispersion and advection processes. The soil gets heated by solar radiation and transfer the heat to the subsurface by thermal conduction. Thermal conduction involves the transfer of heat when materials with different temperatures come in physical contact, where heat flows from material with high temperature to material with low temperature. Thermo-mechanical dispersion involves the transfer of heat as a result of mixing due to flow of water in porous media. Advection involves the transfer of heat due to the movement of water of different temperature.

Natural source of heat in subsurface are solar radiation on surface of the earth, geothermal activity form the earth's interior, from volcanic and tectonic activities. Temperature variation in the shallow vadose zone varies both with depth and time, while temperature variation in deep vadose varies only with depth (Constantz, Tyler, & Kwiccklis, 2003). Temperature affects the evaporation, infiltration, ponding and seepage in the soil water system. Various factors in the soil water system, such as fluid viscosity, soil water content, and soil physical and chemical properties, interact with temperature changes in the system, therefore, influence the temperature effects on soil water flow processes (Zhang, Zhang, & Kang, 2003).

3.1 Heat transport equation

The governing equation of advection dispersion heat transport in unsaturated zone is given in equation 3.1 (Healy & Ronan, 1996):

$$\frac{\partial}{\partial t}[\theta C_w + (1-\phi)C_s]T = \nabla \bullet K_T(\theta)\nabla T + \nabla \bullet \theta C_w D_H \nabla T - \nabla \theta C_w v T + q C_w T^* \qquad (3.1)$$

Where the terms θ, C_w, ϕ, C_s, T, K_T, D_H, v, q, T^* and t refer to volumetric moisture content, heat capacity of water [$Jm^{-3}\ ^oC$], porosity [-], heat capacity of the solid matrix [$Jm^{-3}\ ^oC$], temperature [^oC], thermal conductivity of water [$Wm^{-1}\ ^oC$], hydrodynamic dispersion tensor [L^2T^{-1}] , water velocity [LT^{-1}] , rate of fluid source [L^{-1}], temperature of fluid source [^oC] and time [T] respectively.

Change in energy stored in the domain of interest over a simulation period is given by the left hand side term of equation 3.1. The first, second, third and last term on the right hand side of equation 3.1 represent thermal conduction, thermo-mechanical dispersion, advective transport and heat sources-sink term respectively.

Advection or convection of heat involves the transport of heat by movement of fluid from one place to the other at the velocity of water flow in the porous media. The velocity of advective transport is given in equation 3.2 as:

$$v_i = \frac{K_r(h)K}{\theta}\left(\frac{\partial h}{\partial i}\right) \tag{3.2}$$

where i stands for direction of flow in this case X or Z. Peclet number is usually used to control numerical errors related to grid size or spatial discretization. Peclet number can be mathematically expressed in equation 3.3 as;

$$P_e = \frac{|v|L}{D} \tag{3.3}$$

where the terms $|v|$, L and D refer to the magnitude of velocity vector, grid cell width and dispersion coefficient respectively. Thermal conduction occurs due to temperature gradient while thermo-mechanical dispersion occurs due to mixing caused by local variations in ve-

locity around some mean velocity of flow. The hydrodynamic dispersion tensor is given in equation 3.4 (Healy, 1990):

$$D_{Hij} = \alpha_T |v| \delta_{ij} + (\alpha_L - \alpha_T)(v_i v_j)/|v| \tag{3.4}$$

where α_T is transverse dispersivity of the porous medium [L], α_L is longitudinal dispersivity of porous medium [L], $|v|$ is the magnitude of hydraulic flux density vector [LT^{-1}], δ_{ij} is Kronecker delta operator (equal to one if i = j otherwise it is zero) and v_i is i th component of hydraulic flux density vector.

$$|v| = \left(v_x{}^2 + v_z{}^2\right)^{1/2} \tag{3.5}$$

$$D_{Hxx} = \alpha_L \frac{v_x{}^2}{|v|} + \alpha_T \frac{v_z{}^2}{|v|} \tag{3.6}$$

$$D_{Hzz} = \alpha_L \frac{v_z{}^2}{|v|} + \alpha_T \frac{v_x{}^2}{|v|}$$

The source/sink term accounts for inject or removal of heat in to the domain of interest in form of fluid source or sink. The potential source can be fluid injected in to the well, stream flow loss and irrigation. The potential ways to remove heat from the porous medium are withdrawal from the well, springs, evaporation and evaporation.

3.2 Initial and boundary conditions for heat transport

The initial condition for heat transport accounts for temperature distribution in the unsaturated zone domain of interest at the beginning of simulation and can be mathematically written as equation 3.7.

$T(x,z,t) = T_0(x,z)$ at $t=0$ (3.7)

Boundary conditions for heat transport can be set as heat flux or fixed temperature. At the inflow heat flux boundaries the temperature must be specified. At the outflow heat flux boundary cells temperature will be set internally by the program to the temperature of the finite difference cells where the water flow out. Upper boundary condition often considered to be the average annual air temperature and lower boundary condition can be the temperature at the water table (Constantz, Tyler, & Kwiccklis, 2003).

Chapter Four: Solute transport in unsaturated zone

Solute transport is a process by which solutes are mainly transported in the subsurface through the movement of water. The chemical constitutes of ground water play significant role on its quality and feasibility for various purposes. The main sources of water to recharge ground water come from rainfall and snow melt. Rainfall and snowmelt have very little dissolved mineral matter (Schwartz & Zhang, 2003). Therefore, the water that recharges the ground water picks up most of its dissolved minerals on its pathway through the soil and vadose zone. It is clear that the use of fertilizers, pesticides and unsafe disposal of chemical wastes like hazardous and radioactive wastes in unsaturated zone significantly affect the chemistry of ground water and ultimately the degree of pollution and contamination of ground water. Hence, it is very important to simulate the solute transport pattern in unsaturated zone in order to be able to see the distribution and quantity of solutes in the unsaturated zone before reaching the ground water. This would help to map potential ground water contaminants coming from unsaturated zone which helps to evaluate various remedial measures designed to protect ground water resource.

4.1 Solute transport equation in unsaturated zone

The advection dispersion equation for solute transport without any chemical reaction in variably saturated condition is given in equation 4.1 (Bear, 1979):

$$\frac{\partial(\theta C)}{\partial t} = \nabla \cdot \theta \overline{D}_h \cdot \nabla C - \nabla \cdot \theta \hat{v} C + SS \tag{4.1}$$

where the terms θ, C, t, D_h, $\hat{v}$ and SS refer to volumetric moisture content, concentration of chemical constitute [ML^{-3}], time [T], hydrodynamic dispersion tensor [L^2T^{-1}], fluid velocity vector [LT^{-1}] and source/sink terms [$ML^{-3}T^{-1}$] respectively.

Change in solute concentration in the domain of interest over the period of simulation is given by left hand side term of equation 4.1. The first, second and last term on the right side of equation 4.1 accounts for hydrodynamic dispersion, advection and source/sink respectively.

Hydrodynamic dispersion accounts for mechanical dispersion and molecular diffusion. Mechanical dispersion is more prominent at greater flow velocities while molecular diffusion is prominent at lower flow velocity. The causes of hydrodynamic dispersion are: range in pore size which results in the solutes to arrive at various times at the end of a soil column, transverse diffusion into stagnate pores, while direct flow through other pores cause solutes to arrive at various times and molecular diffusion ahead of the wetting front as it varies with time (Tindall & Kunkel, 1999).

Mechanical dispersion accounts for spreading of solute through flow channel in the porous media. Normally, dispersion takes place in longitudinal (along the flow line) direction and transverse direction (in direction perpendicular to the flow direction) and the longitudinal dispersion is always larger than transverse dispersion.

Molecular diffusion can be expressed by Fick's Law and depends on molecular diffusion coefficient. Hydrodynamic dispersion tensor is given in equation 4.2 (Healy, 1990) as:

$$\overline{D}_h = \overline{D} + \overline{D}_m \tag{4.2}$$

$$D_{ij} = \alpha_T |v| \delta_{ij} + (\alpha_L - \alpha_T) v_i v_j / |v| \tag{4.3}$$

$$D_{m_{ij}} = D_d \tau_{ij} \tag{4.4}$$

where the term $\bar{D}$, D_m, α_T, α_L, v, δ_{ij}, v_i, D_d and τ_{ij} refer to mechanical dispersion [L^2/T], molecular diffusion [L^2/T], transverse dispersivity of porous medium [L], longitudinal dispersivity porous medium [L], magnitude of the velocity vector [LT^{-1}], Kronecker delta function, which is equal to 1 when i = j and zero otherwise, i^{th} component of the velocity vector [LT^{-1}], coefficient of molecular diffusion of solute in water [L^2T^{-1}] and tortuosity respectively.

In this VS2DRT α_T, α_L and tortuosity are constants and tortuosity is uniformly aligned with the x and z axes so that $\tau_{xx} = \tau_{zz} = \tau$ and $\tau_{xz} = \tau_{zx} = \tau$ (Healy, 1990). The components of hydrodynamic dispersion in 2D are given in equation 4.5 (Healy, 1990):

$$D_{H_{xx}} = \alpha_L \frac{v_x^{\,2}}{|v|} + \alpha_T \frac{v_z^{\,2}}{|v|} + D_m$$

$$D_{H_{zz}} = \alpha_L \frac{v_z^{\,2}}{|v|} + \alpha_T \frac{v_x^{\,2}}{|v|} + D_m \qquad (4.5)$$

$$D_{H_{xz}} = D_{H_{zx}} = (\alpha_L - \alpha_T) v_X v_Z / |v|$$

The source/sink term accounts for inject or removal of solute in to the domain of interest in form of fluid source or sink. The potential source can be fluid injected in to the well, polluted stream flow loss and irrigation.

4.2 Initial and boundary conditions for solute transport

Initial solution condition accounts for spatial distribution of solute at the beginning of the simulation. And mathematically it may be represented using equation 4.6 as:

$C(x,z,t) = C_0(x,z)$ at $t=0$ (4.6)

The boundary conditions for solute transport can be fixed concentration or fixed mass flux of solute. The concentration solute in the water entering the system must be specified and for water leaving the system concentration of solute in the exiting water is set to be equal to the concentration of solute in cell where water is exiting with exception of the case of evaporation. In case of evaporation the water assumed to be solute free (Healy, 1990).

Chapter Five: Chemical reactions in unsaturated zone

Various chemical reactions occur in the unsaturated zone between aqueous chemical constitutes in porous and solid matrix as well as among aqueous chemical constitutes. The chemical reactions my result in the transfer of chemical constitutes in to or from the liquid phase through desorption, dissolution and sorption, precipitation and decay processes respectively. The chemical reactions are simulated in VS2DRT based on ion-association aqueous model or ion interaction model within PHREEQC. It has capabilities to simulate both equilibrium and kinetic reactions. Geochemical databases are used to store chemical reactions and their corresponding equilibrium constants, as well as other parameters such as Debye-Hückel parameters, charge, molar volume, and gram-formula weight (Lichtner, 1996). In PHREEQC the chemical species contained in the system are divided into primary and secondary species. Primary species are total number of species minus the number of reactions. Secondary species equals to the number of reactions. In PHREEQC chemical reactions are written in terms of primary species. For any linearly independent set of chemical reactions, chemical reactions could be written in canonical form as given in equation 5.1 (Lichtner, 1996):

$$\sum_{j=1}^{N_c} \tilde{v}_{ij} A_j = A_i \qquad (i= N_c +1,\ldots,N) \text{ and } N_c = N - N_r \tag{5.1}$$

where N, N_c and N_r represents total number of species involved in the reactions, number of primary species and secondary species respectively, $\bar{v}_{ij}$ stoichiometric coefficients for j^{th} and i^{th} primary and secondary species, A_j, A_i represents j^{th} and i^{th} primary and secondary species respectively. The stoichiometric coefficient measures the degree to which a chemical species take part in a reaction.

5.1 Equilibrium reaction

Equilibrium reactions are governed by mass action law which relates activities of the reactant and products species to equilibrium constant. Equilibrium constant K is given in equation 5.2 as:

$$K = \frac{\prod a_{pi}^{cp}}{\prod a_{rj}^{cr}} \tag{5.2}$$

where a_{pi} and a_{rj} represent activities of i^{th} product and j^{th} reactant species respectively, cp and cr stand for stoichiometric coefficients of i^{th} product and j^{th} reactant species in the chemical reaction. Equilibrium constants are temperature dependent and the activity of an aqueous species is a product of its activity coefficient and molality. Activity coefficients of the aqueous species are functions of species charge and ionic strength, and can be determined using WATEQ Debye-Hückel, Davies or extended Debye-Hückel equations 5.3, 5.4 and 5.5 respectively.

$$\log \gamma_i = -\frac{AZ_i^2\sqrt{\mu}}{1+Ba_i^0\sqrt{\mu}} \qquad \text{for I < 0.1mol/kg} \tag{5.3}$$

$$\log \gamma_i = -AZ_i^2\left(\frac{\sqrt{\mu}}{1+\sqrt{\mu}} - 0.3\mu\right) \qquad \text{for I < 0.5 mol/kg} \tag{5.4}$$

$$\log \gamma_i = -\frac{AZ_i^2\sqrt{\mu}}{1+Ba_i^0\sqrt{\mu}} + b_i\mu \qquad \text{for I < 1mol/kg} \tag{5.5}$$

where Z_i refers to ionic charge of aqueous species i, A and B are temperature dependent parameters, a_i^o and b_i are ion-specific parameters which are determined based on ion radius.

Ionic strength (I) is given in equation 5.6 as:

$$\mu = \frac{1}{2}\sum C_i Z_i^2 \tag{5.6}$$

where C_i and Z_i are molar concentration and charge number of the i^{th} species.

In PHREEQC the default activity coefficient equation used is Davies equation and WATEQ Debye-Hückel equations are used for charged and uncharged species respectively and are set in the database or in the input file through SOLUTION_SPECIES data block.

5.1.1 Heterogeneous ion-exchange

One of the most common reversible chemical reactions which occur in the unsaturated zone is ion-exchange. Ion-exchange is a sorption process which involves exchange of ions between the aqueous solution and the solid matrix. The ion-exchange process in vadose zone depends on cation exchange capacity (CEC) of the soil. CEC refers to the amount of exchangeable equivalents of cationic charge per mass of dry soil. The CEC of a soil is highly dependent on its clay and organic matter content mainly due to presence of high amount of charges on their surface. In PHREEQC ion-exchange is simulated based on heterogeneous mass-action equation and mole-balance equations for the exchange sites. The general mass action equation for ion-exchange can be written as equation 5.7 (Parkhurst & Appelo, 1999):

$$K_{i_e} = a_{i_e} \prod_{m}^{M} a_m{}^{C_{m,ie}} \tag{5.7}$$

where the terms a_{ie}, K_{ie} and $C_{m,ie}$ refer to the activity of an exchange species, the half-reaction selectivity constant and the stoichiometric coefficient of master species, m, in the association half-reaction for exchange species ,i_e, respectively.

EXCHANGE_SPECIES data block of PHREEQC is used to define ion-exchange chemical equations for mole-balance and mass-action expressions, activity coefficient expression for each exchange species and other thermodynamic parameters.

5.1.2 Heterogeneous surface complexation process

Surface complexation is a sorption process where ions in aqueous solution attracted to charged solid matrix surface due to electrostatic forces. Surface complexation can be modeled for example with double layer model. In double layer model charges on the solid surface are neutralized by equal and opposite charges in the aqueous solution. In PHREEQC surface complexation is simulated based on heterogeneous mass-action equation and mole-balance equations for the surface sites and charge-potential relations for each surface. The mass action equation for surface complexation reactions may include electrostatic potential or not. The general mass-action equation for surface species can be written as equation 5.8 (Parkhurst & Appelo, 1999):

$$K_{i_{sk}}^{\text{int}} = \left(a_{i_{sk}} \prod_{m}^{M} a_{m}^{-Cm,i_{sk}} \right) e^{\frac{F\psi_S}{RT}\Delta z_{I_{i_{sk}}}} \tag{5.8}$$

where the terms ΔZ_{isk}, K^{int}_{isk} , $i_{(sk)}$, $C_{m,ie}$, F, ψ_s, R and T refer to the net change in surface charge due to the formation surface species, the intrinsic equilibrium constant, the i^{th} surface species for surface-site type k in surface s, the stoichiometric coefficient of master species, m, in the association half-reaction for surface species ,$i_{(sk)}$, the Faraday constant, the potential surfaces (volt), the gas constant and the temperature (Kelvin) respectively.

5.1.3 Heterogeneous mineral dissolution/precipitation

Heterogeneous mineral dissolution/precipitation process involves transfer of chemical species in to and out of the aqueous solution respectively and could be model in VS2DRT using PHRREQC's EQULIBIRUM-PHASES data block. In general pure phase equilibria can be represented with equation 5.9 (Parkhurst & Appelo, 1999):

$$K_p = \prod_m^{M_{aq}} a_m{}^{C_{m,p}} \tag{5.9}$$

where the term $C_{m,p}$ refers stoichiometric coefficient of master species m in dissolution reaction. Saturation index for the mineral, SI_p, is given in equation 5.10:

$$SI_p = \log \prod_m^{M_{aq}} a_m{}^{C_{m,p}} \tag{5.10}$$

5.2 Kinetic reaction

Slow homogeneous and heterogeneous chemical reactions in unsaturated zone are controlled by the rate of kinetic reactions. First order radioactive decay and biodegradation can be an example for the kinetic reactions in soil. PHREEQC models kinetic reactions using user defined rate equations written in Basic language statements. A general rate expression for a kinetic reaction of minerals and other solids is given in equation 5.11 (Parkhurst & Appelo, 1999):

$$R_k = r_k \frac{A_0}{V} \left(\frac{m_k}{m_{0k}} \right)^n \tag{5.11}$$

where the terms r_k, $A_{0,}$ V, m_{0k} and m_k refer to the specific rate [T^{-1}], the initial surface area of the solid [L^2], the amount of solution, the initial moles of solid and the moles of solid at a given time respectively.

Chapter Six: Numerical solutions for water flow, heat transport and multi-solute transport

Finite difference method is used to solve unsaturated water transport equation including advection, dispersion, diffusion, equations of heat and multi-solute transport subjected to initial and boundary conditions. Finite difference numerical approximation of unsaturated water flow results in a set of simultaneous nonlinear algebraic equations. To obtain the solution for unsaturated water flow and transport the simultaneous nonlinear algebraic equations was linearized using a modified Newton-Raphson Method. Strongly implicit procedure (SIP) is used to solve the linearized simultaneous algebraic equations, as well as simultaneous algebraic equations for heat and multi-solute transports.

6.1 Numerical implementation for unsaturated water flow

6.1.1 Spatial discretization of unsaturated water flow

Block centered finite difference approach is used to approximate spatial derivatives of unsaturated flow. Schematic representation rectangular and cylindrical grid-block systems are presented in the figure 6.1 and 6.2 respectively.

The form of unsaturated flow equation for each grid block is given in equation 6.1 (Lappala, Healy, & Weeks, 1987):

$$\begin{aligned} &v\rho\left(C_m + sS_m\right)\frac{\partial H}{\partial t} \\ &-\hat{C}_{n-1/2,j}\left(H_{n-1,j} - H_{n,j}\right) - \hat{C}_{n,j-1/2}\left(H_{n,j-1} - H_{n,j}\right) - \hat{C}_{n+1/2,j}\left(H_{n+1,j} - H_{n,j}\right) \\ &-\hat{C}_{n,j+1/2}\left(H_{n,j+1} - H_{n,j}\right) - \rho q v = 0 \end{aligned} \tag{6.1}$$

where the term $\hat{C}$ represent the conductance and is defined as:

$$\hat{C}_{i-1/2,j} = \left(\frac{\rho K K_r A}{\Delta X} \right)_{i-1/2,j} \tag{6.2}$$

$$\hat{C}_{i,j-1/2} = \left(\frac{\rho K K_r A}{\Delta Z} \right)_{i,j-1/2} \tag{6.3}$$

$$\hat{C}_{i+1/2,j} = \left(\frac{\rho K K_r A}{\Delta X} \right)_{i+1/2,j} \tag{6.4}$$

$$\hat{C}_{i,j+1/2} = \left(\frac{\rho K K_r A}{\Delta Z} \right)_{i,j+1/2} \tag{6.5}$$

where A represents block face area.

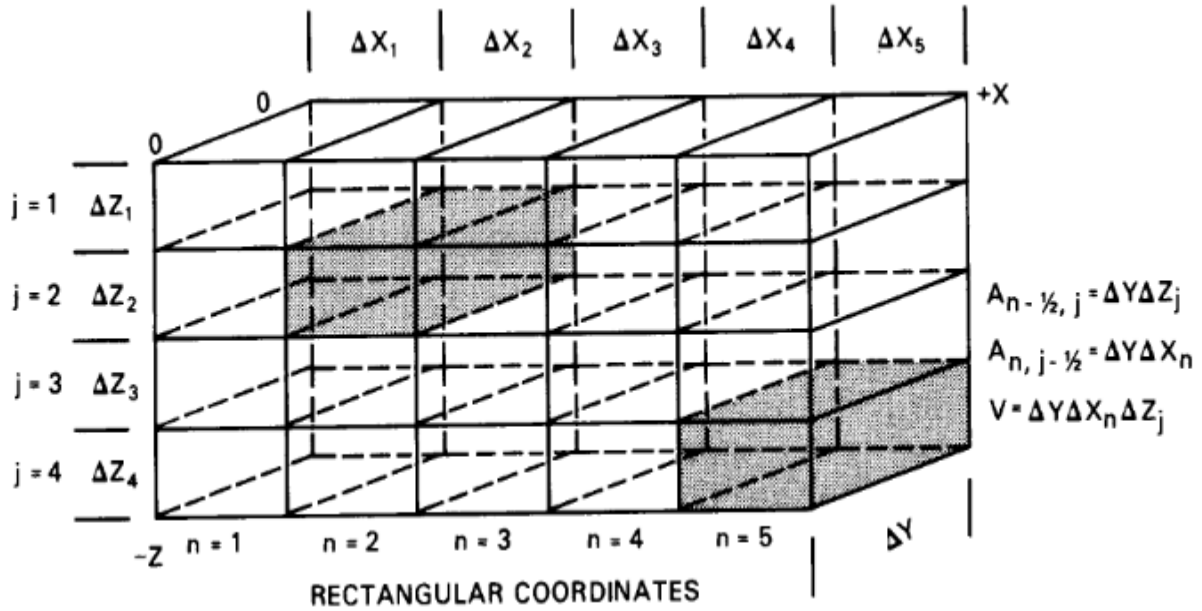

Figure 6.1 Schematic representation of rectangular grid block system (Lappala, Healy, & Weeks, 1987)

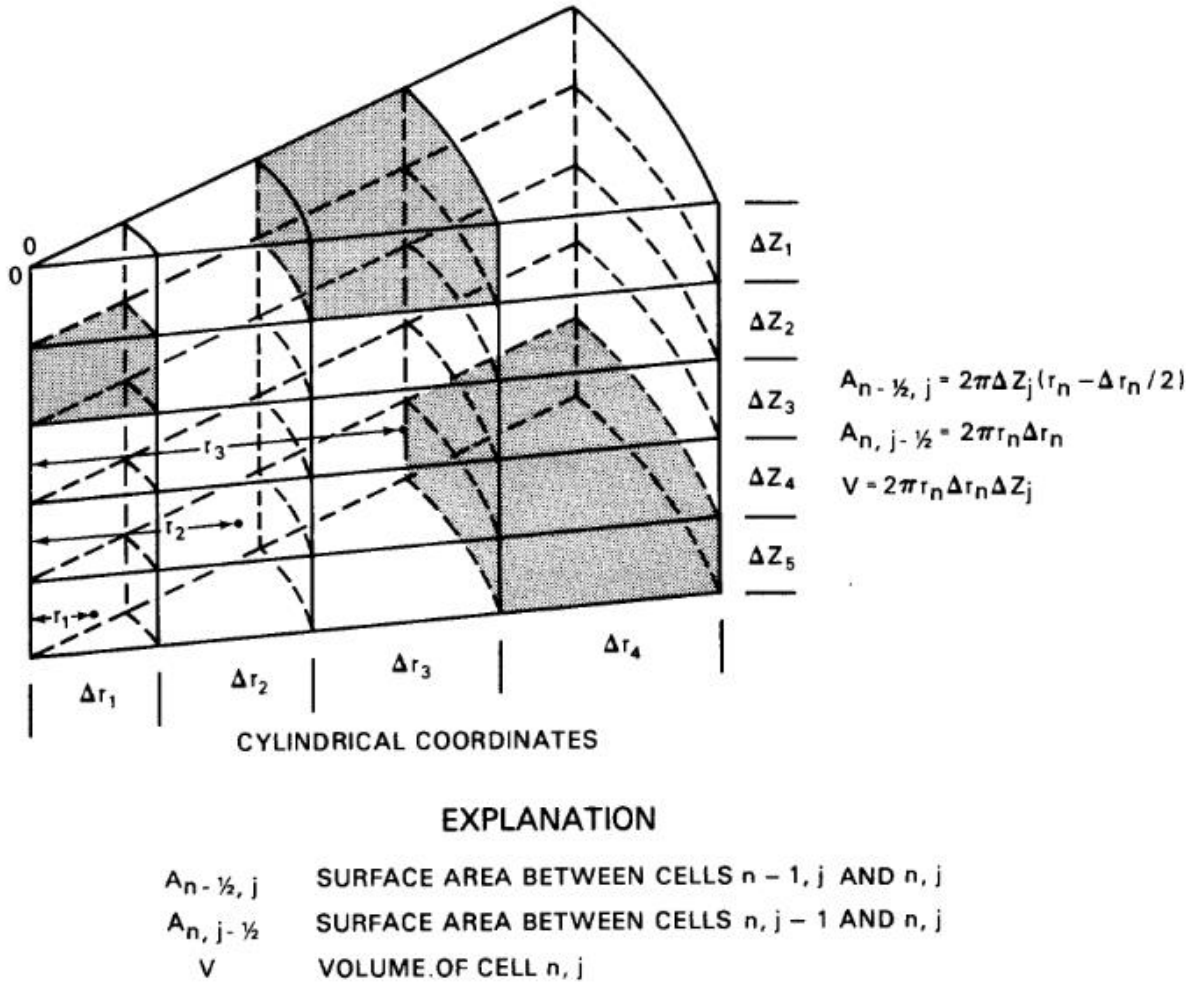

Figure 6.2 Schematic representations of cylindrical grid-block system (Lappala, Healy, & Weeks, 1987)

Averaging the conductance terms for adjacent blocks is essential while using block centered scheme. In VS2DRT the conductance terms of the medium is represented by saturated hydraulic conductivity and relative hydraulic conductivity. Inter-cell saturated hydraulic conductivity of adjacent blocks are determined using distance-weighted harmonic mean of saturated hydraulic conductivity of adjacent cells. Geometric mean or weighted arithmetic mean can be used to determine the averages relative hydraulic conductivity of adjacent blocks or cells.

6.1.2 Temporal discretization of unsaturated water flow

The numerical approximation for the time derivative term *(∂H/∂t)* of Richard's equation is given in equation 6.6 as:

$$\left(\frac{\partial H}{\partial t}\right)^{i-1/2} = \frac{H^{i} - H^{i-1}}{t^{i} - t^{i-1}} \tag{6.6}$$

where the terms *i* and *i-1* represent the current time and previous time steps respectively. Temporal discretization can be in the form of fully implicit or backward difference scheme form. Numerical representation of Richard's equation for 2D flow in terms of spatial and temporal discretization is given in equation 6. 7 (Lappala, Healy, & Weeks, 1987):

$$\begin{aligned} &v\rho\left[c_m + sS_s\right]^{i-1/2}\left(\frac{H_{n,j}^{i} - H_{n,j}^{i-1}}{t^{i} - t^{i-1}}\right) = \\ &\overline{C}_{n-1/2,j}^{\,i-1/2}\left(H_{n-1,j}^{i} - H_{n,j}^{i}\right) + \overline{C}_{n,j-1/2}^{\,i-1/2}\left(H_{n,j-1}^{i} - H_{n,j}^{i}\right) + \\ &\overline{C}_{n+1/2,j}^{\,i-1/2}\left(H_{n+1,j}^{i} - H_{n,j}^{i}\right) + \overline{C}_{n,j+1/2}^{\,i-1/2}\left(H_{n,j+1}^{i} - H_{n,j}^{i}\right) + \left(\rho q v\right)_{n,j}^{i-1/2} \end{aligned} \tag{6.7}$$

Numerically approximation of 2D Richards's equation could be written in matrix form (Lappala, Healy and Weeks, 1987) in equation 6.8:

$$\left[A^{i-1/2}\right]\left\{H^{i}\right\} = \left\{RHS\right\} \tag{6.8}$$

Where A is a square m by m matrix which holds unknown parts of conductance terms, storage and source-sink terms and RHS is a vector which holds known parts of conductance, storage and source-sink terms.

6.1.3 Numerical solution

Modified Newton-Raphson method is used to linearize Richard's matrix equation. Strongly implicit procedure is applied to solve linearized 2D Richard's matrix equation.

The linearized Richard's matrix equation (Lappala, Healy, & Weeks, 1987) is given in equation 6.9 as:

$$\left[\overline{A}\right]^{k-1}\{H*\}^{k} = \beta_s\{RHS\}^{k} - \left[\overline{A}\right]^{k-1}\{H\}^{k-1} \tag{6.9}$$

β_s user defined damping factor, HMAX

In VS2DRT the same iteration loop is used for both linearization and matrix solution of Richard's equation. Steps to solve the linearized Richard's equation are (Lappala, Healy, & Weeks, 1987):

1. Evaluation nonlinear coefficients using the latest value of H

2. Determination of the elements of the $[\overline{A}]$ matrix and *{RHS}* vector

3. Solving linearized Richard's matrix equation for the residuals *{H*}* using the SIP

4. Compute new potentials (H^k) using the equation $H^k = H^{k-1} + w_k H*$

where w_k is a damping factor and $0 < w_k <= 1$

5. Test for convergence by checking whether *H** is less than a user–specified tolerance limit.

6. Proceeds to the next time step if convergence is reached, otherwise step 1 to 5 will be repeated until convergence is reached during the user specified maximum iteration limit. For case where convergence could not be reached the length of time step could be adjusted to a maximum of three times and repeats the steps 1 to 5. If still convergence is not reached the program either proceeds to the next time step or terminates.

6.2 Numerical implementation for heat transport

6.2.1 Spatial discretization of heat transport

Spatial discretization of 2D advection dispersion heat transport can be written in equation 6.10 modified from (Healy, 1990):

$$\hat{A}\ T_{n-1,j} + \hat{B}T^{i}_{n,j-1} + \hat{C}T_{n+1,j} + \hat{D}\ T_{n,j+1} + \hat{E}\ T_{n,j} = RHS \tag{6.10}$$

The values of coefficients $\hat{A}$, $\hat{B}$, $\hat{C}$, $\hat{D}$ and $\hat{E}$ are computed using equations 6.10a, 6.10b, 6.10c, 6.10d, 6.10e, 6.10f, 6.10g, 6.10h, 6.10i and 6.12. RHS would be computed using equations 6.10rhs and 6.11.

$$\hat{A} = TC\left[(A)_{n-1/2,j}\left[\frac{K_{T\,xx\,n-1/2,j} + C_w\theta_{n-1/2,j}D_{H\,xx\,n-1/2,j}}{1/2\left(\Delta x_n + \Delta x_{n-1}\right)} + \frac{1}{2}C_w\theta_{n-1/2,j}v_{x\,n-1/2,j}\right] + \hat{G} - \hat{H}\right] \tag{6.10a}$$

$$\hat{B} = TC\left[(A)_{n,j-1/2}\left[\frac{K_{T\,zz\,n,j-1/2} + C_w\theta_{n,j-1/2}D_{H\,zz\,n,j-1/2}}{1/2\left(\Delta z_j + \Delta z_{j-1}\right)} + \frac{1}{2}C_w\theta_{n,j-1/2}v_{z\,n,j-1/2}\right] + \hat{F} - \hat{I}\right] \tag{6.10b}$$

$$\hat{C} = TC\left[(A)_{n+1/2,j}\left[\frac{K_{T\,xx\,n+1/2,j} + C_w\theta_{n+1/2,j}D_{H\,xx\,n+1/2,j}}{1/2\left(\Delta x_n + \Delta x_{n+1}\right)} + \frac{1}{2}C_w\theta_{n+1/2,j}v_{x\,n+1/2,j}\right] - \hat{G} + \hat{H}\right] \tag{6.10c}$$

$$\hat{D} = TC\left[(A)_{n,j+1/2}\left[\frac{K_{T\,zz\,n,j+1/2} + C_w\theta_{n,j+1/2}D_{H\,zz\,n,j+1/2}}{1/2\left(\Delta z_j + \Delta z_{j+1}\right)} + \frac{1}{2}C_w\theta_{n,j+1/2}v_{z\,n,j+1/2}\right] - \hat{F} + \hat{I}\right] \tag{6.10d}$$

$$\hat{E} = -\hat{A} - \hat{B} - \hat{C} - \hat{D} - \frac{V}{\Delta t}\left(2C_w\theta + (1-\phi)C_s\right) + TC\left[\left(A\theta v_x\right)_{n-1/2,j} + \left(A\theta v_z\right)_{n,j-1/2} + \left(A\theta v_x\right)_{n+1/2,j} + \left(A\theta v_z\right)_{n,j+1/2}\right] \tag{6.10e}$$

$$RHS = \frac{V}{\Delta t} T_{n,j} \left(C_w \theta + (1-\phi) C_s \right) -$$
$$2(1-TC)\left[\hat{A}\ T_{n-1,j} + \hat{B}\ T_{n,j-1} + \hat{C}\ T_{n+1,j} + \hat{D}\ T_{n,j+1} + \hat{E}\ T_{n,j} \right] -$$
$$\left(\hat{F} + \hat{G} \right) T_{n-1,j-1} + \left(\hat{H} + \hat{F} \right) T_{n-1,j+1} + \left(\hat{I} + \hat{G} \right) T_{n+1,i-1} - \left(\hat{H} + \hat{I} \right) T_{n+1,j+1}$$

(6.10rhs)

where

$$\hat{F} = \frac{1}{2}\left[\frac{A\left(K_{T\ xz\ n-1/2,j} + C_w \left(\theta D_{H\ xz} \right)_{n-1/2,j} \right)}{\Delta z_j + 1/2\left(\Delta z_{j+1} + \Delta z_{j-1} \right)} \right] \quad (6.10f)$$

$$\hat{G} = \frac{1}{2}\left[\frac{A\left(K_{T\ zx\ n,j-1/2} + C_w \left(\theta D_{H\ zx} \right)_{n,j-1/2} \right)}{\Delta x_n + 1/2\left(\Delta x_{n-1} + \Delta x_{n+1} \right)} \right] \quad (6.10g)$$

$$\hat{H} = \frac{1}{2}\left[\frac{A\left(K_{T\ zx\ n,j+1/2} + C_w \left(\theta D_{H\ zx} \right)_{n,j+1/2} \right)}{\Delta x_n + 1/2\left(\Delta x_{n-1} + \Delta x_{n+1} \right)} \right] \quad (6.10h)$$

$$\hat{I} = \frac{1}{2}\left[\frac{A\left(K_{T\ xz\ n+1/2,j} + C_w \left(\theta D_{H\ xz} \right)_{n+1/2,j} \right)}{\Delta z_j + 1/2\left(\Delta z_{j-1} + \Delta z_{j+1} \right)} \right] \quad (6.10i)$$

$$TC = \begin{cases} 1, \text{for fully implicit} \\ 1/2, \text{for time centered} \end{cases}$$

In presence of source/sink term RHS and $\hat{E}$ terms would be modified to consider source/sink effect in the simulation. The modification could be done using equations 6.11 and 6.12:

$$RHS = RHS + qC_w T^* V \qquad \text{If } qV > 0 \quad (6.11)$$

$$\hat{E} = \hat{E} - qC_w T^* V \qquad \text{If } qV < 0 \quad (6.12)$$

6.2.2 Temporal discretization of heat transport

The time derivative of 2D advection dispersion heat transport equation can be approximated using equation 6.13 as follows:

$$\frac{\partial[\theta C_w + (1-\phi)C_s]T}{\partial t} = \frac{TC_w \partial\theta}{\partial t} + \frac{(\theta C_w + (1-\phi)C_s)\partial T}{\partial t}$$
$$\approx T^{i-1/2} C_w \frac{\theta^i - \theta^{i-1}}{t^i - t^{i-1}} + \left(\theta^{i-1/2} C_w + (1-\phi)C_s\right)\frac{T^i - T^{i-1}}{t^i - t^{i-1}} \quad (6.13)$$

Where i represents current time step, i-1 represent previous time step, T^i, T^{i-1}, θ^i and θ^{i-1} represents current time step temperature, previous time step temperature, current time step volumetric moisture content and previous time step volumetric moisture content at a given node respectively.

Spatial and temporal discretization equations 2D heat transport equation could be given in equation 6.14 as:

$$\hat{A}^{i+1} T_{n-1,j}^{i+1} + \hat{B}^{i+1} T_{n,j-1}^{i+1} + \hat{C}^{i+1} T_{n+1,j}^{i+1} + \hat{D}^{i+1} T_{n,j+1}^{i+1} + \hat{E}^{i+1} T_{n,j}^{i+1} = RHS \quad (6.14)$$

6.2.3 Numerical solution

At each node in the finite difference grid the advection dispersion heat transport equation have to be solved. Finite difference approximation at each nodal point in the finite difference grid gives a set of simultaneous equations which could be solved as matrix in equation 6.15.

$$\overline{A}\,\overline{T}^{\,i} = \overline{RHS} \quad (6.15)$$

where A is a pentagonal square coefficient matrix T^i is the vector of unknown temperatures at the i time level and RHS is the vector defined above.

The matrix equation for 2D advection dispersion heat transport equation is solved using an iterative matrix solver applying strongly implicit procedure according to equation 6.16:

$$\overline{A}\,\Delta\overline{T}^{\,i,k} = \overline{RHS}^{\,k} - \overline{A}\,\overline{T}^{\,i,k-1} \quad (6.16)$$

where $\Delta\bar{T}^{i,k} = \bar{T}^{i,k} - \bar{T}^{i,k-1}$ and k represents the iteration index

Steps involved to solve the advection dispersion heat transport equation are:

1. Determination of the elements of matrix $[\bar{A}]$ and $\{RHS\}$ vector
2. Solving advection dispersion heat transport equation for the residuals, $\Delta\bar{T}$ using the SIP.
3. Compute new temperature (T^k) using the equation $\vec{T}^k = \vec{T}^{k-1} + w_k\Delta\bar{T}$, where w_k is a damping factor and $0 < w_k <= 1$
4. Test for convergence by checking whether $\Delta\bar{T}$ is less than a user–specified tolerance limit.
5. Proceed to the next time step if convergence is reached, otherwise step 1 to 4 will be repeated until convergence is reached during the user specified maximum iteration limit. For cases where convergence could not be reached the length of time step could be adjusted to a maximum of three times and repeats the steps 1 to 4. If still convergence could not be reached the program either proceeds to next time step or terminates.

In VS2DRT there is an option either to use fully implicit or time centered differencing. The demerit of time-centered differencing methods is that it can cause oscillation. Although, fully implicit differencing method would avoid the oscillation problems of time-differencing, it is prone to numerical dispersion.

6.3 Numerical implementation for multi-solute transport

6.3.1 Spatial discretization of multi-solute transport

Spatial discretization of 2D advection dispersion multi-solute transport can be given in equation 6.17 modified from (Healy, 1990):

$$\hat{A}C^{l}_{n-1,j} + \hat{B}C^{l}_{n,j-1} + \hat{C}C^{l}_{n+1,j} + \hat{D}C^{l}_{n,j+1} + \hat{E}\,C^{l}_{n,j} = RHS \tag{6.17}$$

The values of coefficients $\hat{A}$, $\hat{B}$, $\hat{C}$, $\hat{D}$ and $\hat{E}$ are computed using equations 6.17a, 6.17b, 6.17c, 6.17d, 6.17e, 6.17f, 6.17g, 6.17h, 6.17i and 6.19. RHS would be computed using equations 6.17rhs and 6.18.

$$\hat{A} = TC\left[\left(A\theta\right)_{n-1/2,j}\left[\frac{\overline{\overline{D}}_{hxxn-1/2,j}}{1/2\left(\Delta x_n + \Delta x_{n-1}\right)} + \frac{1}{2}\bar{v}_{xn-1/2,j}\right] + \hat{G} - \hat{H}\right]^{i} \tag{6.17a}$$

$$\hat{B} = TC\left[\left(A\theta\right)_{n,j-1/2}\left[\frac{\overline{\overline{D}}_{hzzn,j-1/2}}{1/2\left(\Delta z_j + \Delta z_{j-1}\right)} + \frac{1}{2}\bar{v}_{zn,j-1/2}\right] + \hat{F} - \hat{I}\right]^{i} \tag{6.17b}$$

$$\hat{C} = TC\left[\left(A\theta\right)_{n+1/2,j}\left[\frac{\overline{\overline{D}}_{hxxn+1/2,j}}{1/2\left(\Delta x_n + \Delta x_{n+1}\right)} + \frac{1}{2}\bar{v}_{xn+1/2,j}\right] - \hat{G} + \hat{H}\right]^{i} \tag{6.17c}$$

$$\hat{D} = TC\left[\left(A\theta\right)_{n,j+1/2}\left[\frac{\overline{\overline{D}}_{hzzn,j+1/2}}{1/2\left(\Delta z_j + \Delta z_{j+1}\right)} + \frac{1}{2}\bar{v}_{zn,j+1/2}\right] - \hat{F} + \hat{I}\right]^{i} \tag{6.17d}$$

$$\hat{E} = -\hat{A} - \hat{B} - \hat{C} - \hat{D} - \frac{V}{\Delta t}\left(2\theta_{n,j}^{i} - \theta_{n,j}^{i-1}\right) + TC\left[\left(A\theta\bar{v}_x\right)_{n-1/2,j} + \left(A\theta\bar{v}_z\right)_{n,j-1/2} + \left(A\theta\bar{v}_x\right)_{n+1/2,j} + \left(A\theta\bar{v}_z\right)_{n,j+1/2}\right]^{i} \quad (6.17e)$$

$$RHS = \frac{V}{\Delta t}C_{n,j}^{i-1}\left(\theta^{i-1}\right) - 2\left(1-TC\right)\left[\hat{A}^{i-1}C_{n-1,j}^{i-1} + \hat{B}^{i-1}C_{n,j-1}^{i-1} + \hat{C}^{i-1}C_{n+1,j}^{i-1} + \hat{D}^{i-1}C_{n,j+1}^{i-1} + \hat{E}^{i-1}C_{n,j}^{i-1}\right] - \left(\hat{F}^{i} + \hat{G}^{i}\right)C_{n-1,j-1}^{i} + \left(\hat{H}^{i} + \hat{F}^{i}\right)C_{n-1,j+1}^{i} + \left(\hat{I}^{i} + \hat{G}^{i}\right)C_{n+1,i-1}^{i} - \left(\hat{H}^{i} + \hat{I}^{i}\right)C_{n+1,j+1}^{i} \quad (6.17rhs)$$

where

$$\hat{F} = \frac{1}{2}\left[\frac{\left(A\theta\overline{\overline{D}}_{h\,xz}\right)_{n-1/2,j}}{\Delta z_j + 1/2\left(\Delta z_{j+1} + \Delta z_{j-1}\right)}\right] \quad (6.17f)$$

$$\hat{G} = \frac{1}{2}\left[\frac{\left(A\theta\overline{\overline{D}}_{h\,zx}\right)_{n,j-1/2}}{\Delta x_n + 1/2\left(\Delta x_{n-1} + \Delta x_{n+1}\right)}\right] \quad (6.17g)$$

$$\hat{H} = \frac{1}{2}\left[\frac{\left(A\theta\overline{\overline{D}}_{h\,zx}\right)_{n,j+1/2}}{\Delta x_n + 1/2\left(\Delta x_{n-1} + \Delta x_{n+1}\right)}\right] \quad (6.17h)$$

$$\hat{I} = \frac{1}{2}\left[\frac{\left(A\theta\overline{\overline{D}}_{h\,xz}\right)_{n+1/2,j}}{\Delta z_j + 1/2\left(\Delta z_{j-1} + \Delta z_{j+1}\right)}\right] \quad (6.17i)$$

$$TC = \begin{cases} 1, \textit{for fully implicit} \\ 1/2, \textit{for time centered} \end{cases}$$

In the presence of source/sink term RHS and $\hat{E}$need to be modified to consider source/sink effect in the simulation. The modification could be done using equations 6.18 and 6.19:

$$RHS = RHS + qC_w T^{*}V \qquad \text{if } qV > 0 \quad (6.18)$$

$$\hat{E} = \hat{E} - qC_w T^{*}V \qquad \text{if } qV < 0 \quad (6.19)$$

6.3.2 Temporal discretization of multi-solute transport

The time derivative term in equation 4.1 could be approximated using equation 6.20 as follows:

$$\frac{\partial \theta C}{\partial t} = \frac{C \partial \theta}{\partial t} + \theta \frac{\partial C}{\partial t} \approx C^{i-1/2} \frac{\theta^i - \theta^{i-1}}{t^i - t^{i-1}} + \left(\theta^{i-1/2}\right) \frac{C^i - C^{i-1}}{t^i - t^{i-1}} \tag{6.20}$$

where i represents current time step, i-1 represent previous time step, C^i, C^{i-1}, θ^i and θ^{i-1} represents current time step l^{th} species concentration, previous time step l^{th} concentration, current time step volumetric moisture content and previous time step volumetric moisture content at a given node respectively.

Spatial and temporal discretization of multi-solute transport equation is given in equation 6.21 as:

$$\hat{A}^i C^i_{n-1,j} + \hat{B}^i C^i_{n,j-1} + \hat{C}^i C^i_{n+1,j} + \hat{D}^i C^i_{n,j+1} + \hat{E}^i C^i_{n,j} = RHS \tag{6.21}$$

6.3.3 Numerical solution

At each node of the finite difference grid solute transport equation is solved for each solute. Finite difference approximation at each nodal point in the finite difference grid gives a set of simultaneous equations which could be solved as matrix equation in equation 6.22.

$$\overline{A}\,\overline{C}^{\,i} = \overline{RHS} \tag{6.22}$$

where A represents pentagonal square coefficient matrix, l^{th} C is the vector of unknown concentration at the i time level and RHS is the vector above.

Equation 6.22 will be solved by strongly implicit procedure iterative matrix solver in equation 6.23:

$$\bar{A}\Delta\bar{C}^{i,k} = \overline{RHS}^{k} - \bar{A}\bar{C}^{i,k-1} \tag{6.23}$$

where $\Delta\bar{C}^{i,k} = \bar{C}^{i,k} - \bar{C}^{i,k-1}$ and k represents iteration index

1. Determination of the elements of matrix $[\bar{A}]$ and $\{RHS\}$ vector
2. Solving advection dispersion solute transport equation for the residuals, $\Delta\bar{C}$ using the SIP.
3. Compute new concentration ($\bar{C}^{k}$) using the equation $\bar{C}^{k} = \bar{C}^{k-1} + w_k\Delta\bar{C}$, where w_k is a damping factor and $0<w_k<=1$
4. Test for convergence by checking whether $\Delta\bar{C}$ is less than a user–specified tolerance limit.

The code proceeds to the next time step if convergence is reached, otherwise step 1 to 4 will be repeated until convergence is reached during the user specified maximum iteration limit. For case where convergence could not be reached the length of time step could be adjusted to a maximum of three times and repeats the steps 1 to 4. If still convergence could not be reached the program either proceeds to next time step or exits.

6.4 Numerical solutions for chemical equilibrium and kinetic reaction equations

In PHREEQC a set of functions, *f,* are derived by substituting the equations for the moles of species into mole- and charge-balance equations to define heterogeneous equilibrium. These functions include $f_{H2O,}$, f_{μ} , f_{Ptotal} , f_{p} , f_{Pss} , f_{Sk} , f_{e} , f_{Alk} , $f_{m,}$ $f_{z,}$ $f_{\psi s}$ and $f_{z,s}$ are given in equations

from 6.24 to 6.47 along with their total derivatives (Parkhurst & Appelo, 1999) . Their corresponding master unknowns are $\ln a_{Alk}$, $\ln a_e$, n_g, $\ln a_{e^-}$, $\ln a_{H2O}$, $\ln a_m$, $\ln W_{aq}$, N_{gas}, n_p, n_{ss}, $\ln a_{sk}$, $\ln a_{H^+}$, μ,and $\ln a_{\psi s}$ (Parkhurst & Appelo, 1999).

The function used for activity of water, $f_{H2O,}$ in the numerical methods is given in equation 6.24. The total derivative of f_{H2O} is given in equation 6.25:

$$f_{H_2O} = W_{aq}\left(a_{H_2O} - 1\right) + 0.017\sum_{i}^{N_{aq}} n_i \tag{6.24}$$

$$df_{H_2O} = W_{aq} a_{H_2O} d\ln\left(a_{H_2O}\right) + \left(a_{H_2O} - 1\right) W_{aq} d\ln\left(W_{aq}\right) + 0.017\sum_{i}^{N_{aq}} dn_i \tag{6.25}$$

where a_{H2O} is the activity of water, W_{aq} is the mass of solvent water in aqueous solution and n_i is the moles of aqueous species i in the solution respectively.

The function used for ionic strength, $f_{\mu,}$ in the numerical methods is given in equation 6.26. The total derivative of f_{μ} is also given in equation 6.27:

$$f_{\mu} = W_{aq}\mu - \frac{1}{2}\sum_{i}^{Naq} z_i^2 n_i \tag{6.26}$$

$$df_{\mu} = \mu W_{aq} d\ln\left(W_{aq}\right) + W_{aq} d\mu - \frac{1}{2}\sum_{i}^{N_{aq}} z_i^2 dn_i \tag{6.27}$$

where μ refers to the ionic strength.

The function used for fixed-pressure multicomponent gases, f_{Ptotal}, in the numerical methods is given in equation 6.28. The total derivative of f_{Ptotal} is given in equation 6.29:

$$f_{P\,total} = P_{total} - \sum_{g}^{N_g} P_g \tag{6.28}$$

$$df_{P\,total} = -\sum_{g}^{N_g}\sum_{m}^{M_{aq}} C_{m,g} P_g \, d\ln a_m \tag{6.29}$$

where P_{total}, N_g, $C_{m,g}$ and P_g refer to total pressure, total number of gas components in the gas phase, the stoichiometric coefficient of aqueous master species m and partial pressure of gas component g in the gas phase respectively.

The function used for phase equilibrium, f_p, in the numerical methods is given in equation 6.30. The total derivative of f_p is given in equation 6.31.

$$f_P = \left(\ln K_p + [\ln(10)] SI_{P;target}\right) - \sum_{m}^{M_{aq}} C_{m,p} \ln(a_m) \tag{6.30}$$

$$df_P = -\sum_{m}^{M_{aq}} C_{m,p} \, d\ln(a_m) \tag{6.31}$$

where K_p, $SI_{p,target}$ and $C_{m,p}$ refer to pure phase equilibria, target saturation index for the phase and the stoichiometric coefficient of master species m respectively.

The function used for each component of an ideal solution, f_{Pss}, in the numerical methods is given in equation 6.32. The total derivative of f_{Pss} is given in equation 6.33.

$$f_{P\,ss} = \ln\left(\frac{\sum_{m}^{M_{aq}} a_m^{C_{m,Pss}}}{K_{P_{ss}}}\right) - \ln\left(\frac{n_{p_{ss}}}{N_{total}}\right) \tag{6.32}$$

$$df_{P\,ss} = \sum_{m}^{M_{aq}} C_{m,P_{ss}} \, d\ln a_m - \frac{1}{n_{P_{ss}}}\left(\frac{N_{total} - n_{P_{ss}}}{N_{total}}\right) dn_{P_{ss}} + \sum_{j_{ss}}^{N_{ss}, j_{ss} \neq P_{ss}} \frac{1}{N_{total}} dn_{j_{ss}} \tag{6.33}$$

$$N_{total} = \sum_{j_{ss}}^{N_{ss}} n_{j_{ss}} \tag{6.34}$$

where $C_{m,Pss}$, K_{Pss}, n_{Pss} and N_{ss} refer to the stoichiometric coefficient of master species m in the dissolution reaction for component p in the solid solution *ss*, solid-solution equilibria, mole of each component in each solid solution n_{Pss} and the number of components in solid solution *ss* respectively.

The function used for surface site type S_k, f_{Sk}, in the numerical methods is given in equation 6.35. The total derivative of f_{Sk} is given in equation 6.36.

$$f_{S_k} = T_{S_k} - \sum_{i_{(S_k)}}^{N_{S_k}} b_{S_k,i_{(S_k)}} n_{i_{(S_K)}} \tag{6.35}$$

$$df_{S_k} = \Delta T_{S_k} - \sum_{i_{(S_k)}}^{N_{SK}} b_{S_k,i_{(S_k)}} dn_{i_{(S_K)}} \tag{6.36}$$

where T_{S_k}, N_{s_k} and $bs_k, i_{(s_k)}$ refer to the moles of the surface site type, the number of surface species for the site type and the number of surface sites occupied by the surface species $i_{(s_k)}$ respectively.

The function used for exchange site, f_e, in the numerical methods is given in equation 6.37. The total derivative of f_e is given in equation 6.38.

$$f_e = T_e - \sum_{i_e}^{N_e} b_{e,i_e} n_{i\,e} \tag{6.37}$$

$$df_e = \Delta T_e - \sum_{i_e}^{N_e} b_{e,i_e} dn_{i\,e} \tag{6.38}$$

The function used for alkalinity, f_{Alk}, in the numerical methods is given in equation 6.39. The total derivative of f_{Alk} is given in equation 6.40.

$$f_{Alk} = T_{Alk} - \sum_{i}^{N_{aq}} b_{Alk,i} n_i \tag{6.39}$$

$$df_{Alk} = -\sum_{i}^{N_{aq}} b_{Alk,i} dn_i \tag{6.40}$$

where T_{Alk} and $b_{Alk,i}$ refer to the number of equivalents of alkalinity in the solution and the alkalinity contribution of aqueous species *i* respectively.

The function used for mole balance of elements, f_m, in the numerical methods is given in equation 6.41. The total derivative of f_m is given in equation 6.42.

$$f_m = \left(T_m - \sum_{p}^{N_p} b_{m,p} n_p - \sum_{ss}^{SS} \sum_{P_{ss}}^{N_{ss}} b_{m,p_{ss}} n_{p_{ss}} \right) - \sum_{i}^{N_{aq}} b_{m,i} n_i - \sum_{e}^{E} \sum_{i_e}^{N_e} b_{m,i_e} n_{i_e} - \sum_{s}^{S} \sum_{k}^{K_s} \sum_{i_{(s_k)}}^{N_{sk}} b_{m,i_{(s_k)}} n_{i(S_k)} - \sum_{g}^{N_g} b_{m,g} n_g - \sum_{s}^{S} \sum_{i}^{N_{aq}} b_{m,i} n_{i,s} \tag{6.41}$$

$$df_m = -\sum_{p}^{N_p} b_{m,p} dn_p - \sum_{ss}^{ss} \sum_{P_{ss}}^{N_{ss}} b_{m,P_{SS}} dn_{P_{SS}} - \sum_{i}^{N_{aq}} b_{m,i} dn_i - \sum_{e}^{E} \sum_{i_e}^{N_e} b_{m,i_e} dn_{i_e} - \sum_{s}^{S} \sum_{k}^{K_s} \sum_{i_{(s_k)}}^{N_{sk}} b_{m,i_{(s_k)}} dn_{i(S_k)} - \sum_{g}^{N_g} b_{m,g} dn_g - \sum_{s}^{S} \sum_{i}^{N_{aq}} b_{m,i} dn_{i,s} \tag{6.42}$$

where the terms T_m, N_p, SS, N_{ss}, N_{aq}, N_{s_k}, E, N_e, S, K_s, N_g, n_p, n_i, n_{i_e}, $n_{p_{ss}}$, $n_{i_{(s_k)}}$, n_g, $n_{i,s}$ and b_m refer to total moles of the element in the system, the number of phases in the pure phase assemblage, the number of solid solutions in the solid-solution assemblage, the number of solid solutions, the number of aqueous species, the number of surface species for surface type s_k, the number of exchangers in the exchange assemblage, the number of exchange species for exchange site *e*, the number of surfaces in the surface assemblage, the number of surface types for surface *s*, the number of gas phase components, moles for pure phase in the pure-phase assemblage, moles of aqueous species ,moles for exchange species of exchange site *e*, moles for components in solid solution, moles for surface species for surface type s_k,

moles for gas components, moles of aqueous species in the diffuse layer of surface s and moles of element *m* per mole of each entity respectively.

The function used for charge balance, f_z, in the numerical methods is given in equation 6.43. The total derivative of f_z is given in equation 6.44.

$$f_z = \left(T_z - \sum_i^{N_{aq}} z_i n_i - \sum_s^S \sum_k^{K_s} \sum_{i(sk)}^{N_{sk}} z_{i(s_k)} n_{i(s_k)} + \sum_s^S \sum_i^{N_{aq}} z_i n_{i,s} \right) - \sum_e^E \sum_{i_e}^{N_e} z_{i_e} n_{i_e} \tag{6.43}$$

$$df_z = -\sum_i^{N_{aq}} z_i dn_i - \sum_S^S \sum_k^{K_s} \sum_{i_{(s_k)}}^{N_{S_k}} z_{i_{(s_k)}} dn_{i_{(s_k)}} - \sum_e^E \sum_{i_e}^{N_e} z_{i_e} dn_{i_e} \tag{6.44}$$

The function used for charge potential, $f_{\psi s}$, in the numerical methods is given in equation 6.45. The total derivative of $f_{\psi s}$ is given in equation 6.46.

$$f_{\psi_s} = \sqrt{8000 \varepsilon \varepsilon_0 RT} \sqrt{\mu} \sinh\left(\frac{F\psi_s}{2RT} \right) - \frac{F}{A_{surf}} \sum_k^{K_s} \sum_{i_{(s_k)}}^{N_{sk}} z_{i_{(s_k)}} n_{i_{(s_k)}} \tag{6.45}$$

$$df_{\psi_s} = \frac{\sqrt{8000 \varepsilon \varepsilon_0 RT}}{2} \frac{1}{\sqrt{\mu}} \sinh\left(\frac{F\psi_s}{2RT} \right) d\mu + \sqrt{8000 \varepsilon \varepsilon_0 RT} \sqrt{\mu} \cosh\left(\frac{F\psi_s}{2RT} \right) d \ln a_{\psi_s}$$
$$- \frac{F}{A_{surf}} \sum_k^{K_s} \sum_{i_{(s_k)}}^{N_{sk}} z_{i_{(s_k)}} dn_{i_{(s_k)}} \tag{6.46}$$

where $\varepsilon, \varepsilon_0, \psi_s, A_{surf}$, R and F refer to the dielectric constant of water (78.5, dimension-less), the permittivity of free space (8.854x10-12 $CV^{-1}m^{-1}$), the potential at the surface, surface area of the material (m^2), the gas constant (8.314$Jmol^{-1}K^{-1}$) and Faraday constant (96,493.5C/mol) respectively.

The function used for charge balance which includes surface charge and diffuse-layer charge, $f_{z,s}$, in the numerical methods is given in equation 6.47. The total derivative of $f_{z,s}$ is given in equation 6.48.

$$f_{z,s} = \sum_{k}^{K_s} \sum_{i_{(s_k)}}^{N_{s_k}} z_{i_{(s_k)}} n_{i_{(s_k)}} + \sum_{i}^{N_{aq}} z_i n_{i,s} \tag{6.47}$$

$$df_{z,s} = \sum_{k}^{K_s} \sum_{i_{(s_k)}}^{N_{s_k}} z_{i_{(s_k)}} dn_{i_{(s_k)}} + \sum_{i}^{N_{aq}} z_i dn_{i,s} \tag{6.48}$$

For a set of equations $f_i = 0$, there are x_j sets of unknowns which are solved using Newton-Raphson method by iteratively revising an initial sets of x_j values. A set of equations r_i is formulated as equation 6.48 (Parkhurst & Appelo, 1999) for the residuals of the equations for the current values of x_j.

$$r_i = -\sum_{j}^{J} \frac{\partial f_i}{\partial x_j} dx_j \tag{6.48}$$

J is total number of master unknowns for a set of linear equations which can be solved simultaneously for the unknowns, dx_j. New values of x_j are calculated for k^{th} iteration step using equation 6.49 (Parkhurst & Appelo, 1999) and then new values of r_i are calculated and if they are less than a specified tolerance limit then the process continues iteratively until convergence is achieved.

$$^{k+1}x_j = {}^{k}x_j + dx_j \tag{6.49}$$

Numerical solutions of kinetic reactions are controlled by rate equations. “Stiff” sets of equations form as a result of many geochemical kinetic reactions in which some rates are changing rapidly while others are changing slowly as the reactions unfold in time (Parkhurst & Appelo, 1999). In PHREEQC-2 Runge-Rutta algorithm is used to solve kinetic reaction equations.

Chapter Seven: Coupling procedure

7. 1 Coupled process in reactive transport

Unsaturated zone is a complex system where various physical, chemical and biological processes take place. These processes integrate in many ways and affect the reactive transport. The various coupling processes that are included in VS2DRT are:

1. Heat transport and water flow are coupled through advection of heat and the effect of temperature on viscosity and saturated hydraulic conductivity.
2. Solute transport and water flow are coupled through advection of solute
3. Solute transport and heat transport are coupled through effect of temperature on thermodynamics and chemical reaction rates

Additional coupling processes that are not included in VS2DRT are:

1. The effect of precipitation or dissolution of minerals on porosity and permeability
2. The effect of temperature and solute concentration on fluid density
3. The effect of chemical reactions on heat transport.

7.2 Operator splitting

Solute transport and chemical reactions can be coupled through global implicit method or operator splitting method. Global implicit method involves solving solute transport and chemical reactions simultaneously. The GIMRT (Steefel & Yabusaki, 1996) reactive transport model uses a global implicit approach. Operator splitting involves solving the solute transport and chemical reaction equations separately within a single time step. Sequen-

tial iterative approach (SIA), sequential non-iterative approach (SNIA) and Strang Splitting are the major operator splitting techniques. SIA involves solving the solute transport and reaction independently and iterate between the transport and chemical reaction until some sort of convergence is achieved. SIA approach is used by reactive transport models like HYDROGEOCHEM (Yeh & Tripathi, 1990) and OS3D (Steefel & Yabusaki, 1996). SNIA solves the solute transport first followed by chemical reaction of transported concentrations. PHAST (Parkhurst, Kipp, Engesgaard, & Charlton, 2004) saturated porous media reactive transport model use SNIA approach. Strang Splitting is type of SNIA method which involves solving the transport in the half time step flowed by full time step chemical reaction and followed by half time step transport.

VS2DRT uses SNIA approach and the potential problem with SNIA method is that it assumes the addition of fluid from one cell to another as being rapid enough that the reactions only begin after the physical transport is complete (Steefel & Yabusaki, 1996). SNIA introduces an operator-splitting error of the order of the time-step length and this error can be minimized by using smaller time steps (Parkhurst, Kipp, Engesgaard, & Charlton, 2004; Carrayrou, Mose, & Behra, 2004). SNIA can be mathematically expressed in equations 7.1 and 7.2 (Steefel & Yabusaki, 1996):

$$\frac{\left(C_i^{transp} - C_n^i\right)}{\Delta t} = L(C_i)^n \quad \text{for transport step} \tag{7.1}$$

$$\frac{\left(C_i^{n+1} - C_n^{transport}\right)}{\Delta t} = R_i^{n+1} \quad \text{for reaction step} \tag{7.2}$$

Schematic depiction of the coupling approach used for VS2DRT is presented in figure 7.

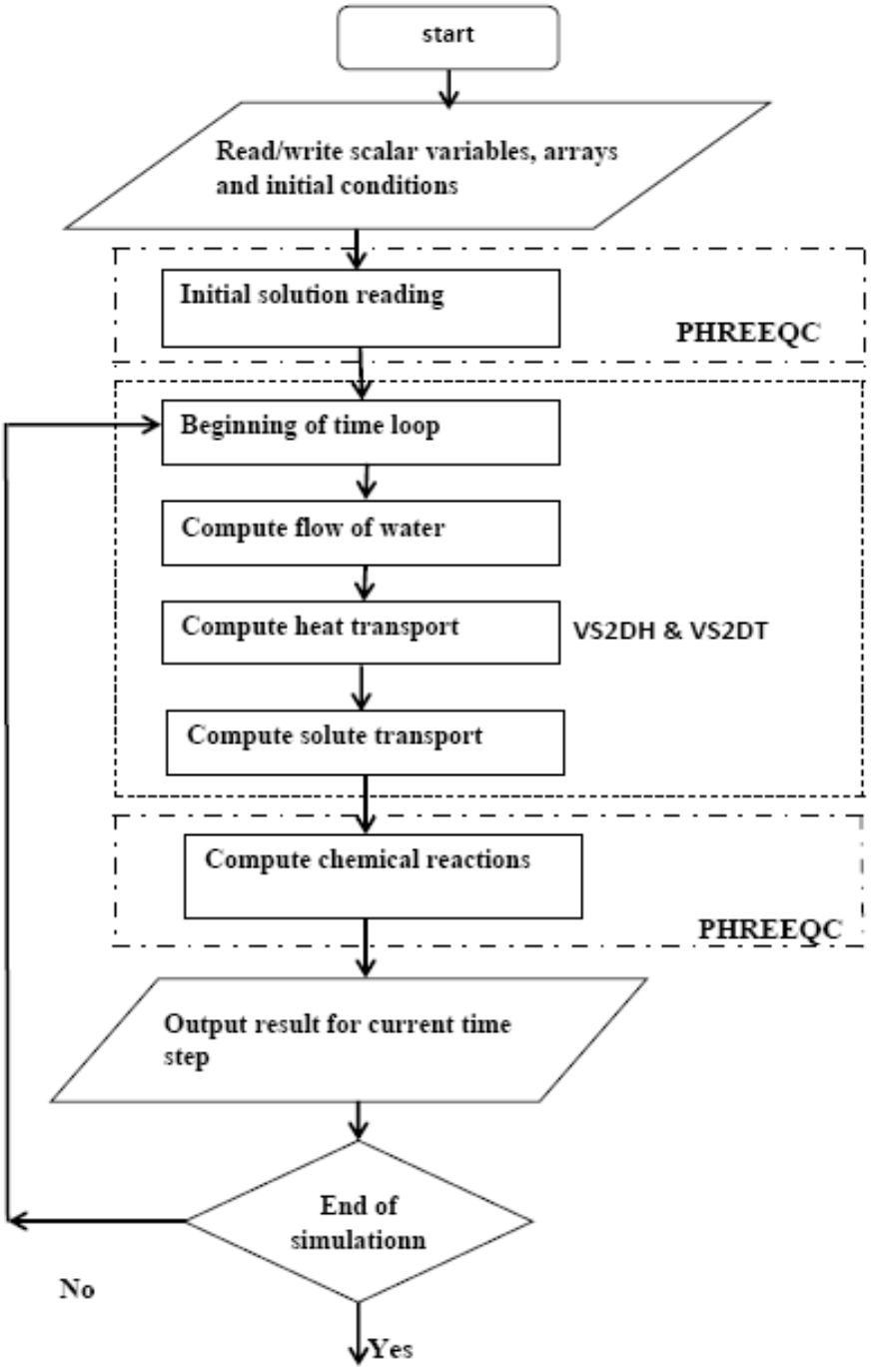

Figure 7 Schematic representation of modeling approach of coupled VS2DRT model.

Chapter Eight: Data input and output for VS2DRT

8.1 VS2DRT pre-processor for non-spatial input

To start a new VS2DRT project in Argus ONE environment one has to open Argus ONE and then click on PIEs menu and select New VS2DRT Project as shown in figure 8.1. Then a new VS2DRT pre-processor window opens to set non-spatial parameters needed by the model. In this window the user can set the units for length, time and energy to be used, choose whether to simulate heat transport, reactive solute transport, evaporation and evapo-transpiration. Additionally, it is used to set initial condition for flow, choice of hydraulic properties functions, evaporation, evapotranspiration, root-water uptake parameters, tem-poral parameters, solver parameters, chemical species, thermodynamic database choice and mass balance output options.

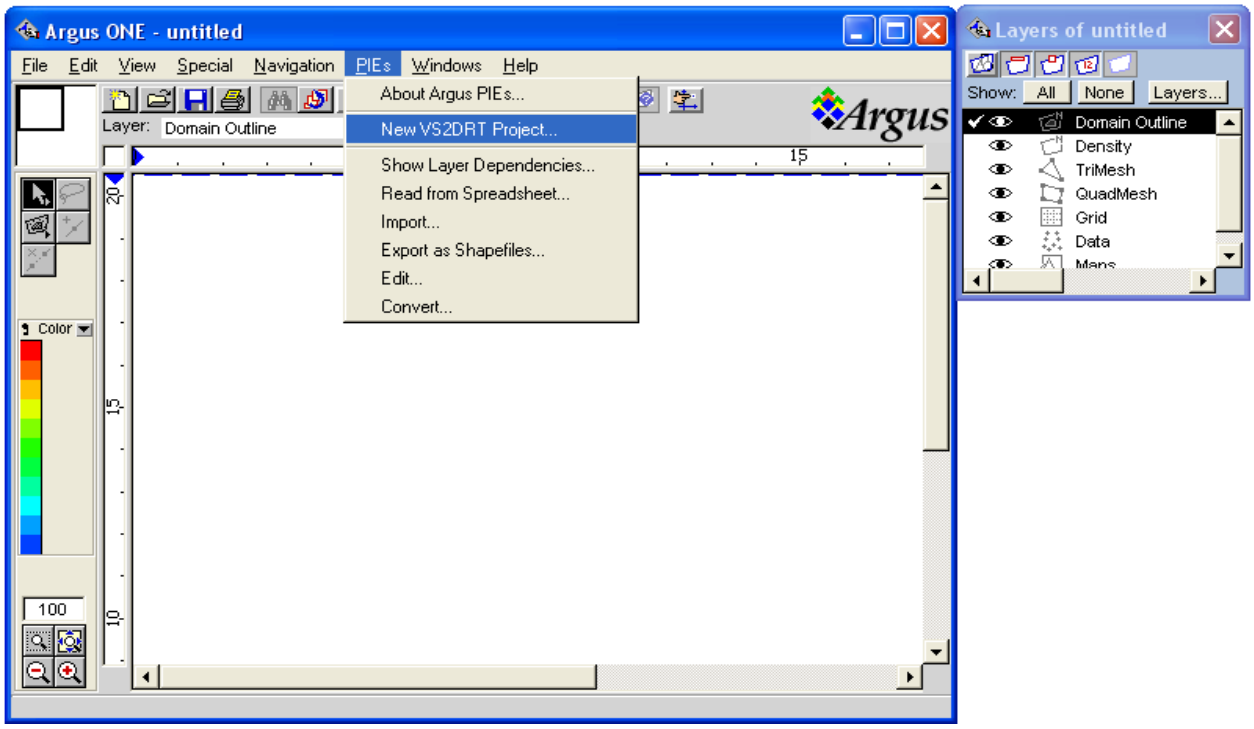

Figure 8.1 Initiating a new VS2DRT project in Argus One Environment

8.1.1 Model description

VS2DRT preprocessor consists of About, Project, Hydraulic, Recharge Periods, Evaporation, Solute, Heat, Solver, Phreeqc input and output menus which are used to set simulation options, choice of hydraulic function, recharge period parameters, solver parameters, initial and boundary solutions, solute, heat and flow mass balance output choices and general output setup. About window gives a brief information and reference to VS2DT, VS2DH and PHREEQC-2 programs which are the basis of VS2DRT program and developers contact address, see figure 8.1.1.

Figure 8.1.1 Brief description about the VS2DRT program

8.1.2 Setting simulation options

Project window shown in figure 8.1.2a is used to set general simulation options like whether to simulate heat transport, reactive solute transport, evaporation or evapotranspiration or any combination of these.

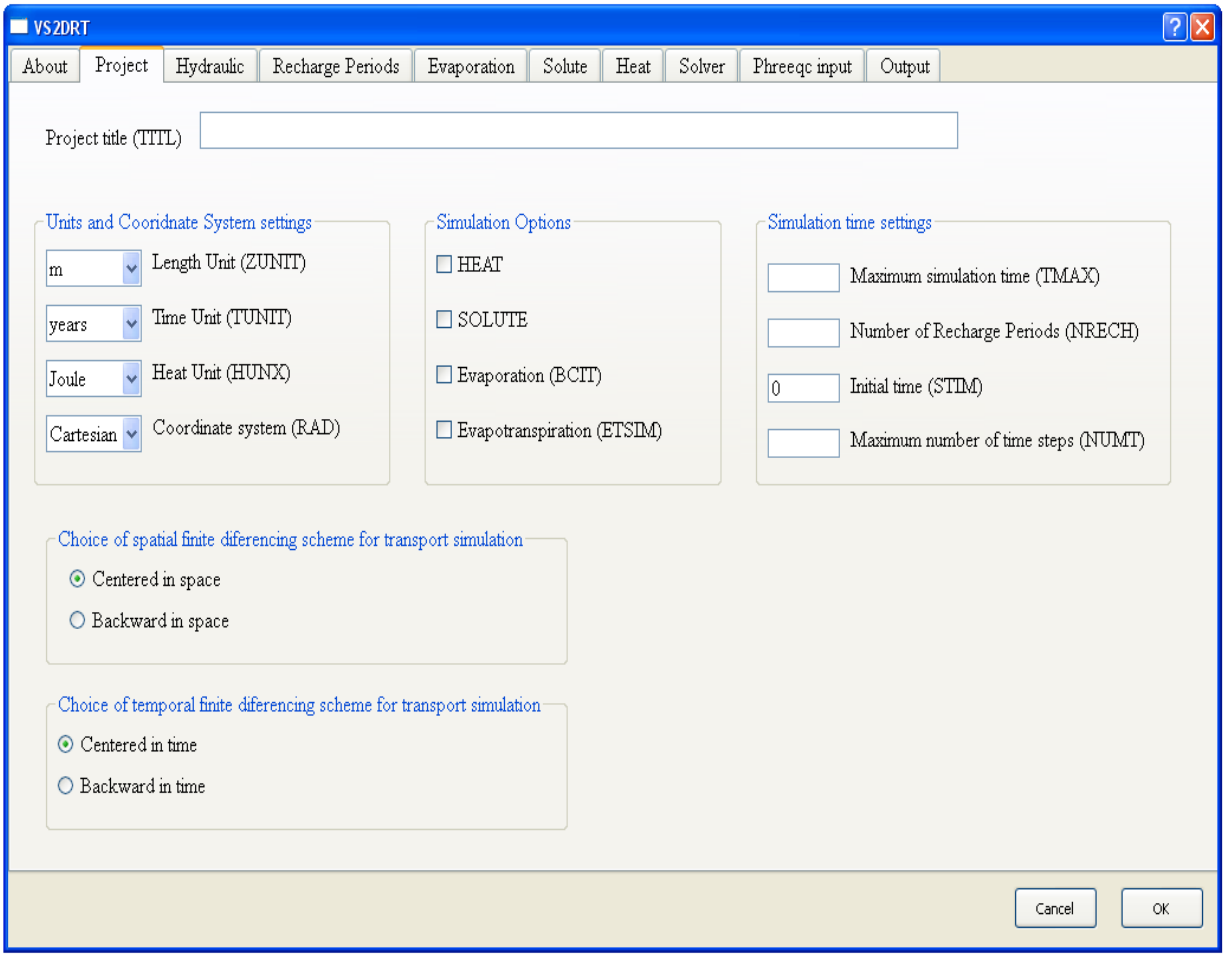

Figure 8.1.2a Setting general simulation parameters in the Project window

The inputs needed here are:

1. Title of the project

2. Geometric units for length, time, heat and available options of units are shown in figures 8.1.2b, 8.1.2c, and 8.1.2d respectively.

3. Coordinate system (Cartesian or Radian) see figure 8.1.2e.

4. Choose whether to simulate heat, solute, evaporation, evapotranspiration or any combination of them as shown figure 8.1.2f.

5. Duration of the simulation, number of recharge periods, initial time and maximum number of time steps

6. Spatial and temporal fine differencing scheme choice for transport simulation which could be centered or backward in space and centered or backward in time respectively as shown figure 8.1.2g.

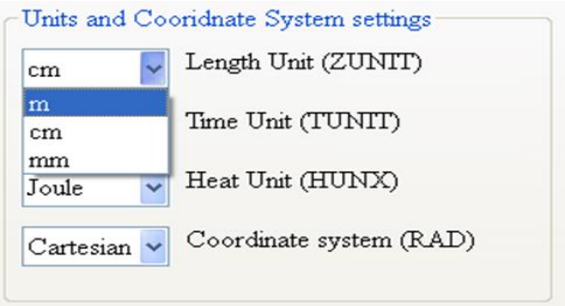

Figure 8.1.2b Choosing length unit

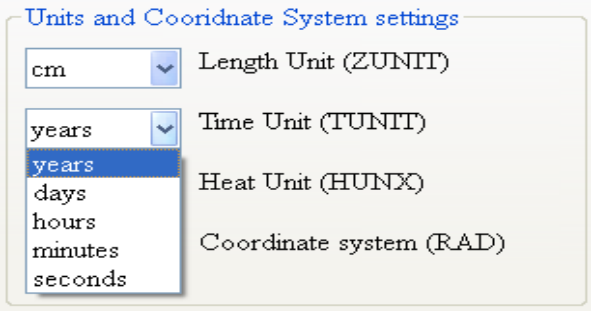

Figure 8.1.2c Choosing time unit

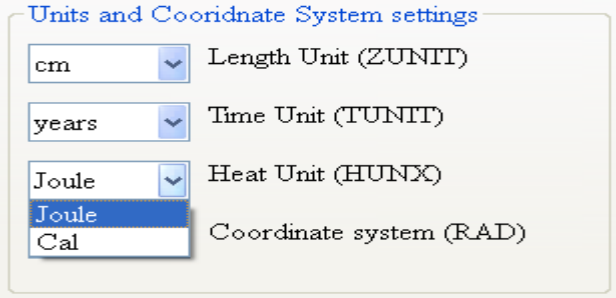

Figure 8.1.2d Choosing heat unit

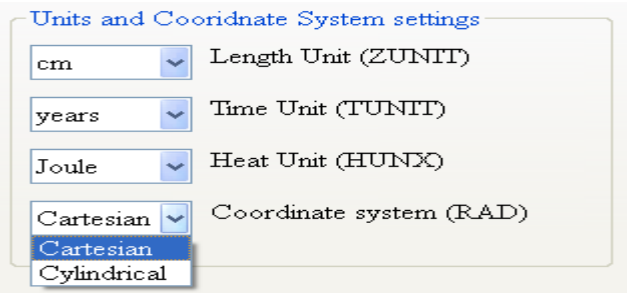

Figure 8.1.2e Choosing coordinate system

Figure 8.1.2f General simulation options for transport and flow

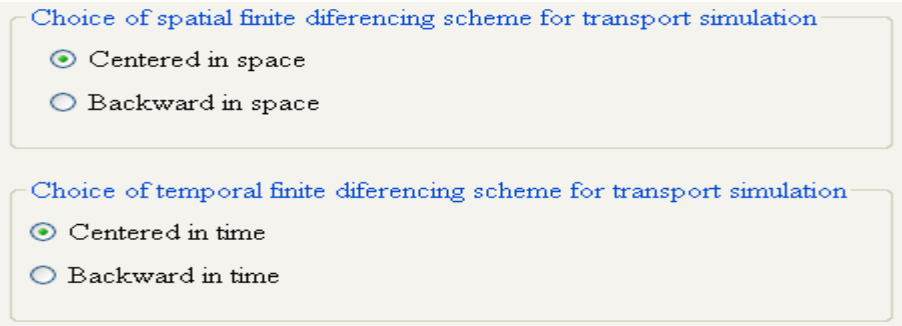

Figure 8.1.2g Choosing finite differencing option for transport simulation

8.1.3 Setting initial conduction and hydraulic properties functions choice

In the hydraulic window shown in figure 8.1.3 the user sets the initial hydraulic condition, choice of hydraulic characteristic functions and weighting function for estimating inter-cell hydraulic conductivity terms. The initial condition could be set either as equilibrium profile, pressure head or moisture content. Hydraulics characteristic functions may be based on Brooks & Corey, Van Genuchten, Haverkamp or Rossi-Nimmo. Inter-cell relative hydraulic conductivity may be estimated either using arithmetic mean, geometric mean or upstream weighting method.

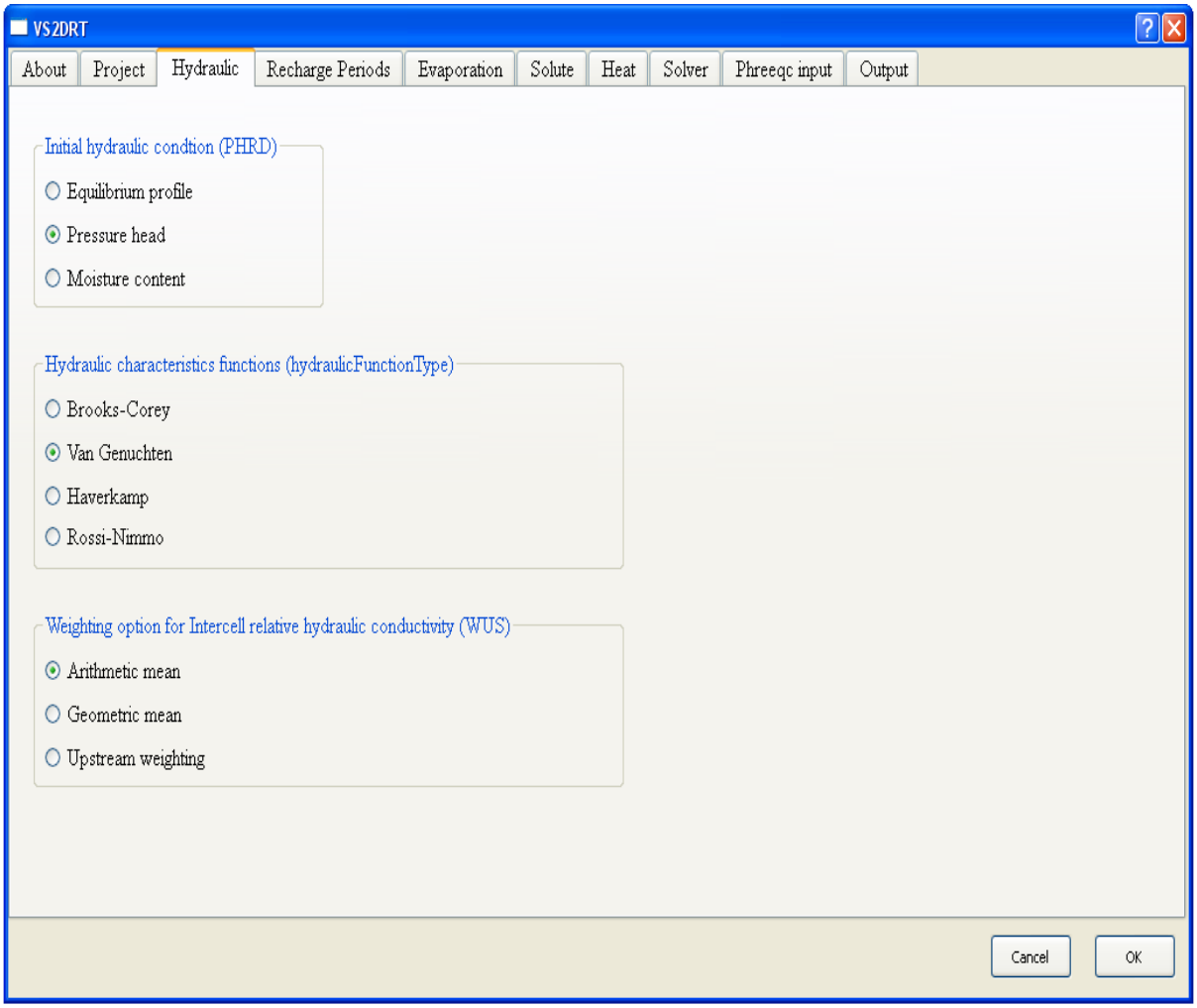

Figure 8.1.3 Setting initial conditions and hydraulic functions in Hydraulic window

8.1.4 Setting recharge period properties

Recharge Periods window is used to set recharge period parameters for each recharge period, as shown in figure 8.1.4. The recharge period parameters that need to be set for each available recharge period are:

1. Length of this recharge period (P.Length)
2. Length of initial time step for this period (DELT)
3. Multiplier for this time length (TMLT)
4. Maximum allowed time step (DLTMX)
5. Minimum allowed time step (DLTMIN)
6. Factor by which time step should be reduced in order to obtain convergence if convergence is not attained at maximum iterations (TRED)
7. Maximum allowed change in head per time step of this recharge period (DSMAX)
8. Steady state head criterion (STERR). The program assumes that steady state is reached when maximum change in head between successive time steps is less than STERR
9. Maximum allowed height of ponded water for constant flux nodes (POND)
10. Print heads, concentrations, temperature, moisture content and /or saturation to output file after each time step (PRNT= true). Enter 1 for true and 0 for false

11. Simulate seepage faces for this recharge period (SEEP). Enter 1 for true and 0 for false

12. Simulate evaporation for this recharge period (BCIT). Enter 1 for true and 0 for false

13. Simulate evapotranspiration for this recharge period (ETSIM). Enter 1 for true and 0 for false

The add button is used to add recharge periods, the clear button is used to clean the content of recharge table and the delete button is used delete a single row of a recharge period. Note that the number of rows in the recharge period must be equal to the number of recharge periods and filled with value. Leaving a recharge period cell empty will cause error on the program. One can use the horizontal bar as well as vertical bars to go through the recharge periods table.

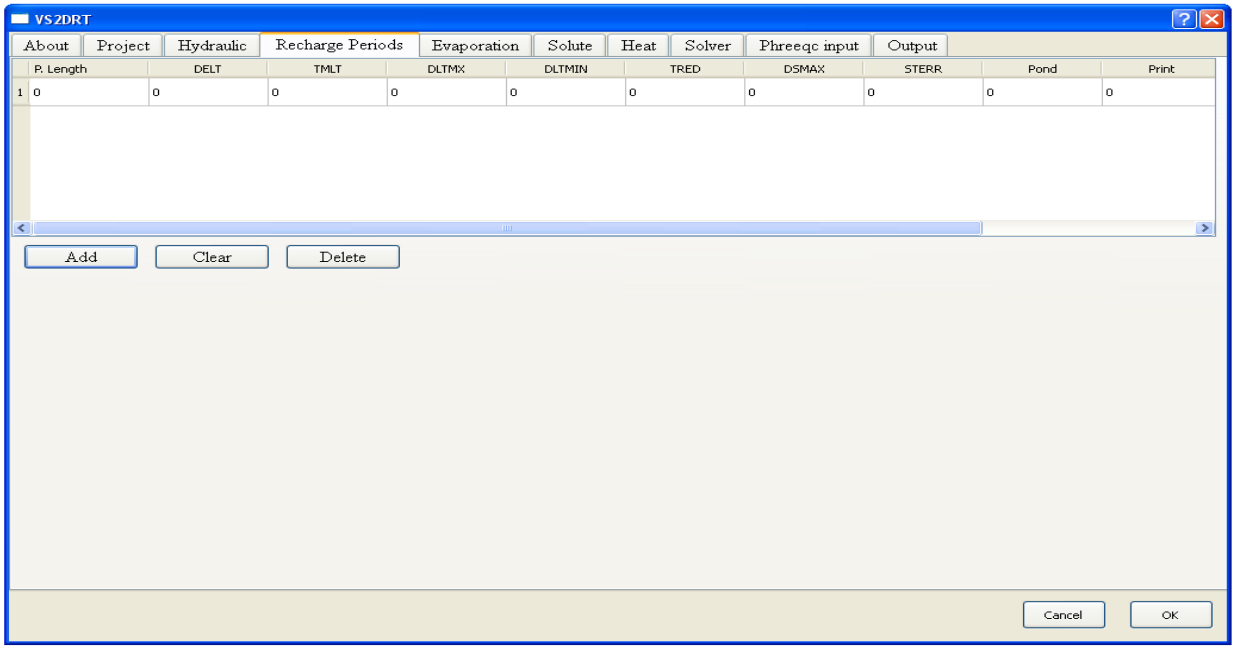

Figure 8.1.4 Recharge period window to input recharge period parameters

8.1.5 Setting evaporation parameters

By default the evaporation window is inactive as shown in figure 8.1.5a and it would get activated if evaporation or evapotranspiration or both of them are selected to be simulated in project widow figure 8.1.5b. Parameters that are needed in evaporation table are evaporation period number (period), potential evaporation rate (PEVAL), surface resistance to evaporation (SRES) and pressure potential of the atmosphere (HA) at the beginning of each evaporation period (figure 8.1.5c). The add button is used to add an evaporation period, the clear button is used to clean the content of evaporation table and the delete button is used delete a single row of evaporation period. Leaving an evaporation period cell empty will cause an error of the program. One can use the horizontal bar as well as vertical bars to go through the evaporation periods table.

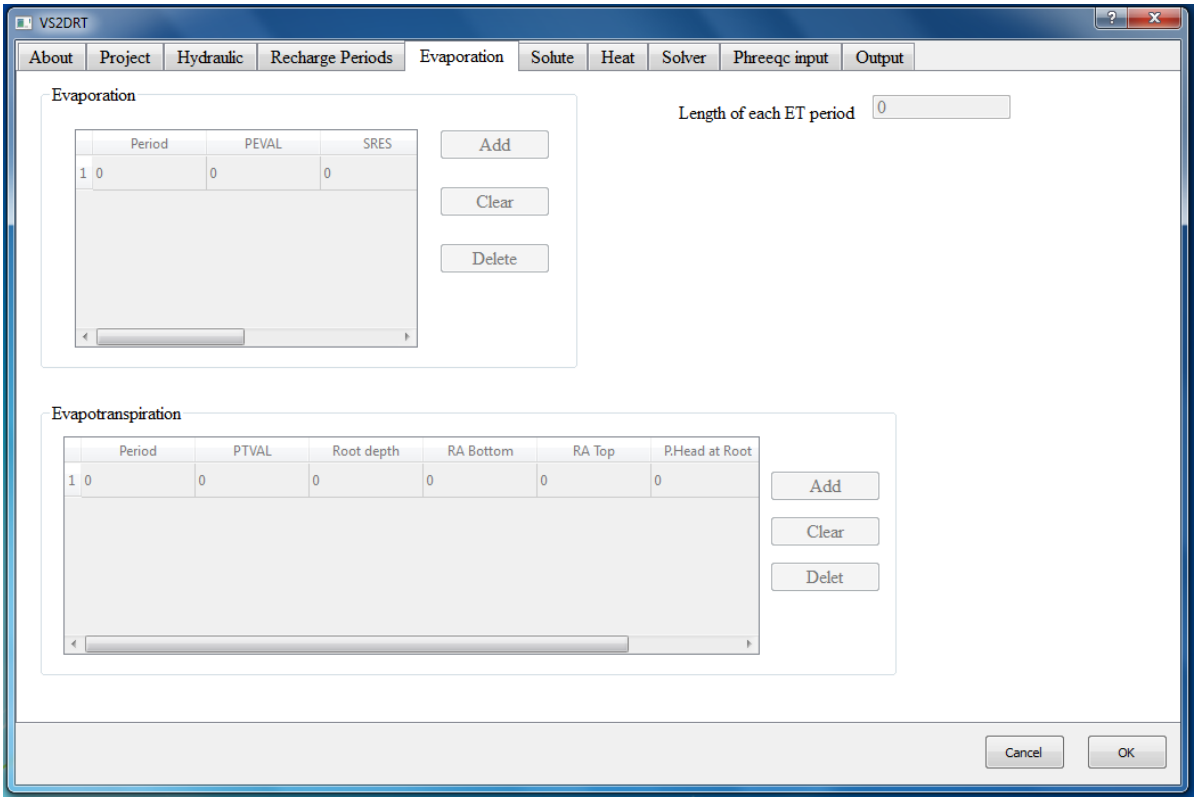

Figure 8.1.5a Inactive evaporation window

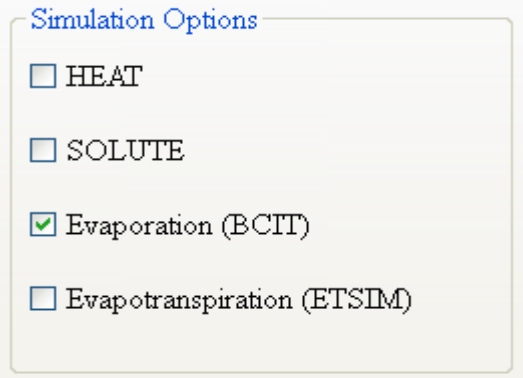

Figure 8.1.5b Selecting evaporation to be simulated in the project widow

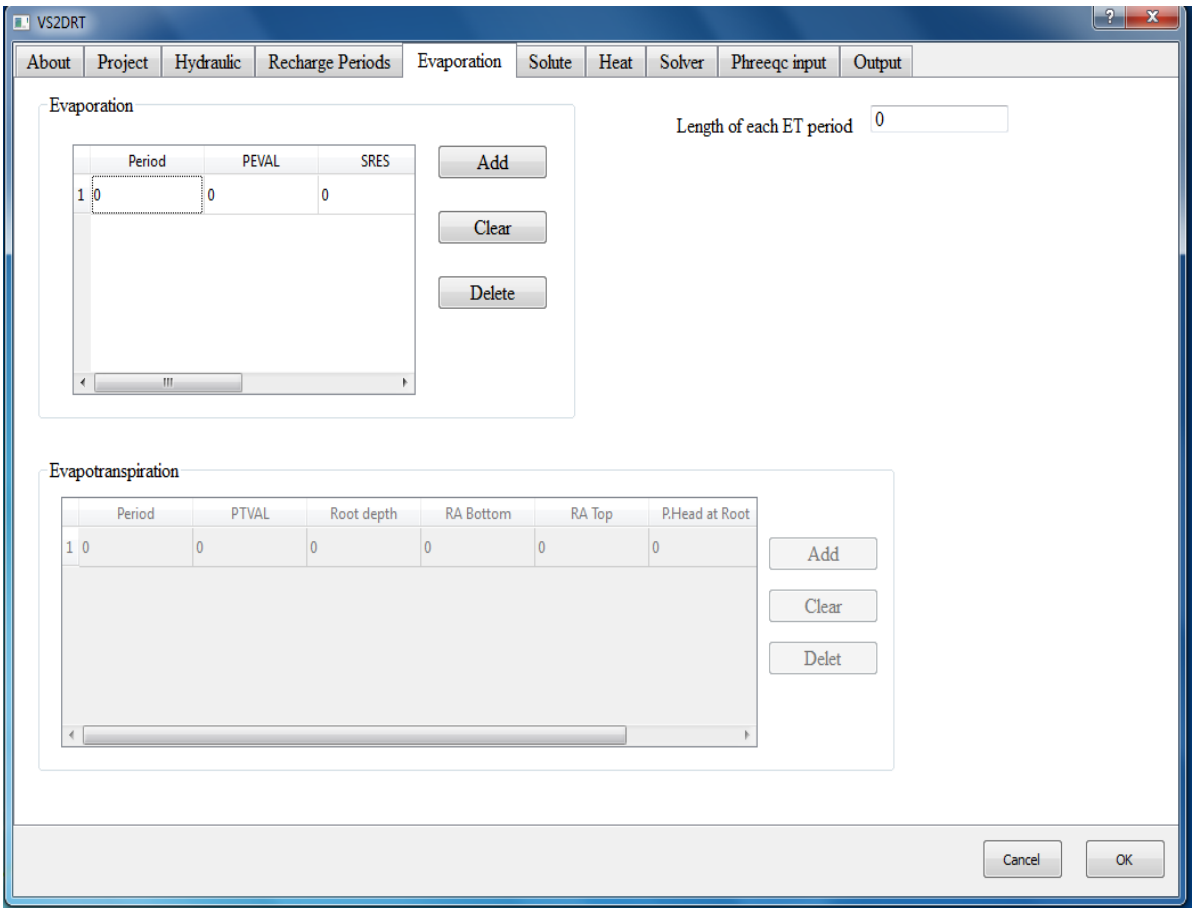

Figure 8.1.5c Activated evaporation table in the evaporation window

8.1.6 Setting evapotranspiration parameters

By default the evapotranspiration table is inactive (figure 8.1.5a) and it gets activated if evapotranspiration is selected to be simulated in the project widow as shown figure 8.1.6a. Parameters that are needed in evapotranspiration table are evapotranspiration period number (Period), potential evapotranspiration rate (PTVAL), root depth, root activity at the base of the root zone (RA Bottom), root activity at top of root zone (RA Top) and pressure head in roots (P.Head at Root) at the beginning of each evaporation period (figure 8.1.6b).

The add button is used to add evapotranspiration period, the clear button is used to clean the content of evapotranspiration table and the delete button is used delete a single row of evap-otranspiration period. Leaving an evapotranspiration period cell empty will cause error on the program. One can use the horizontal bar as well as vertical bars to get evapotranspiration periods.

Figure 8.1.6a Selecting evapotranspiration in the project window

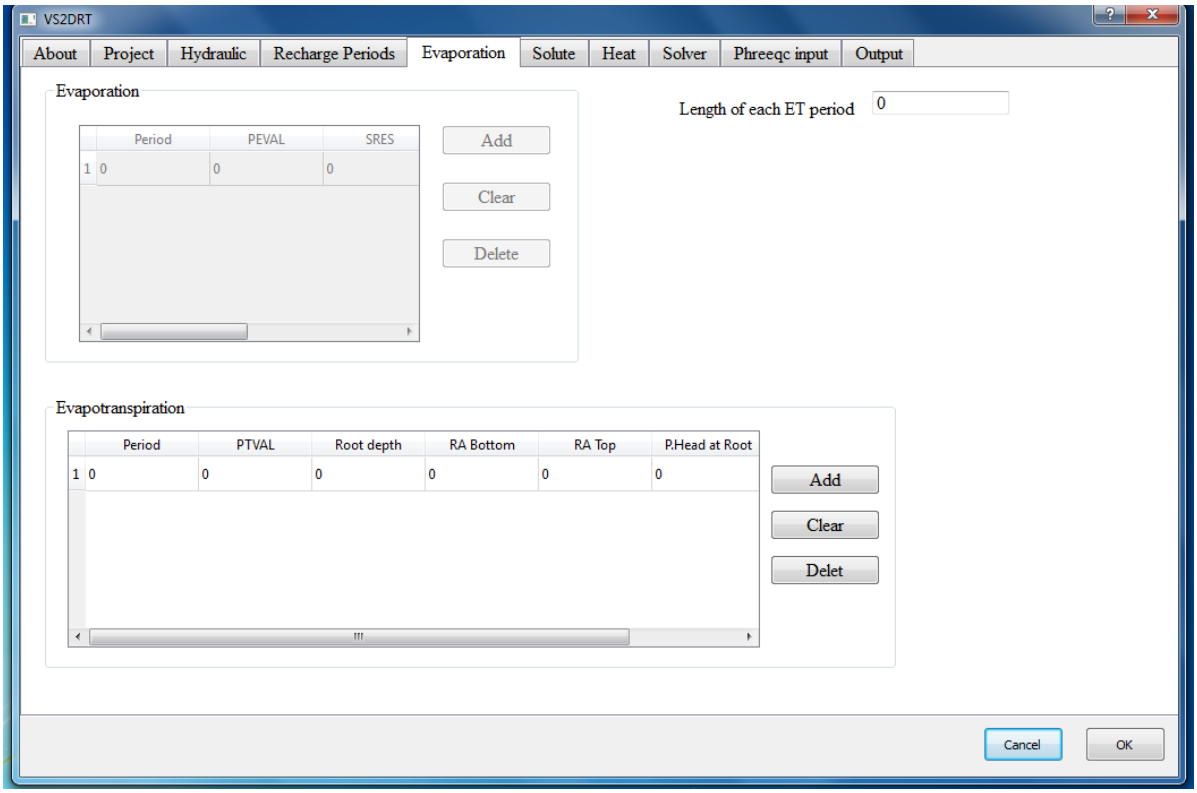

Figure 8.1.6b Activated evapotranspiration table in the evaporation window

In case of simulating both evaporation and evapotranspiration as shown in figure 8.1.6c both evaporation and evapotranspiration tables get activated as shown in figure 8.1.6d.

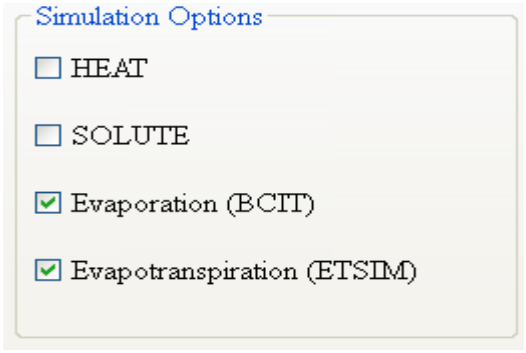

Figure 8.1.6c Selecting evaporation and evapotranspiration options

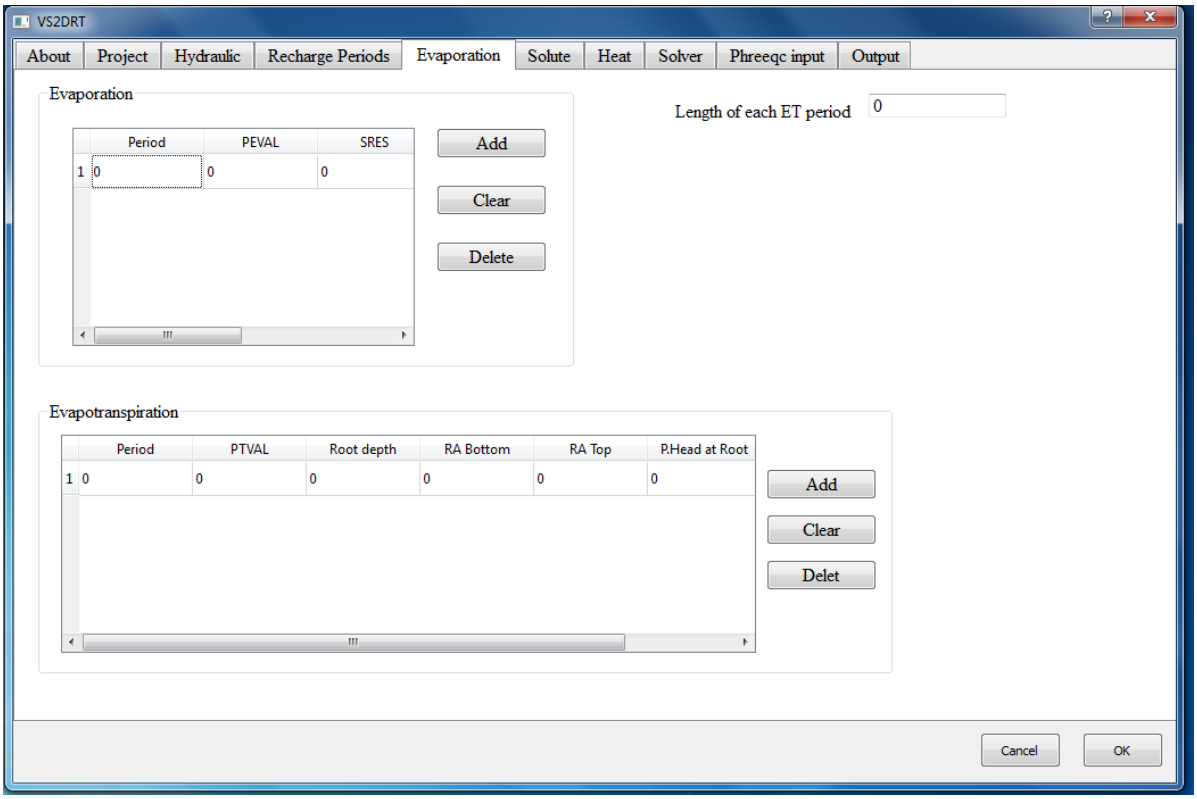

Figure 8.1.6d Activated evaporation and evapotranspiration table in the Evaporation window

8.1.7 Setting reactive transport simulation

In order to simulate reactive transport solute option should be selected in the project window as shown in figure 8.1.7a. The thermodynamic database needed by geochemical model PHREEQC has to be defined in solute window as shown in figure 8.1.7b. The phreeqc.dat is the default database and should be available in each project folder. The user could use other database files as well. Solute mass balance components to be written to output files could be selected in the solute window as shown in figure 8.1.7b as well.

The initial and boundary condition solutions and various equilibrium and kinetic reactions has to be defined in the Phreeqc input window and saved to project folder where the data-base file is also saved (figure 8.1.7c). The solutions and various chemical reactions should

be written according PHREEQC input format and the user should refer to the PHREEQC manual.

Figure 8.1.7a Selecting solute in the Project window

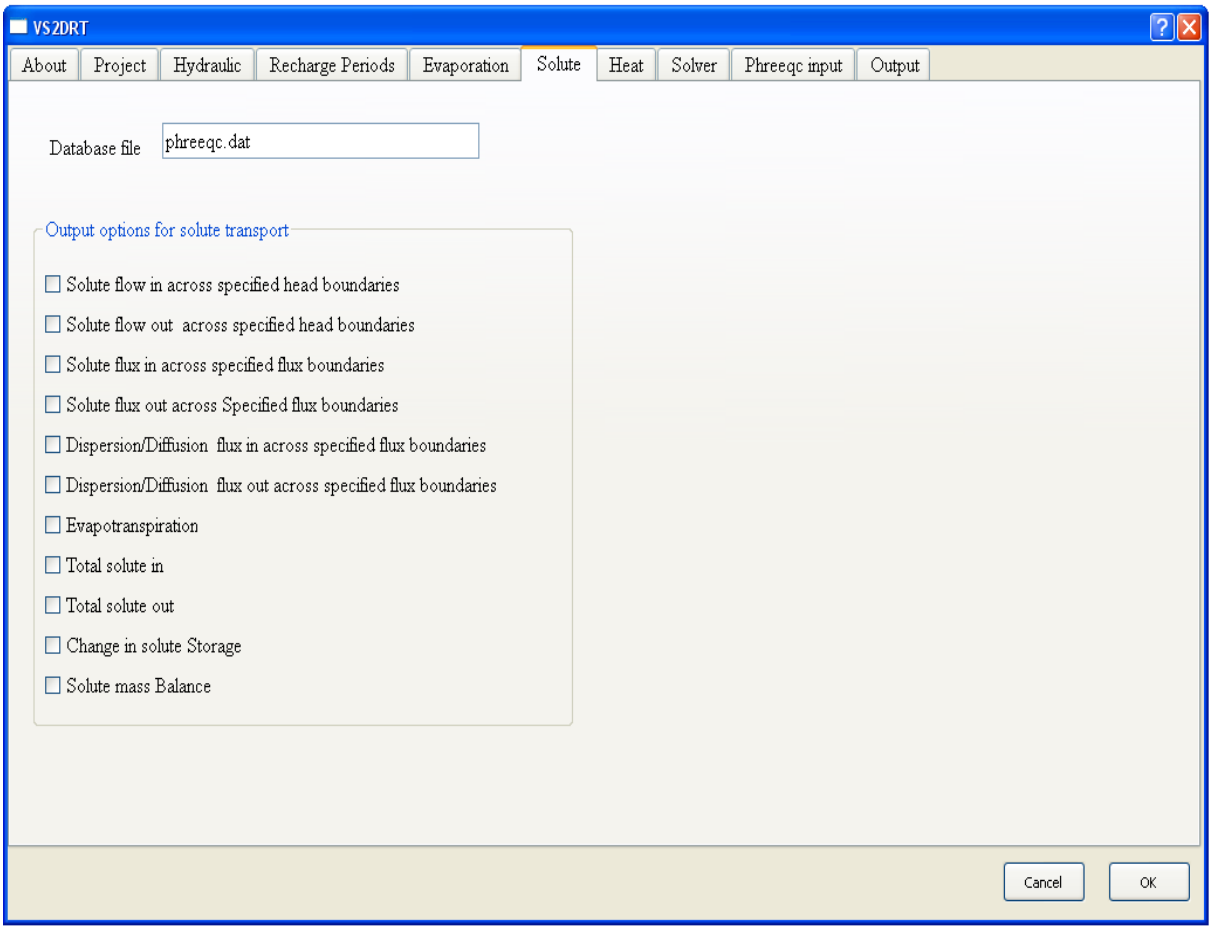

Figure 8.1.7b Database file name and selecting solute mass balance output in the Solute window

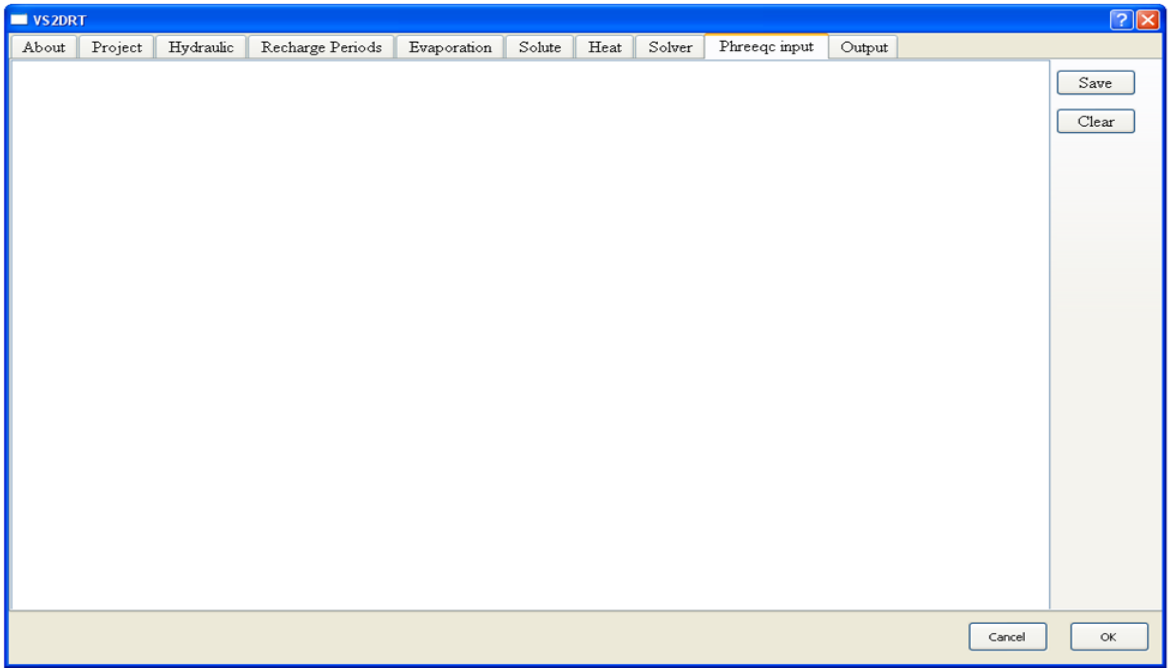

Figure 8.1.7c Phreeqc input window to set initial and boundary solutions and various chemical reactions

8.1.8 Setting heat transport

To simulate heat transport the heat option in project window has to be selected and heat unit has to be set as shown in figure 8.1.8a. The heat mass balance components could be selected in Heat window as presented in figure 8.1.8b.

Figure 8.1.8a Selecting heat transport option in the project window

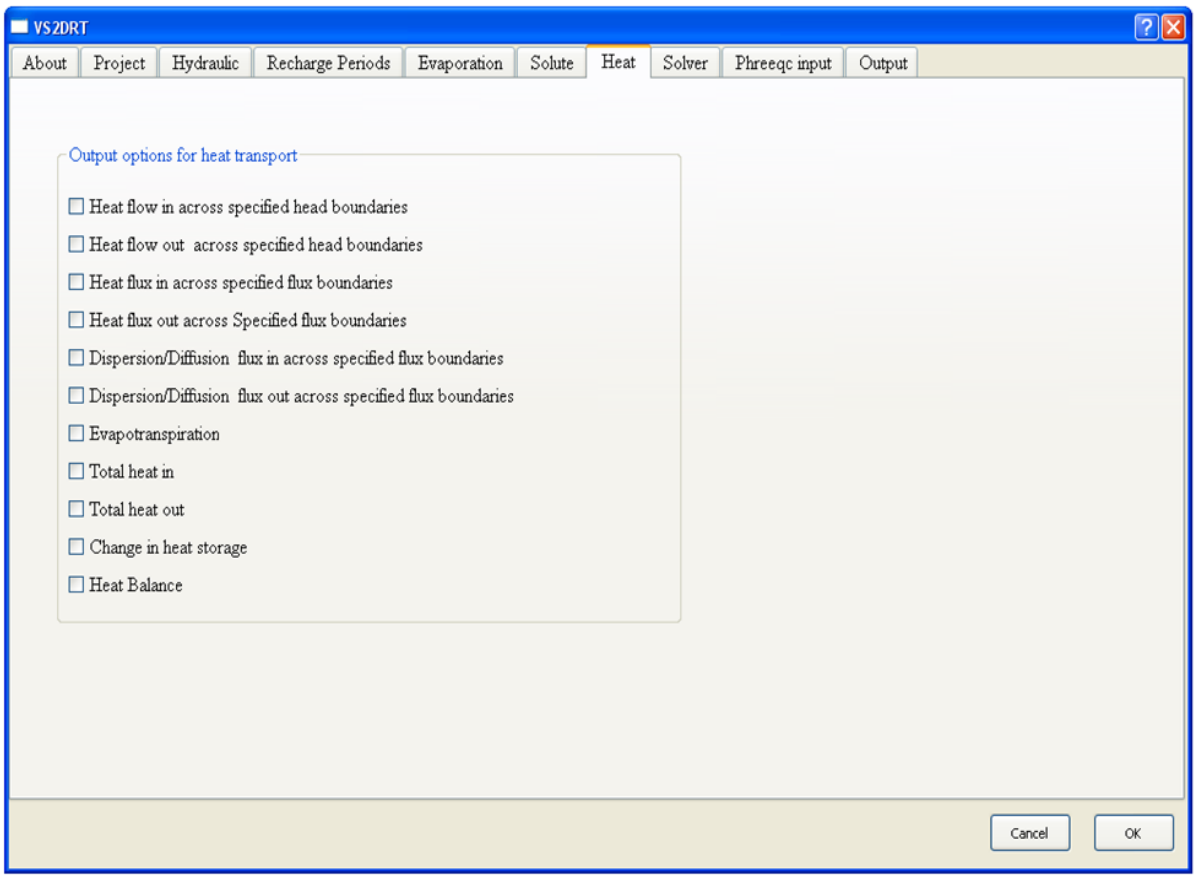

Figure 8.1.8b Heat mass balance selection in the Heat window

8.1.9 Setting solver parameters

Solver window is used to set solver parameters needed to solve flow, heat and solute transport equations (figure 8.1.9). These parameters are:

1. Relaxation parameter for iterative solution (HMAX)
2. Minimum number of iterations per time step (MINIT)
3. Maximum number of iterations per time step (ITMAX)
4. Head closure criterion (EPS)
5. Temperature closure criterion (EPS1)

6. Velocity closure criterion (EPS2)

7. Solute closure criterion (EPS3)

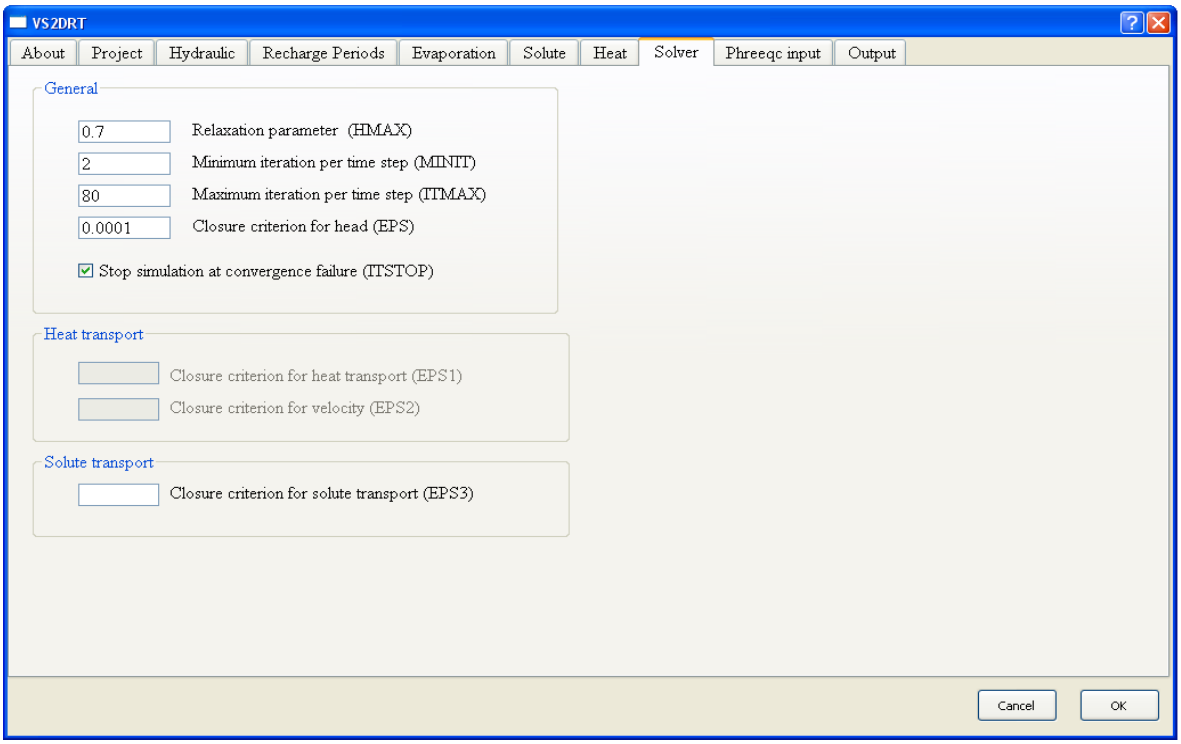

Figure 8.1.9a Solver window to set solver parameters

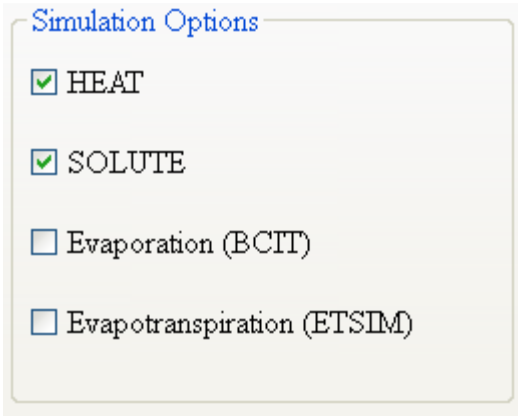

Figure 8.1.9b Setting simulation to simulate heat and reactive transport

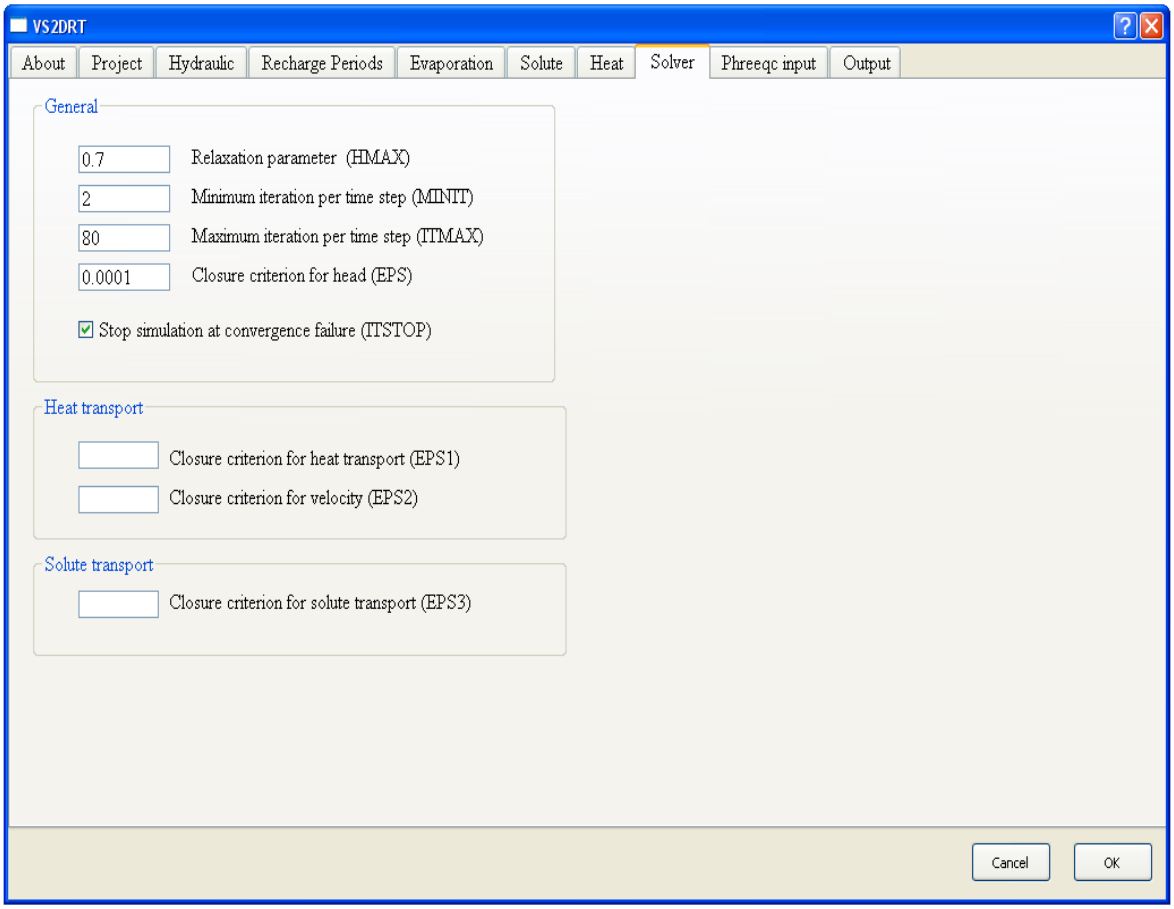

Figure 8.1.9c Setting solver parameters for flow, heat and reactive transport

8.1.10 Setting output potions

The output window is used to determine whether pressure head, total head, volumetric moisture content, saturation, velocity, temperature and chemical constitutes are written to output files at print times. It is also used to specify whether mass balance components should be written to output files at print time or at each time step. Observation point values of pressure head, total head, volumetric moisture content, saturation, velocity, temperature and chemical constitutes may be written to output files at print times or at each time step.

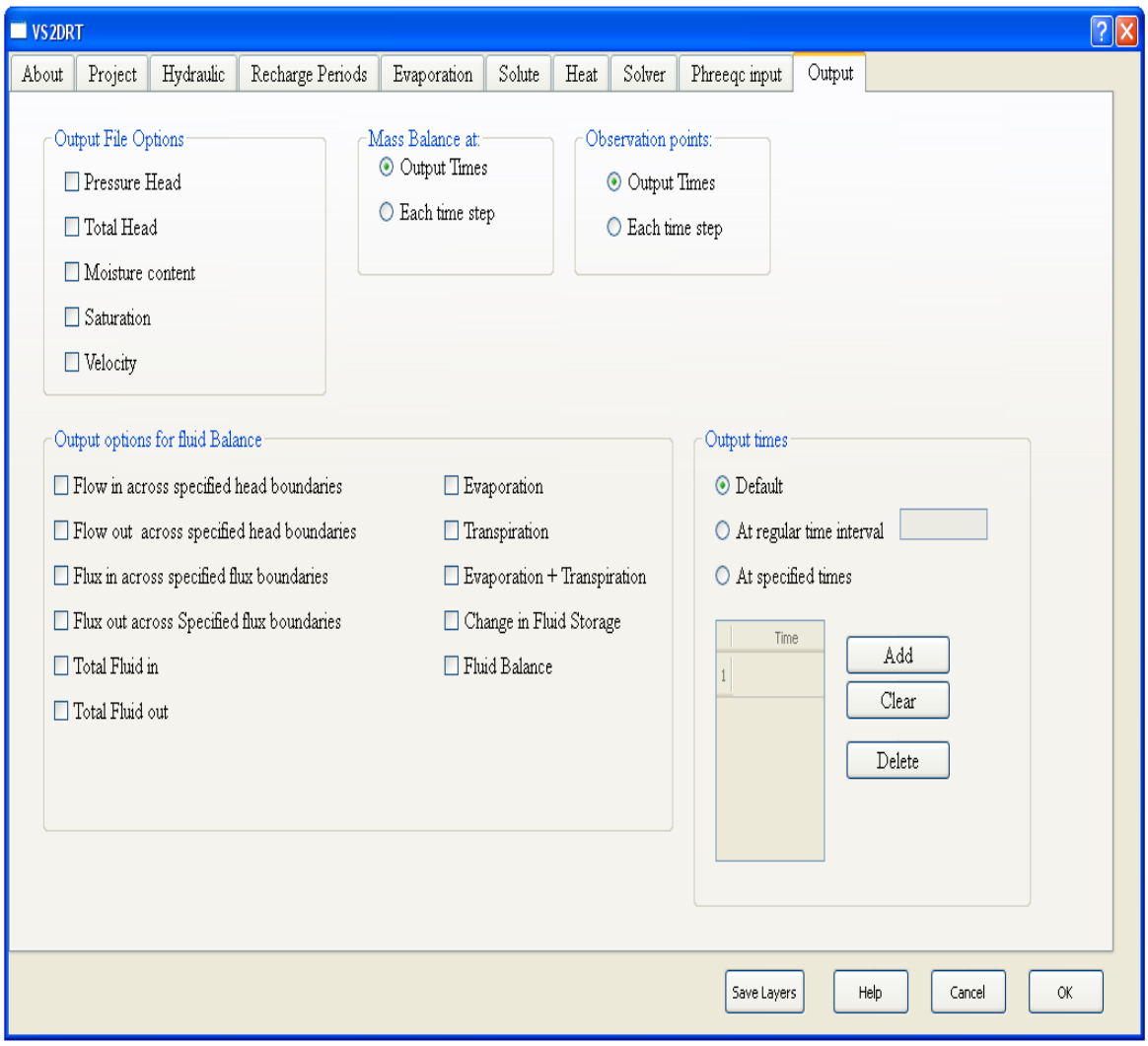

Figure 8.1.10 Output window to set out options and time

8.2 VS2DRT pre-processor for spatial input

Spatial parameters needed for the simulation should be set using VS2DRT pre-processor for spatial input in Argus ONE environment (figure 8.2). VS2DRT pre-processor for spatial input window is created based on the spatial layers created at the end of VS2DRT pre-processor for non-spatial input.

The spatial layers that are used in VS2DRT are:

1. Domain outline
2. Grid density
3. VS2DRT Grid
4. Textural class
5. Equilibrium profile/initial pressure head/initial moisture content
6. Initial Solution
7. Initial temperature
8. Boundary conditions
9. Observation points
10. Source_sink
11. Data
12. Outputs

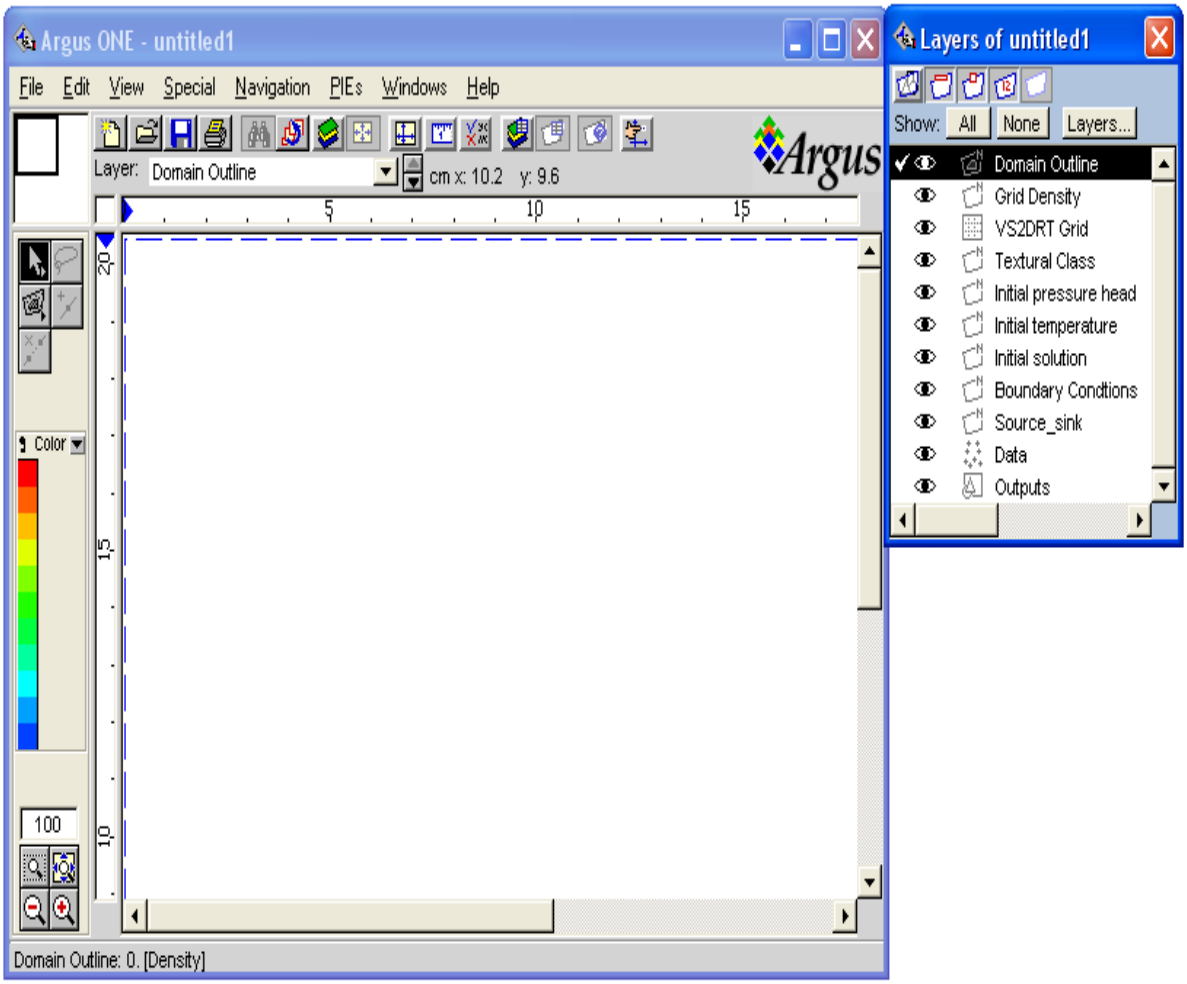

Figure 8.2 VS2DRT pre-processor for spatial input in Argus ONE environment

8.2.1 Simulation domain outline

The spatial domain of interest for the simulation should be outlined in the domain outline layer. Before drawing the domain of interest drawing size and scale and units of the simulation should be set using Argus ONE features. To set drawing size click on special menu and then select Drawing size as shown in figure 8.2.1a and a Drawing size window appears as presented in figure 8.2.1b.

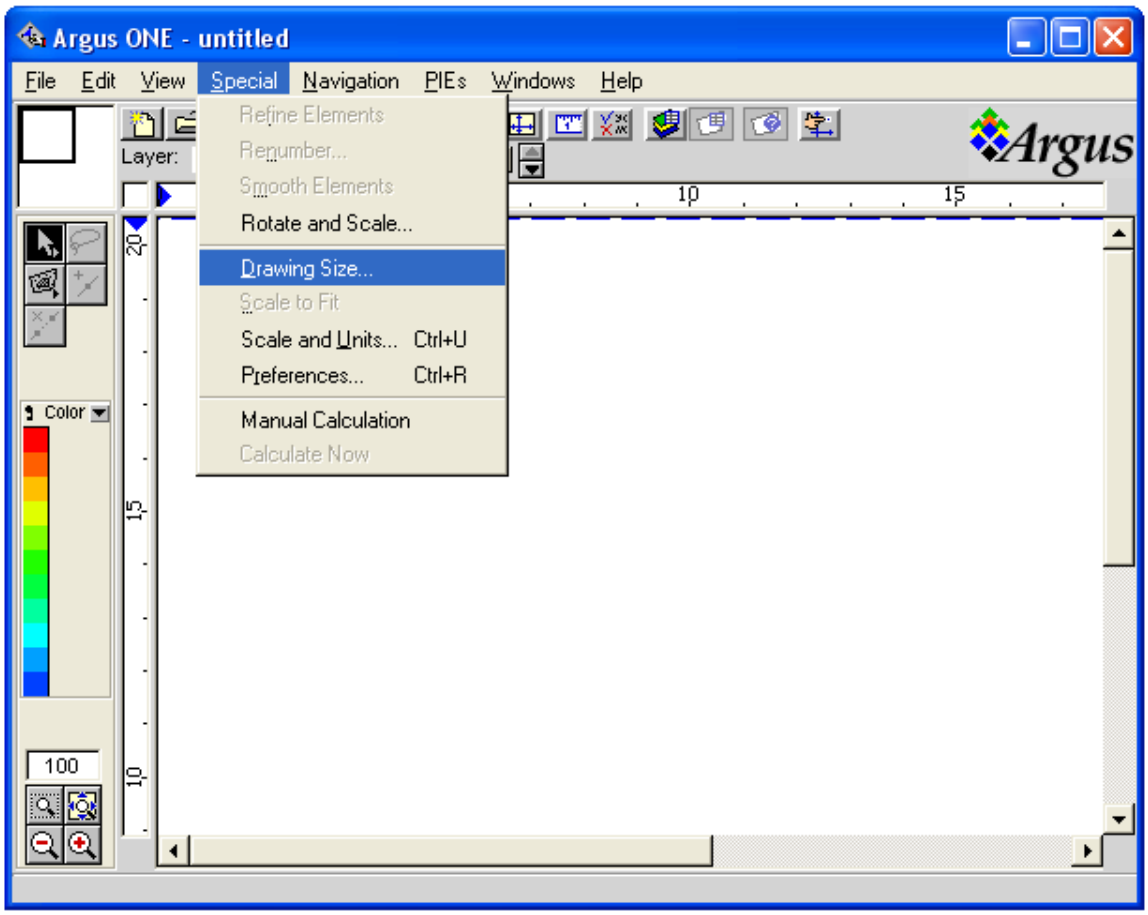

Figure 8.2.1a Schematic representation of selecting drawing size.

To set scale and units click on special menu as show in figure 8.2.1c and select scale and snits and then scale and units window appears as shown in figure 8.2.1d.

To draw domain of interest make sure the current layer is domain outline layer. Then select closed contour by clicking on the closed contour menu as shown in figure 8.2.1e. After drawing a domain of interest Information contour window will appear to set the value of grid density as shown in figure 8.2.1g.

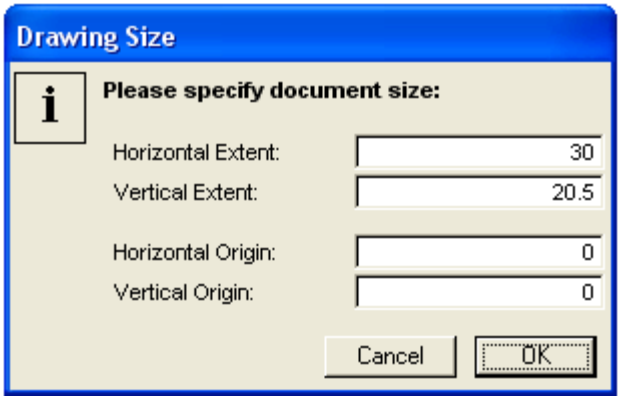

Figure 8.2.1b Drawing size window

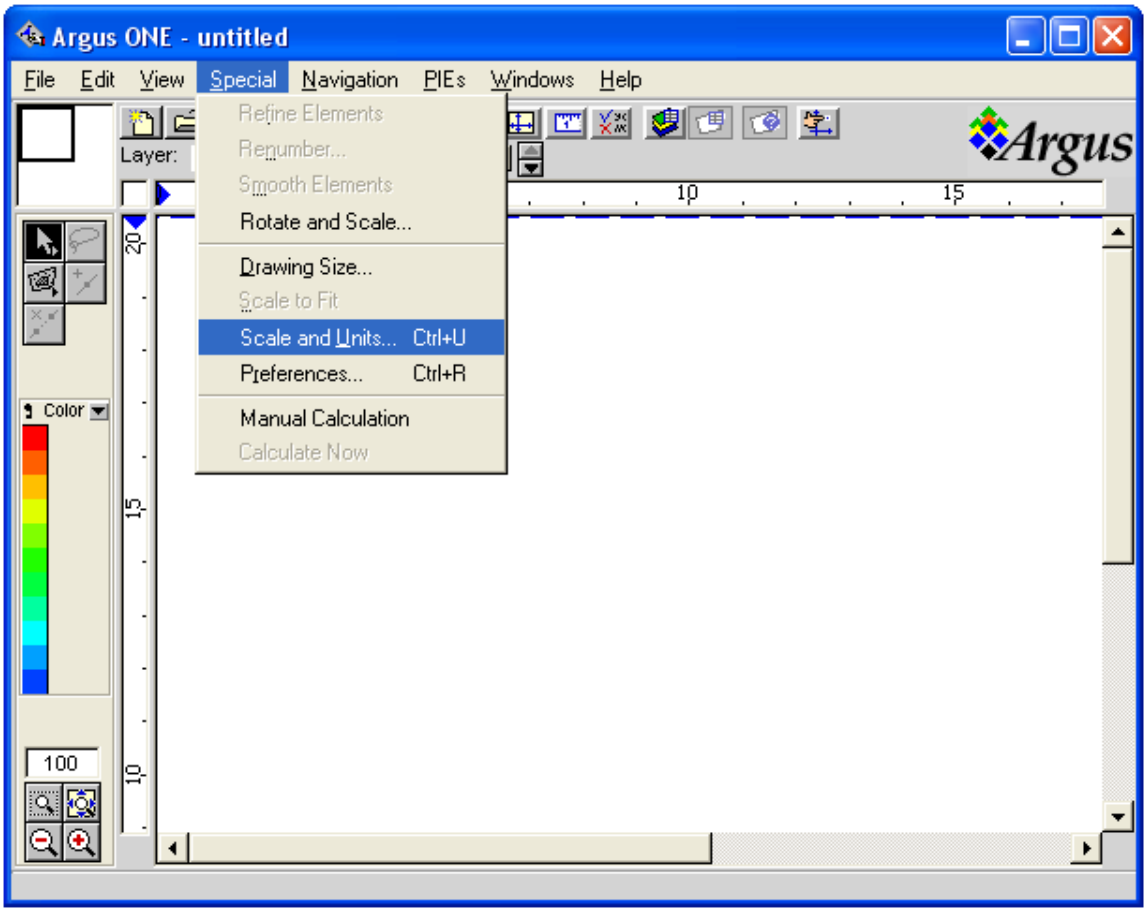

Figure 8.2.1c Schematic representation of selecting scale and units

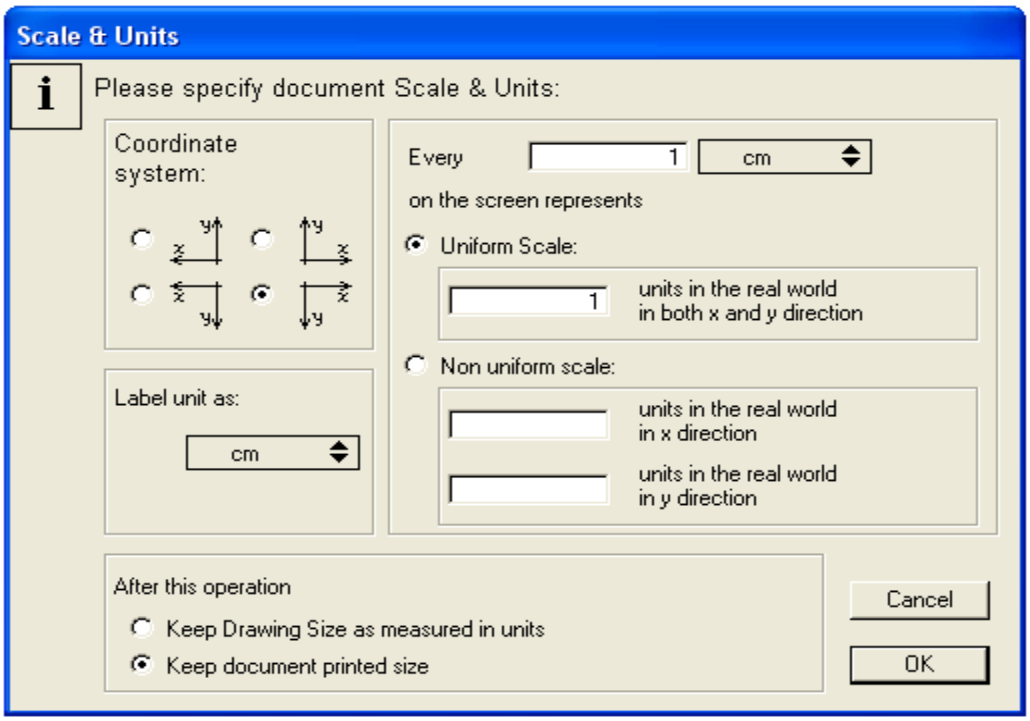

Figure 8.2.1d Scale and units window

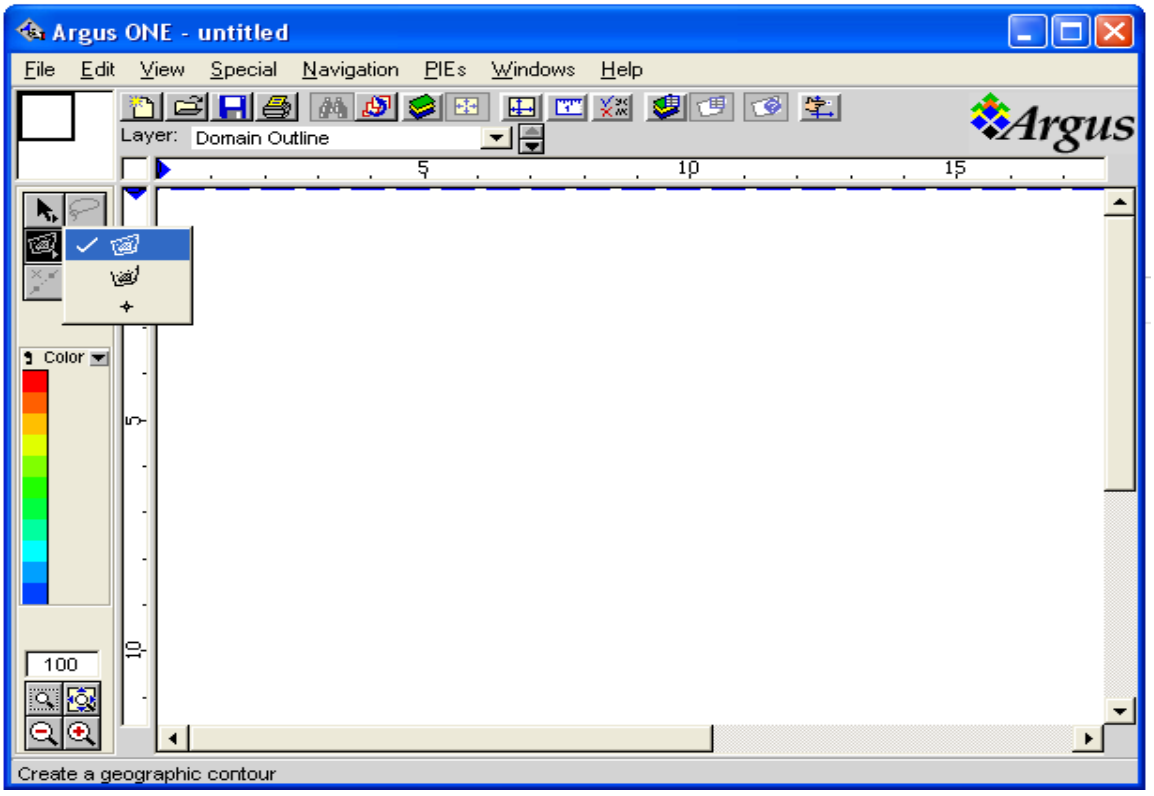

Figure 8.2.1e Selecting closed contour tool to draw the domain of interest

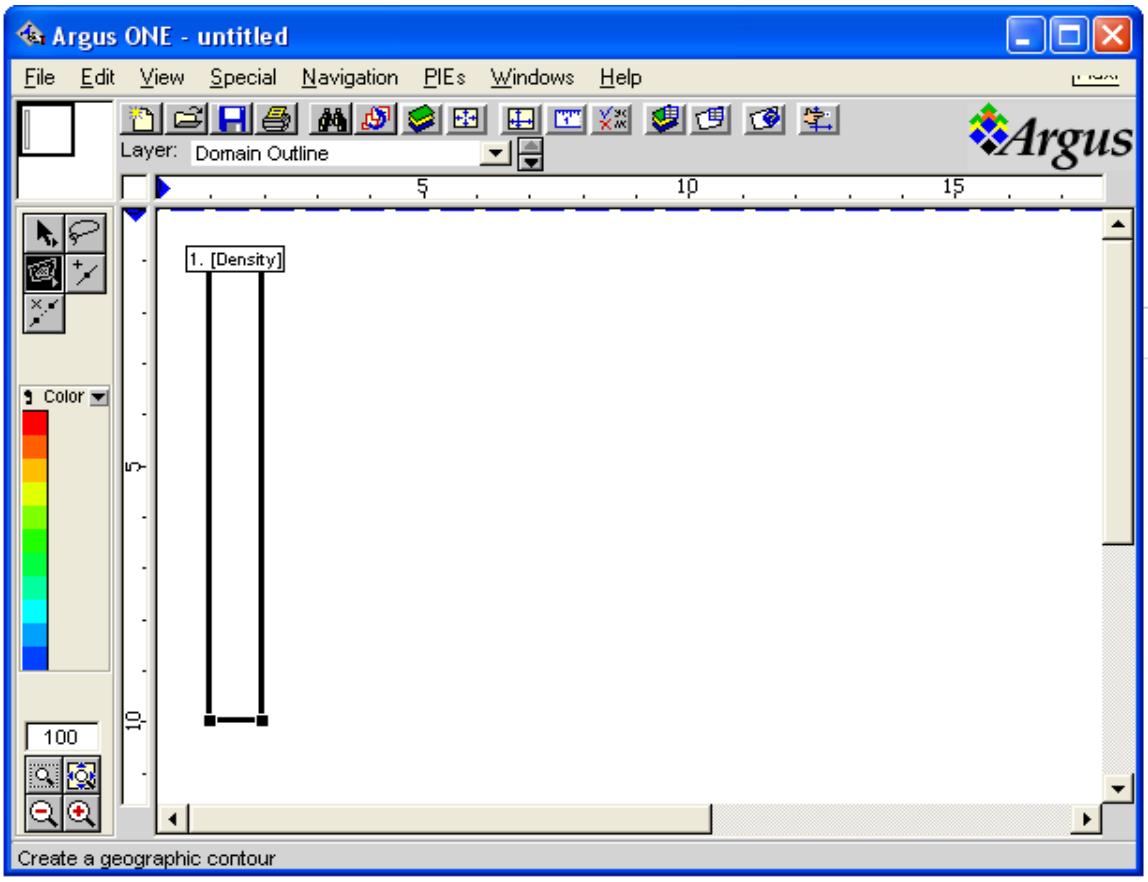

Figure 8.2.1f Schematic representation of domain of interest

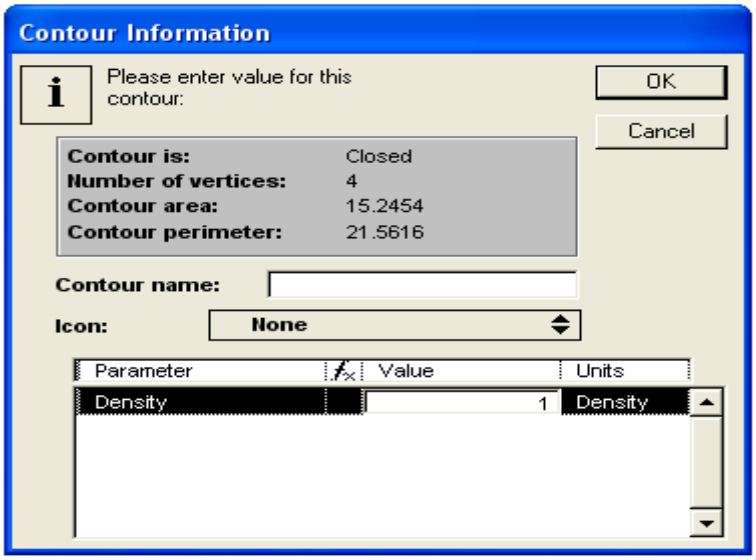

Figure 8.2.1g Schematic presentation of setting grid density value for domain of interest.

8.2.2 VS2DRT Grid

Spatial discretization of domain of interest would be done in VS2DRT Grid layer using Argus ONE finite difference grid module. Select "Magic Wand tool" as shown in figure 8.2.2a and click on the domain of interest outlined and a grid angle window appear as shown in figure 8.2.2b. Set angle of inclination of the grid and click ok. Automatically a grid will be generated as shown in figure 8.2.2c and could be edited by adding or deleting rows, columns using Argus ONE delete and insert menus as shown in figure 8.2.2d and 8.2.2e respectively.

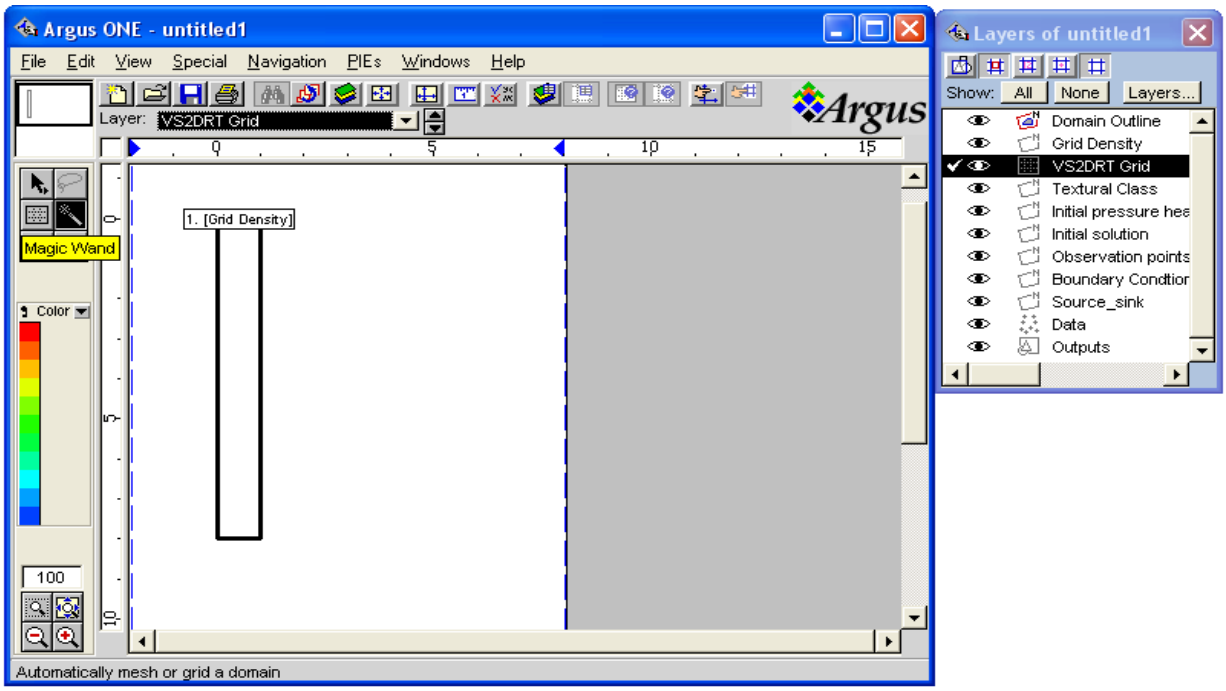

Figure 8.2.2a Schematic representation of selecting Magic Wand tool to generate grid in VS2DRT Grid layer window

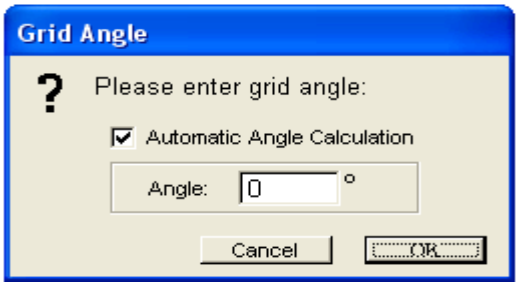

Figure 8.2.2b Grid angle window

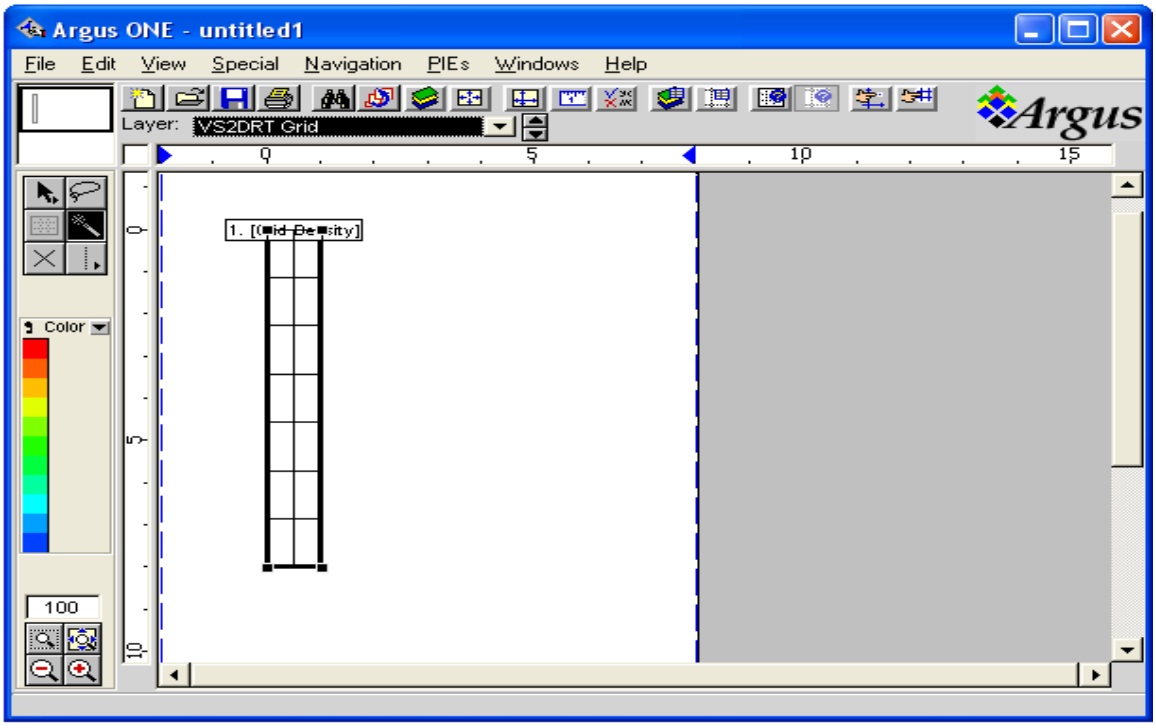

Figure 8.2.2c Schematic representation of grid generated by Magic Wand tool

To insert desired number of rows for 1D simulation one can use row insert tool as shown in figure 8.2.2e and drag it on domain of interest and Grid line generation window opens. Grid line generation windows is used to set required number of row using row spacing or number of rows by selecting distance or count respectively as shown in figure 8.2.2f. Based on the setting on grid line generation windows automatically a new girds will be generated as shown in figure 8.2.2g.

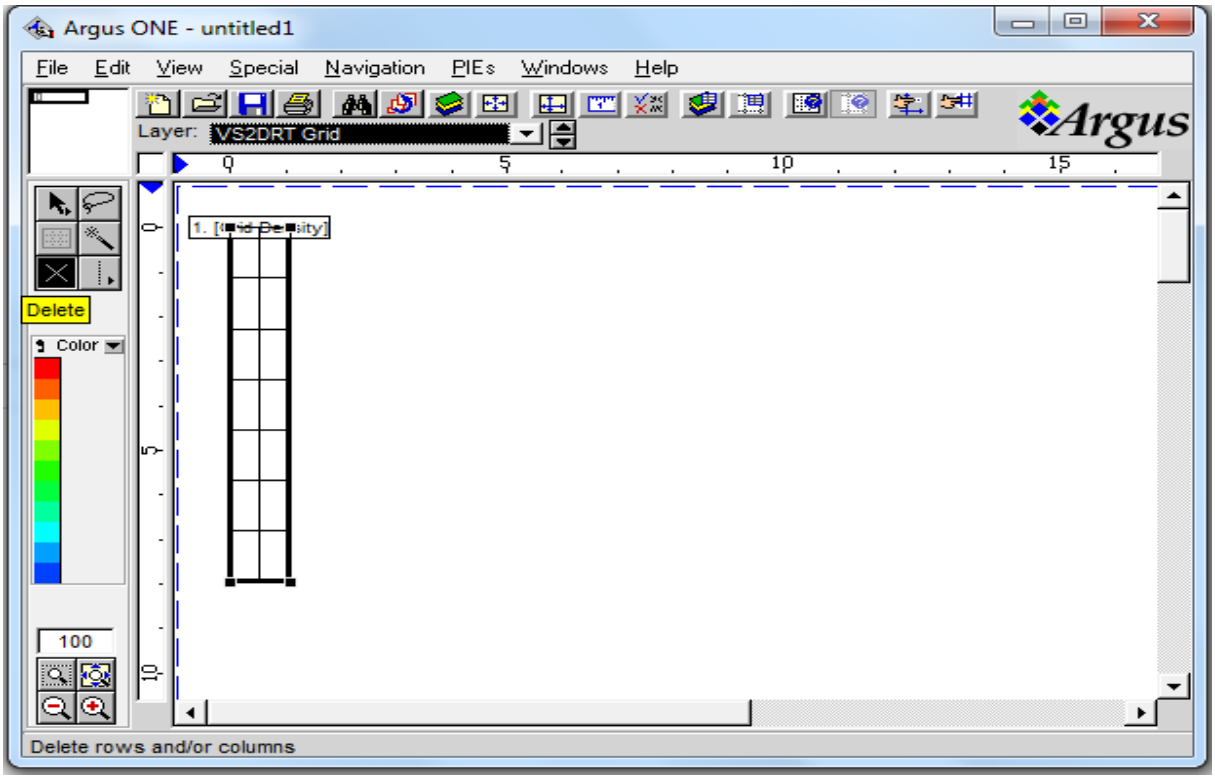

Figure 8.2.2d Schematic representation of selecting the delete tool to remove unwanted grids

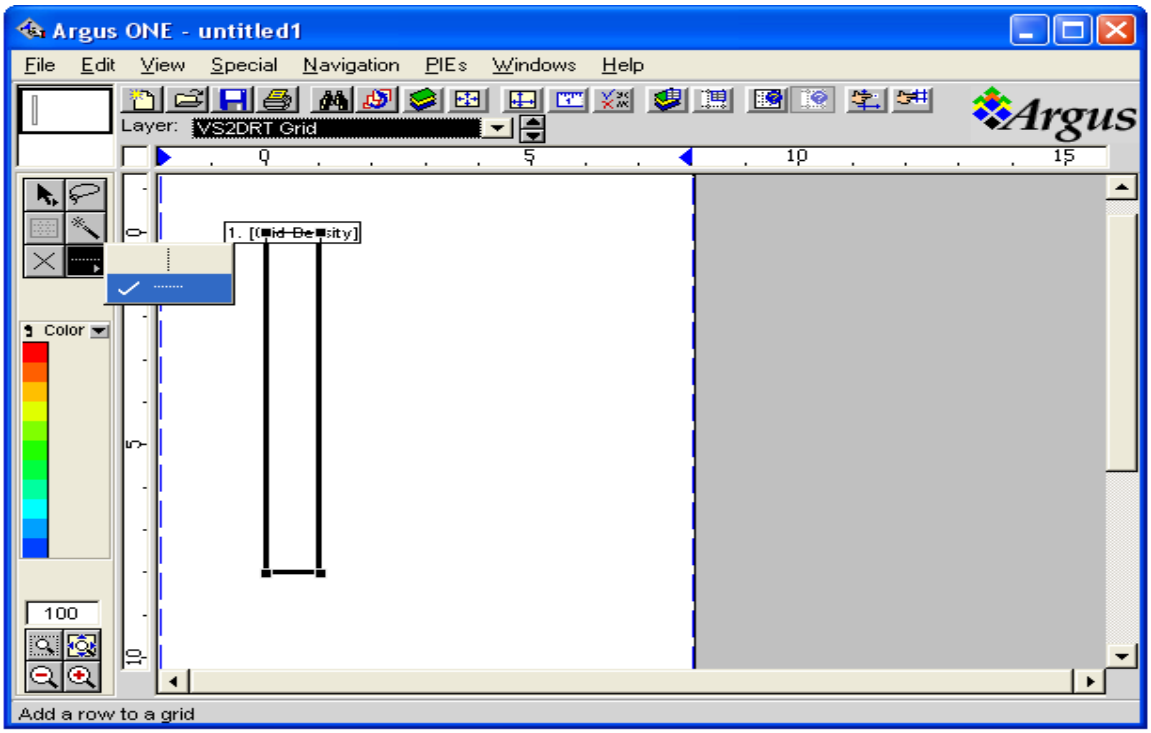

Figure 8.2.2e Schematic representation of row inserting tool to create a 1D column

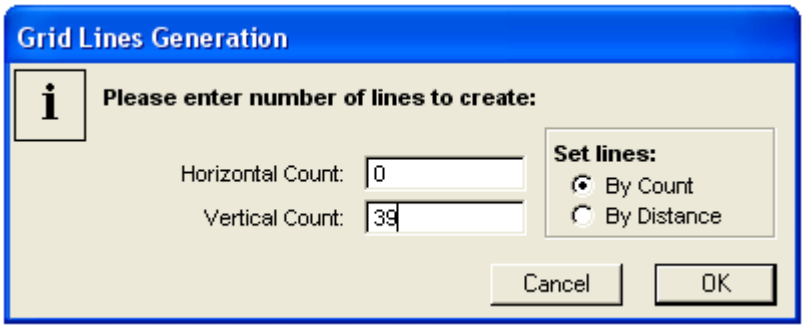

Figure 8.2.2f Grid Lines generation window

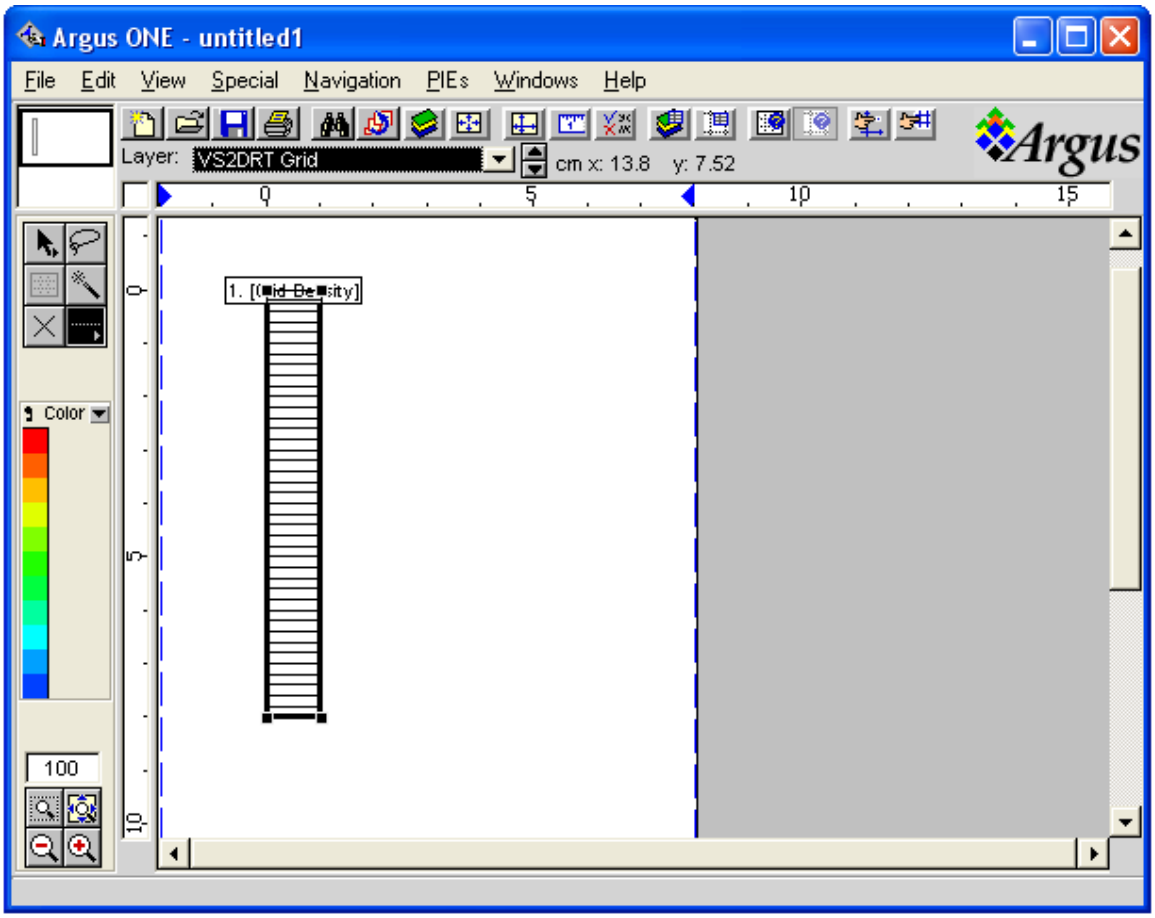

Figure 8.2.2g Schematic representation of 1D grid in column.

8.2.3 Textural Class

Textural class layer is used to set heterogeneous hydraulic, chemical and thermal properties of textural class of the domain of interest. The hydraulic properties needed depending on the choice of hydraulic functions of Brooks & Corey, van Genuchten, Haverkamp or Rossi-Nimmo for a particular simulation. General additional hydraulic properties required for water flow simulation are:

1. Ratio of hydraulic conductivity in the z-coordinate direction to that of in the x-coordinate direction (Kz_Kx)
2. Saturated hydraulic conductivity (Saturated Kh), L/T
3. Specific storage, L^{-1}
4. Porosity

In case of Brooks & Corey models the hydraulic properties required are:

1. Bubbling pressure head which is always has a negative value, L.
2. Residual moisture content
3. Pore-size distribution index

In case of van Genuchten models the hydraulic properties required are:

1. van Genuchten alpha (Alpha), L.
2. Residual moisture content
3. n van Genuchten parameter (Beta)

In case of Haverkamp models the hydraulic properties required are:

1. A prime Haverkamp parameter (A prime) which is always has a negative value, L.
2. Residual moisture content
3. B prime Haverkamp parameter (B prime)
4. Alpha Haverkamp parameter (Alpha) which is always has a negative value, L.
5. Beta Haverkamp parameter (Beta)

In case of Rossi-Nimmo models the hydraulic properties required are:

1. ψ_0 Rossi-Nimmo parameter (Psi_0), L.
2. ψ_D Rossi-Nimmo parameter (Psi_D), L.
3. ψ Rossi-Nimmo parameter (Rossi_lambda)

Thermal properties of the textural class required in cases of heat transport simulation are:

1. Heat longitudinal dispersivity, L.
2. Heat transverse dispersivity, L.
3. Heat capacity of dry solids (Cs), $Q/L^3\,^oC$, where Q is unit of energy.
4. Thermal conductivity of water-sediment at residual moisture (KTr), $Q/L\,^oC$.
5. Thermal conductivity of water-sediment at full saturation (KTs), $Q/L\,^oC$.
6. Heat capacity of water (Cw), $Q/L^3\,^oC$.

Chemical properties of the textural class required in case of reactive transport simulation are:

1. Longitudinal dispersivity, L.
2. Transverse dispersivity, L.
3. Molecular diffusion coefficient, L^2/T.

To set the textural properties of domain of interest select the active layer as Textural Class as shown in figure 8.2.3a. Different textural units would be delineated using closed contour tool as shown in figure 8.2.3b and textural properties as well as thermal and chemical properties of the textural class would be set using contour information window depending on the type of simulation conducted as shown in figure 8.2.3c.

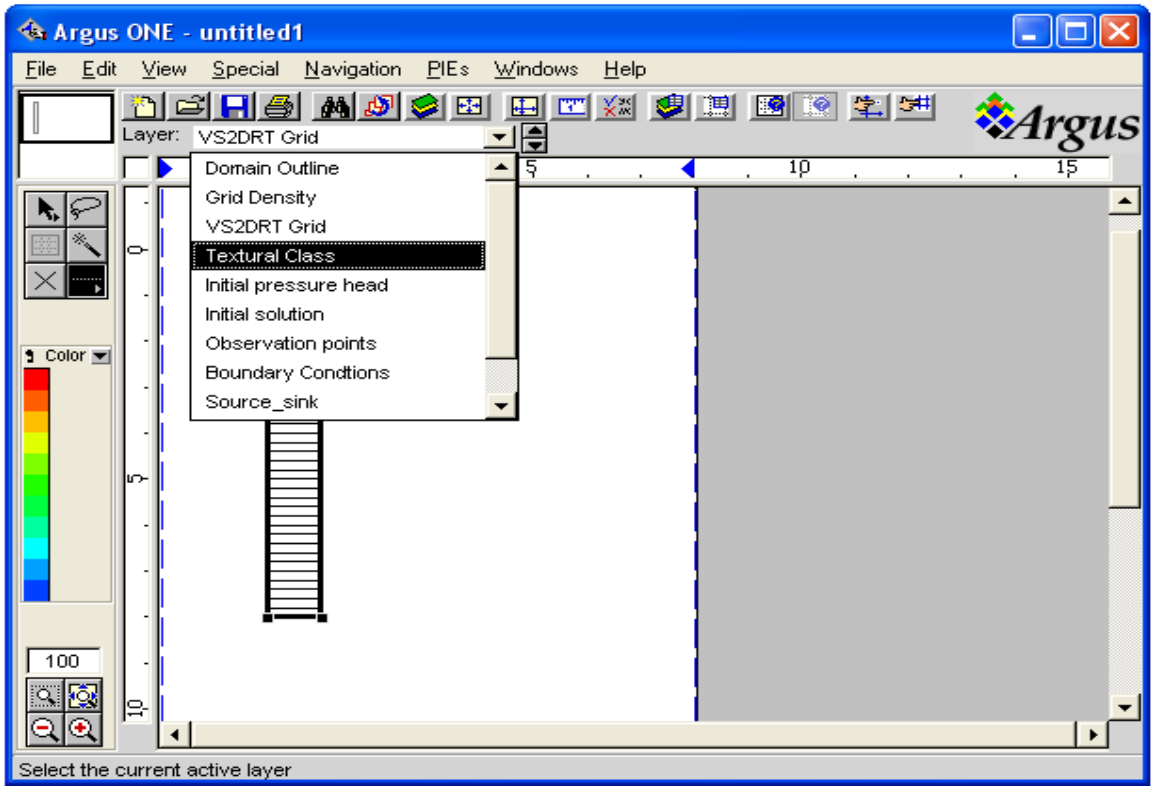

Figure 8.2.3a Schematic representation of selecting textural Class

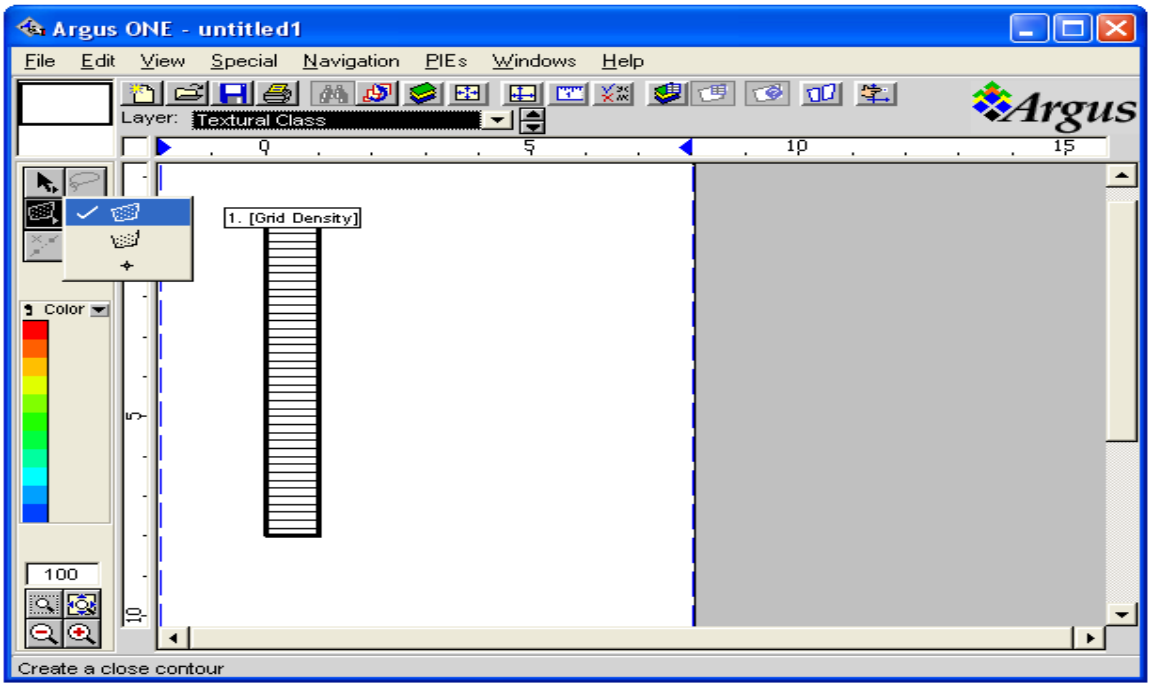

Figure 8.2.3b Schematic representation of selecting closed contour to delineate a textural class

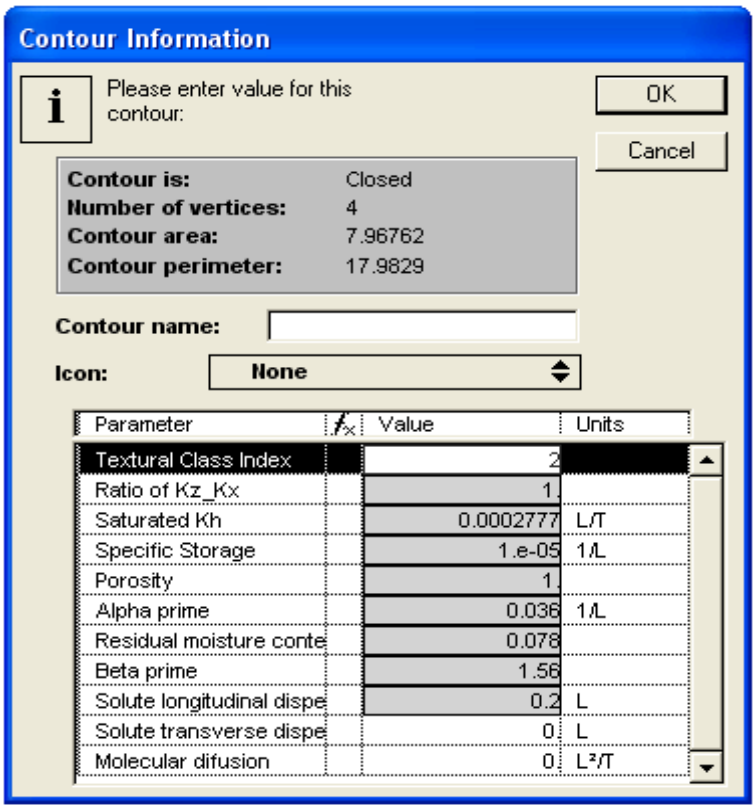

Figure 8.2.3c Schematic representation of setting textural class properties.

8.2.4 Initial condition for flow

The initial condition for flow simulation could be set as pressure head with equilibrium profile, initial pressure head or initial moisture content. To set initial condition for flow the equilibrium profile, initial pressure head or moisture content layer must be the active layer. Closed contour tool could be used to define the initial flow condition in domain of interest in the same way as it is used to delineate domain of interest or textural class as shown in figures 8.2.1e and 8.2.3b.

In case equilibrium profile is chosen as initial condition depth of the ground water table and minimum pressure head above the ground water table are required. Otherwise initial pressure head or moisture content values are required which is also set by the contour value. Figure 8.2.4 presents Contour information window to set value of initial pressure head or initial moisture content. Multiple closed contours can be used if initial flow condition is not uniform in the domain of interest.

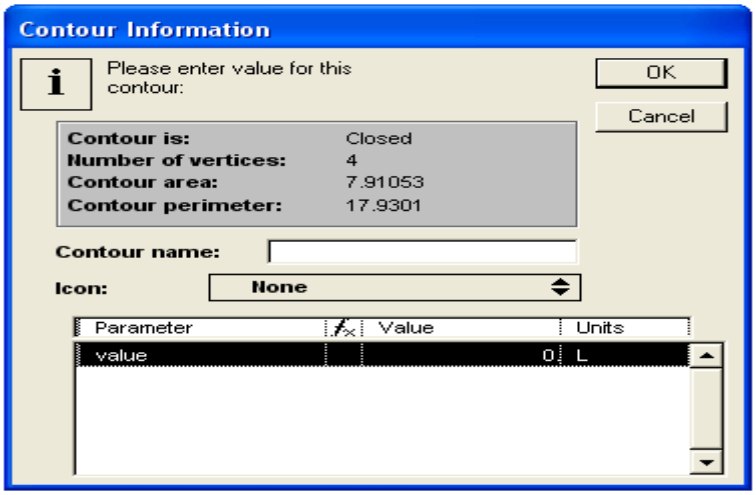

Figure 8.2.4 Schematic representation of setting initial pressure head or initial moisture content in domain of interest.

8.2.5 Initial solution

In order to set initial solution in the domain of interest the active layer should be Initial solution layer. Initial solution can be defined by providing the solution number, pure-phases number, surface number, gas number, solid solution number and kinetics number given in the Phreeqc input file generated by VS2DRT pre-processor for non-spatial input.

The default value for solution number is 1 and for pure-phases number, surface number, gas number, solid solution number and kinetics number is -1. Basics of setting solution, pure-phase, surface, gas, solid solution and kinetics have to be referred from PHREEQC manual.

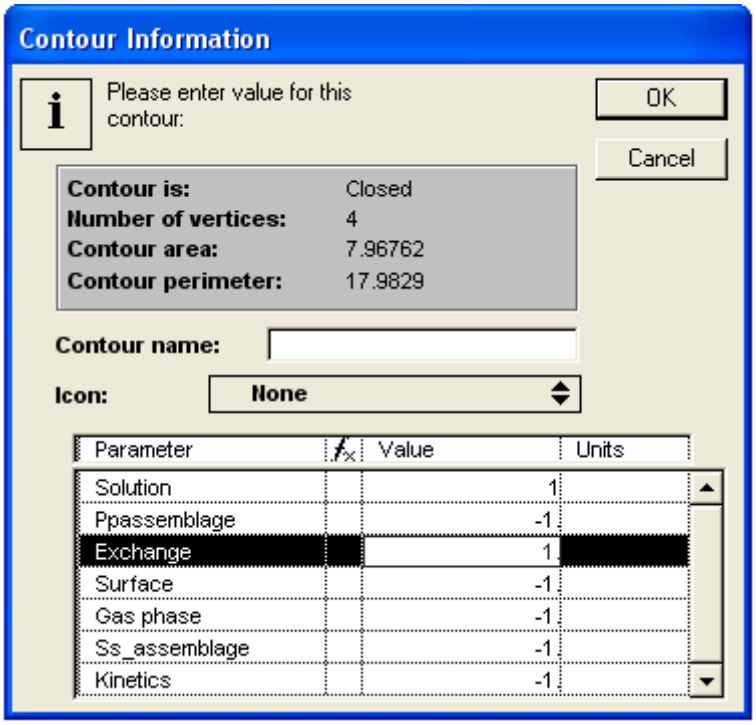

Figure 8.2.5 Schematic representation of setting initial solution

8.2.6 Initial temperature

Initial temperature layer is used to set initial temperature distribution in the domain of interest in case of heat transport using closed contour tool. Initial temperature layer will be avail-

able in case of heat transport simulation. The initial temperature can be set using Argus ONE contour tool in similar ways as the initial pressure head or solution has been set using contour information window as shown in figure 8.2.6a. Thermal properties of the domain of interest will be set in the texture layer along with hydraulic properties and in case of reactive transport also with geochemical property of the medium as shown in figure 8.2.6c. The heat transport boundary condition can be set using boundary layer along with flow, reactive transport boundary conditions as shown in figure 8.2.6b.

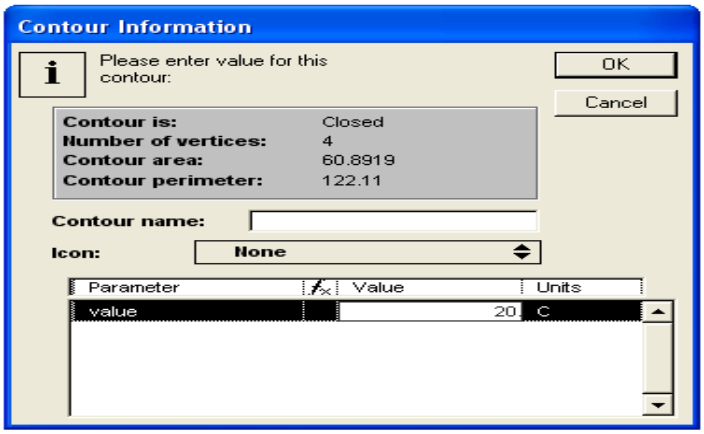

Figure 8.2.6a Schematic representation of setting initial temperature in domain of interest

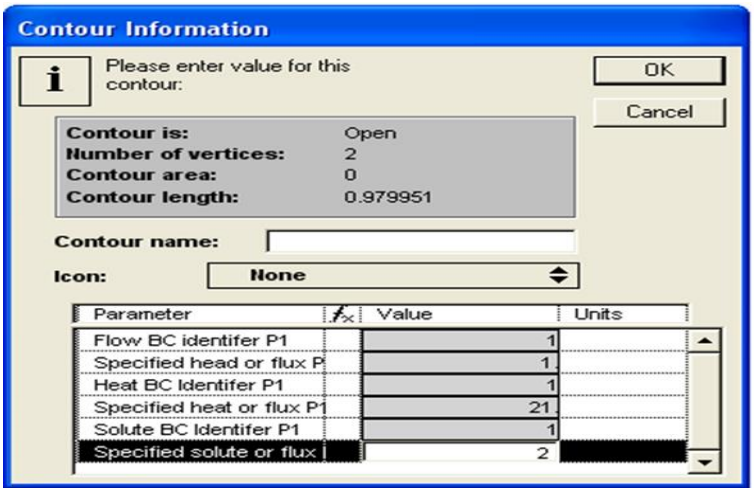

Figure 8.2.6b Setting boundary conditions for flow, heat and reactive transport simulation

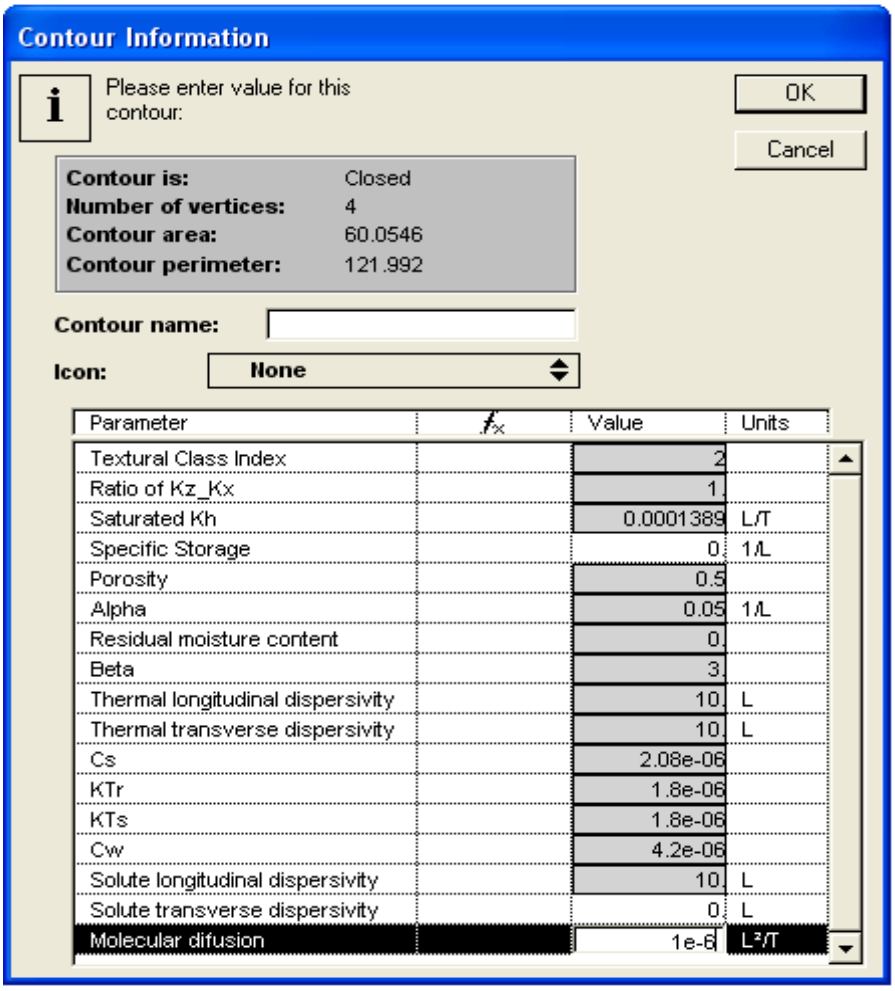

Figure 8.2.6c Setting hydraulic, thermal and geochemical properties of the medium along in case of heat and reactive transport

8.2.7 Observation points

Observation points are used to see the output of the simulation at chosen time at a particular point in space and observation layer is used to set one or more observation points using point contour tool as shown in figure 8.2.7.

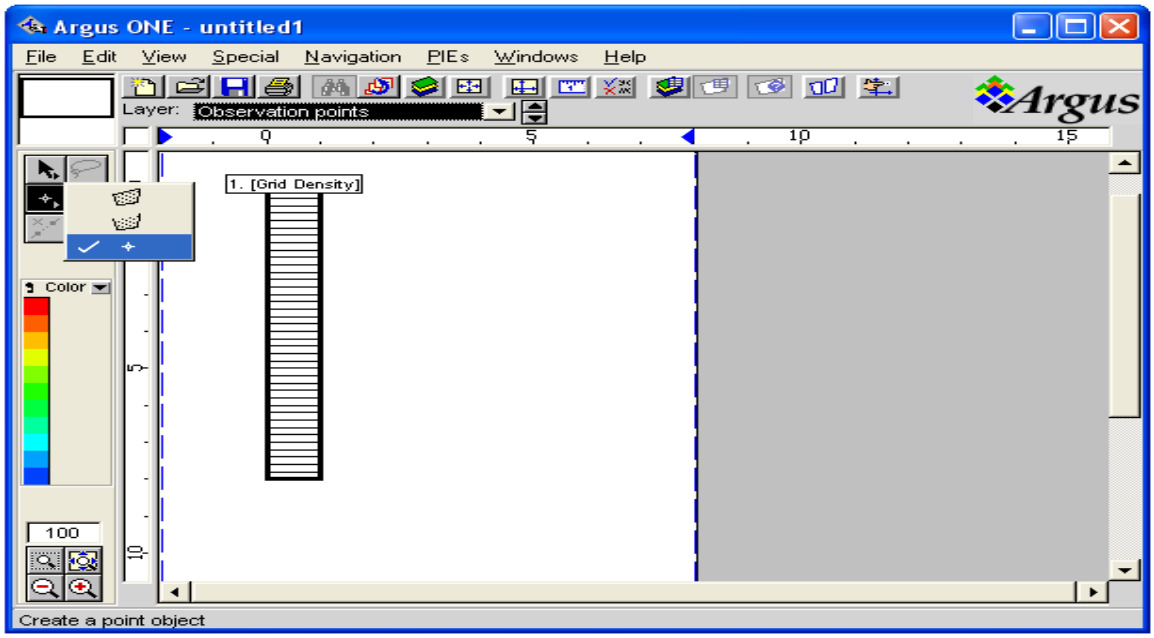

Figure 8.2.7 Setting observation point in the observation layer

8.2.8 Boundary conditions

Boundary conditions layer is used to set flow, heat and/or solute transport boundary conditions for various recharge periods. Possible flow boundary conditions along with their boundary identifier index are presented in table 8.2.8a. The available heat transport boundary conditions are not specified boundary and specified temperature with heat boundary identifier index of 0 and 1 respectively. The available solute transport boundary conditions are not specified boundary and specified concentration with solute boundary identifier index of 0 and 1 respectively. Specified concentration is set by providing solution number of the chemical solution at the boundary or chemical solution flux of water across the boundary.

Table 8.2.8a Possible flow boundary conditions

Flow boundary identifier index	Type of boundary condition
0	No flow across the boundary
1	Specified pressure head
2	Specified flux in units of L/T
3	Possible seepage face
4	Specified total head
5	Evaporation
6	Specified volumetric flow in units of L^3/T
7	Gravity drain

1. No flow across the boundary refers to a boundary where no water inters or leaves in to the domain of interest.

2. Specified pressure head boundary refers to a boundary where pressure head has a specified value.

3. Specified flux in to the domain boundary refers to a boundary where water inters in to the domain of interest in the form of infiltration rate from precipitation and irrigation. Specified flux boundary nodes may change to specified pressure head boundary internally by the program if pressure head at specified flux boundary node exceeds the maximum allowed height of ponding provided by the user. Converted specified pressure head boundary node may return to specified flux boundary node internally if computed flux exceeds the specified flux.

4. Possible seepage face boundary refers to a boundary where seepage might occur if pressure head along the seepage face is zero and water flow out of the domain at same time. In case of possible seepage face only the corresponding flow boundary identifier index should be provided by user.

5. Specified total head boundary condition refers to boundary where specific total head value is defined. If the total head boundary is above the ground water table it will have negative value and if it is below the ground water table it will have a positive value.

6. Evaporation boundary condition refers to boundary where water flow out of the domain of interest in the form of evaporation and evapotranspiration. In case of evaporation boundary condition only the corresponding flow boundary identifier index should be provided by the user.

7. Specified volumetric flow boundary refers to a boundary where water enters or leaves the domain of interest and applicable only in cases when radial coordinate system is used.

8. Gravity drain boundary refers to a boundary where water flow out of the domain vertically due to gravitational force at unit vertical hydraulic gradient.

The heat and solute transport boundary conditions at any particular boundary depends to the corresponding flow boundary condition. Possible combination of boundary conditions for flow and heat and solute transport is presented in the table 8.2.8b.

Table 8.2.8b Possible combination of boundary conditions for flow and heat and solute transport

Flow boundary condition	Heat boundary condition	Solute boundary condition
No flow across the boundary		
Specified pressure head	Specified temperature at the boundary	Specified concentration at the boundary
Specified flux in to the domain in units of L/T	Specified temperature in inflow water	Specified concentration in inflow water
Possible seepage face	no	no
Specified total head	Specified temperature at the boundary	Specified concentration at the boundary
Evaporation	no	no
Specified volumetric flow in units of L^3/T	Specified temperature in-flow water	Specified concentration in the inflow water
Gravity drain		

In the boundary condition layer various boundary conditions could be set using open contour tool of Argus ONE as shown in figure 8.2.8b.

Figure 8.2.8b shows how to set boundary conditions for a given recharge periods using open contour tool and figure 8.2.8c shows contour information window of Argus ONE for to set a boundary conditions for flow and reactive transport. In VS2DRT a particular boundary open contour is supposed to exist in all recharge periods so when a user draws the boundary segment it is required to provide the respective boundary conditions for flow, heat and/or solute transport for all recharge periods through contour information window of Argus ONE. So if

a particular flow boundary segment exist for one recharge period and does not exist for other recharge period then its flow boundary identifier index should be set as 0.

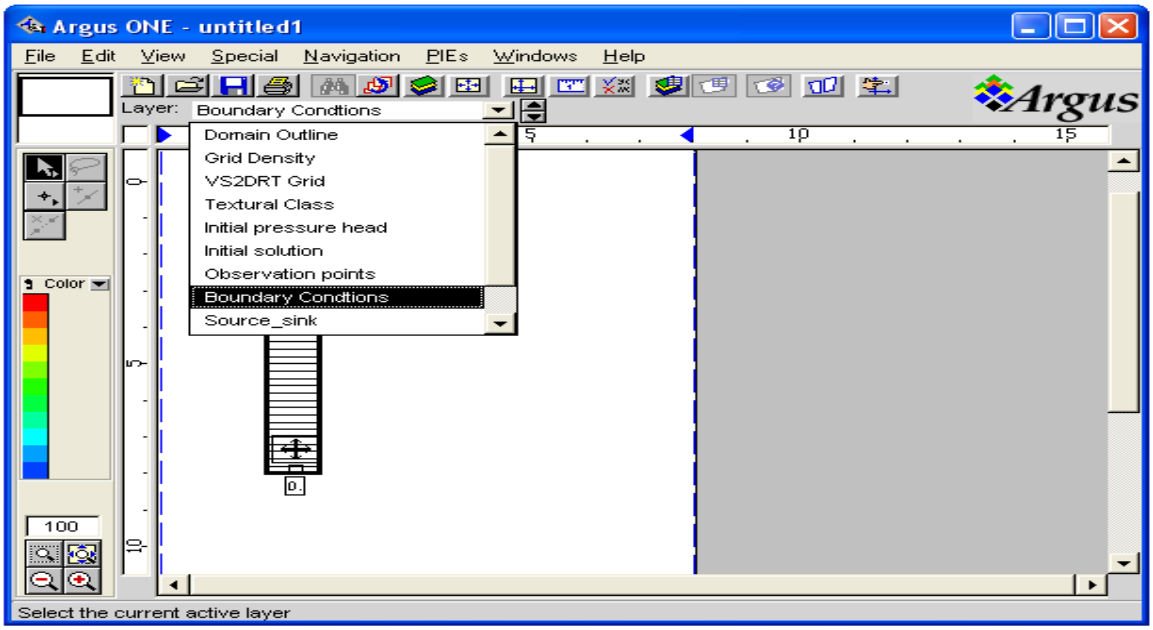

Figure 8.2.8a Selecting boundary conditions layer

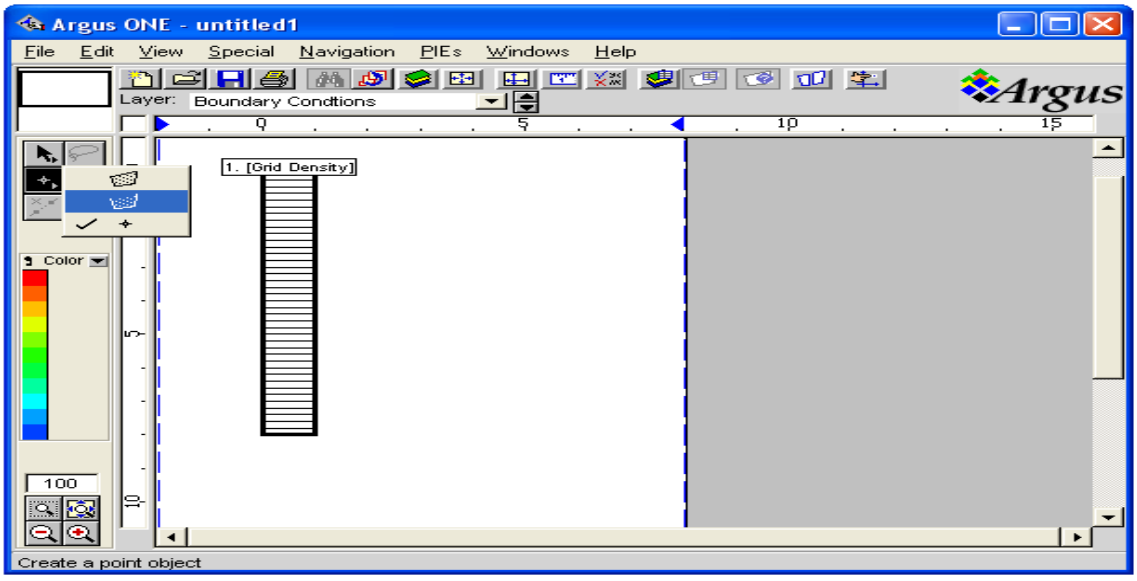

Figure 8.2.8b Schematic representation of selecting open contour tool of Argus ONE to set the boundary conditions

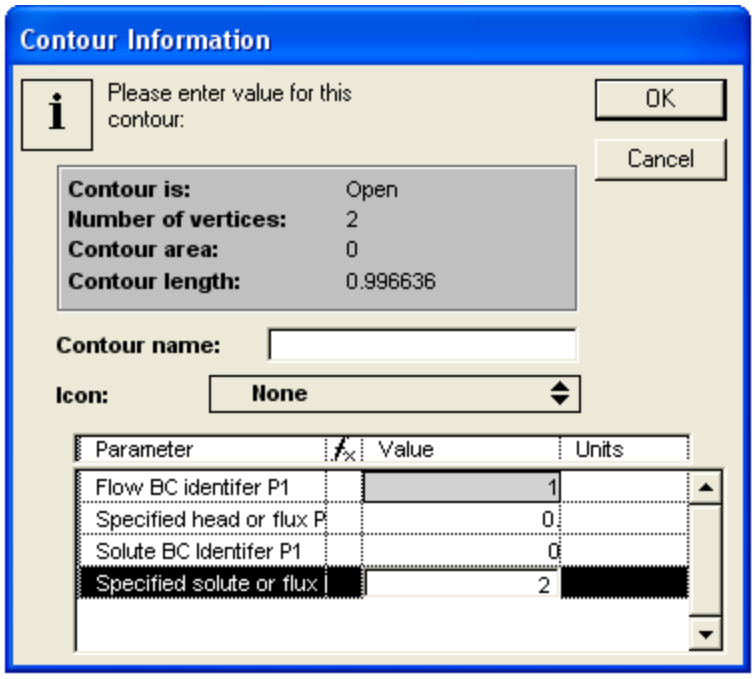

Figure 8.2.8c Schematic representation of setting boundary conditions for flow and solute transport

8.3 VS2DRT post-processor

VS2DRT post-processor deals with running VS2DRT numerical model and presenting the output using Argus ONE post-processor tools.

8.3.1 Running VS2DRT numerical model

To run the numerical model one need to make sure that:

1. Phreeqc input file and database are in the same project folder
2. All necessary spatial, non-spatial and temporal inputs are properly provided
3. Boundary nodes are properly draw along the boundary

To start the simulation the active layer of Argus ONE environment need to be the VS2DRT Grid layer. From PIEs menu by selecting Export VS2DRT one can initiate RunVS2DRT dialog window as shown in figure 8.3.1a and figure 8.3.1b.

To run RunVS2DRT one has to click first on Run VS2DRT button followed by clicking the Ok button to start numerical simulation.

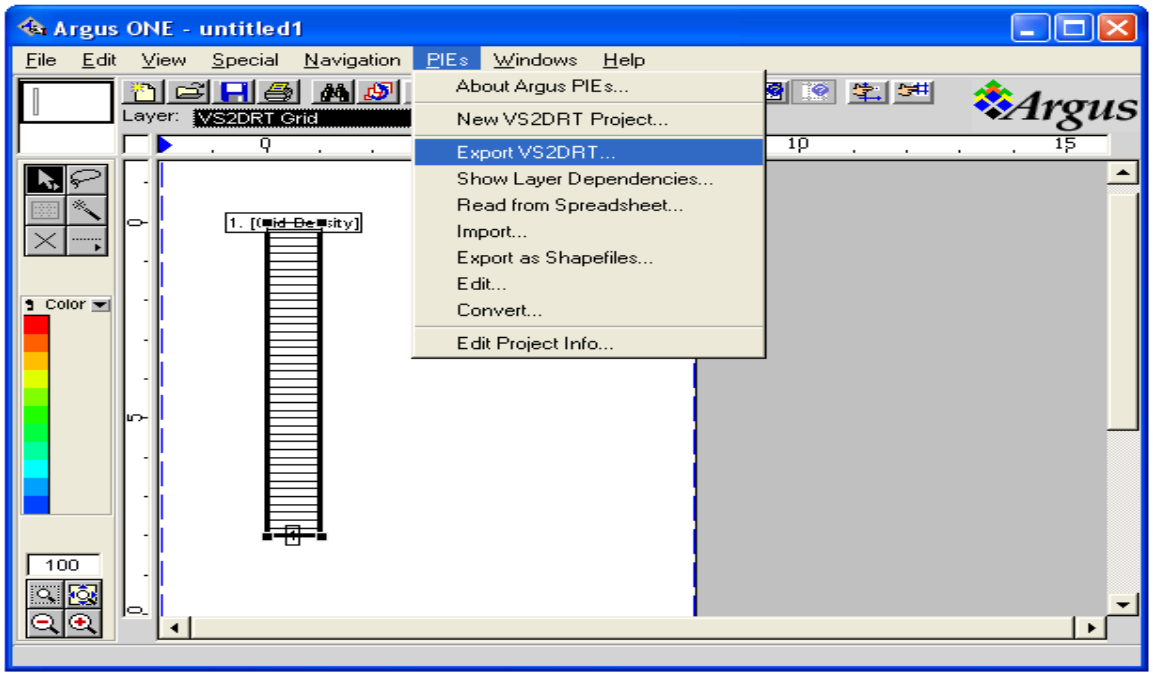

Figure 8.3.1a Schematic representation of selecting ExportVS2DRT menu

Figure 8.3.1b Schematic representation of RunVS2DRT window

8.3.2 Presenting VS2DRT output using Argus ONE post-processor tools

After successfully running the VS2DRT numerical model the output of the simulation can be presented with help of Argus ONE post-processor tools using the Data and Output layers of VS2DRT.

1. Make sure Data is the active layer as shown in figure 8.3.2a.

2. From the file menu select import Data menu as shown in figure 8.3.2 b and then select import text file menu, see figure 8.3.2c. Import Data window will open to set the format of the data file to be imported. For VS2DRT one has to select grid data and read triangulation from layer VS2DRT Grid as shown in figure 8.3.2d.

3. Chose file to import window would be used to select the output of the simulation for pressure head, temperature, moisture content, velocity, saturation or solute concentrations files as shown in figure 8.3.2e .

4. Then make the active layer to be the Outputs layer by selecting outputs layer as shown in figure 8.3.2g.

5. Then select Post-processing popup menu to choose visualization tool of choice, for example in figure 8.3.2 h Color diagram tool to make color map for the output of the simulation.

6. Set the color map parameters as shown in figure 8.3.2i by selecting Data layer as the Layer from which the data will be plotted and the value will be the value of the data on data layer.

7. Get the color map as shown in figure 8.3.2 j.

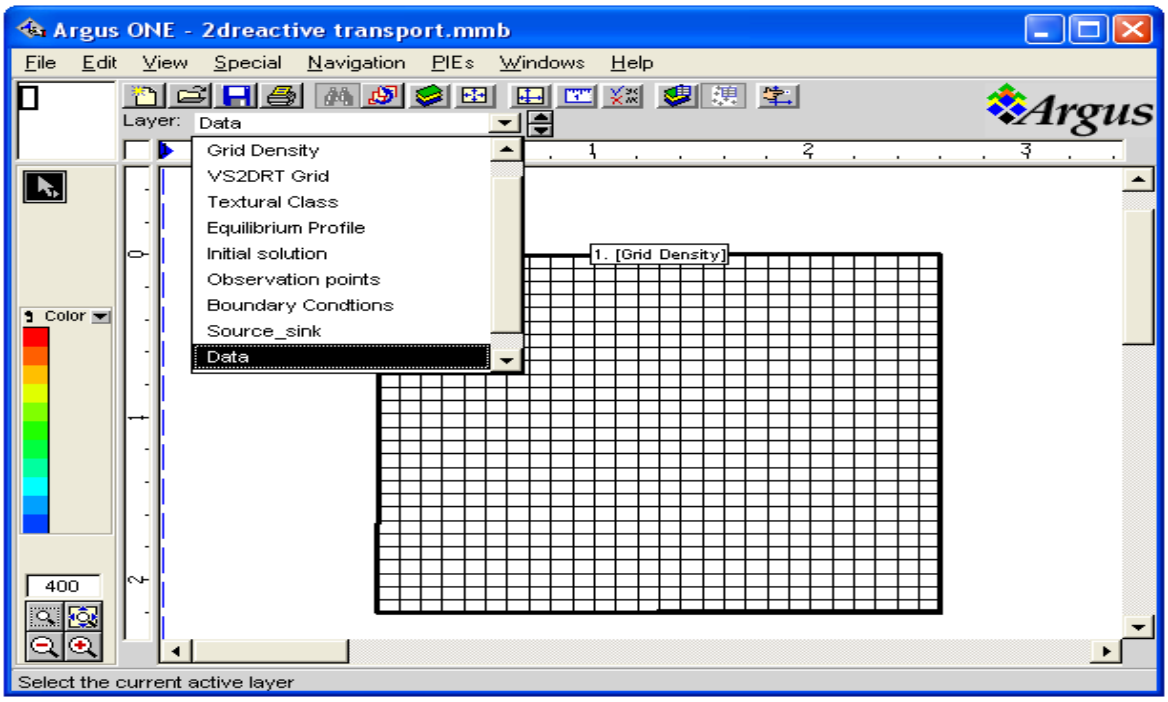

Figure 8.3.2a Schematic representation of selecting the Data layer

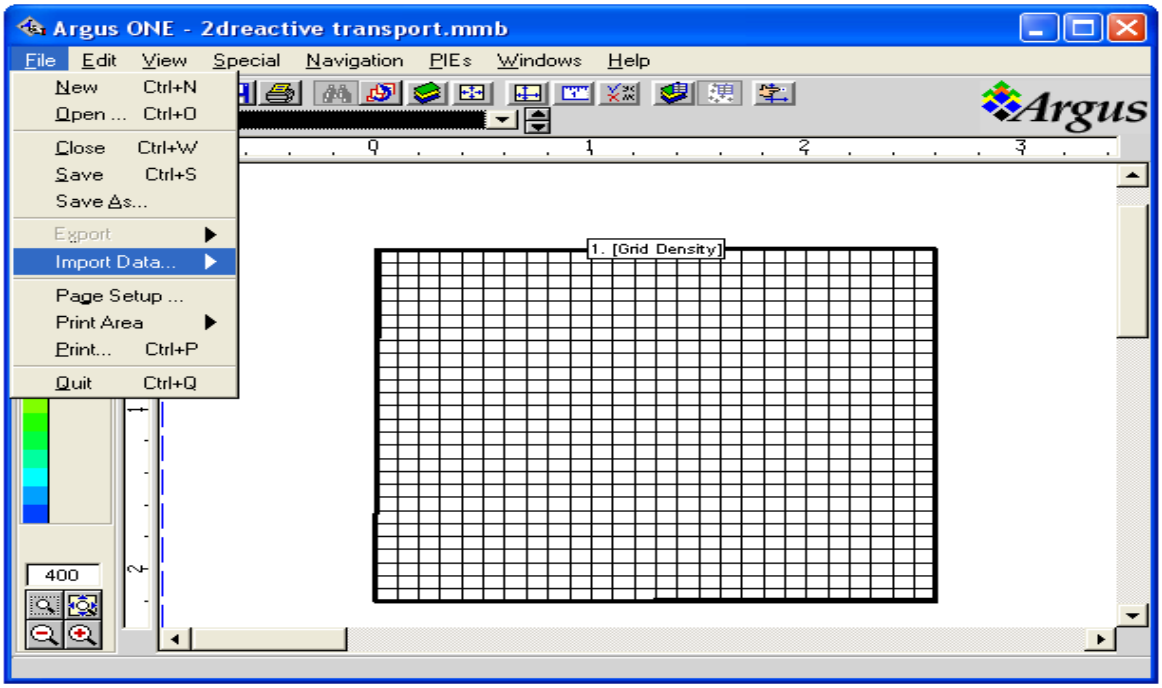

Figure 8.3.2b Schematic representation of selecting the Import Data menu

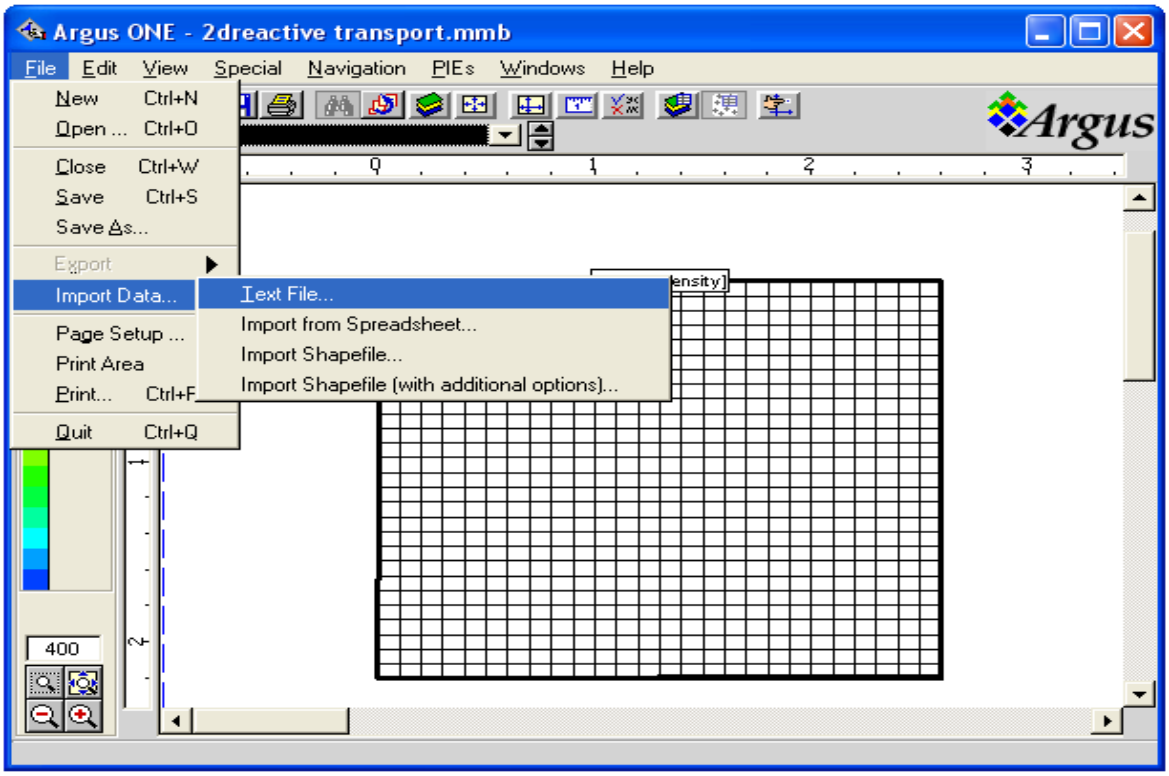

Figure 8.3.2c Schematic representation of selecting Text File menu from Import Data menu

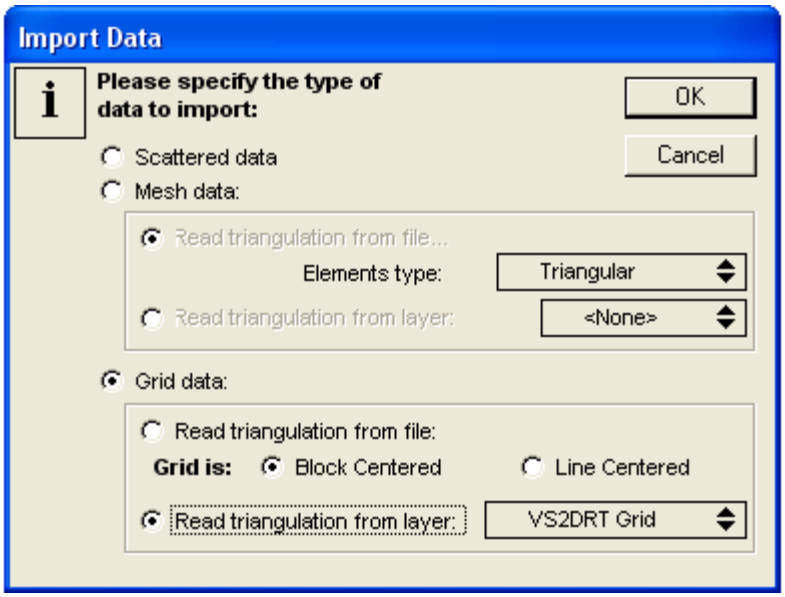

Figure 8.3.2d Schematic representation of the Import Data window

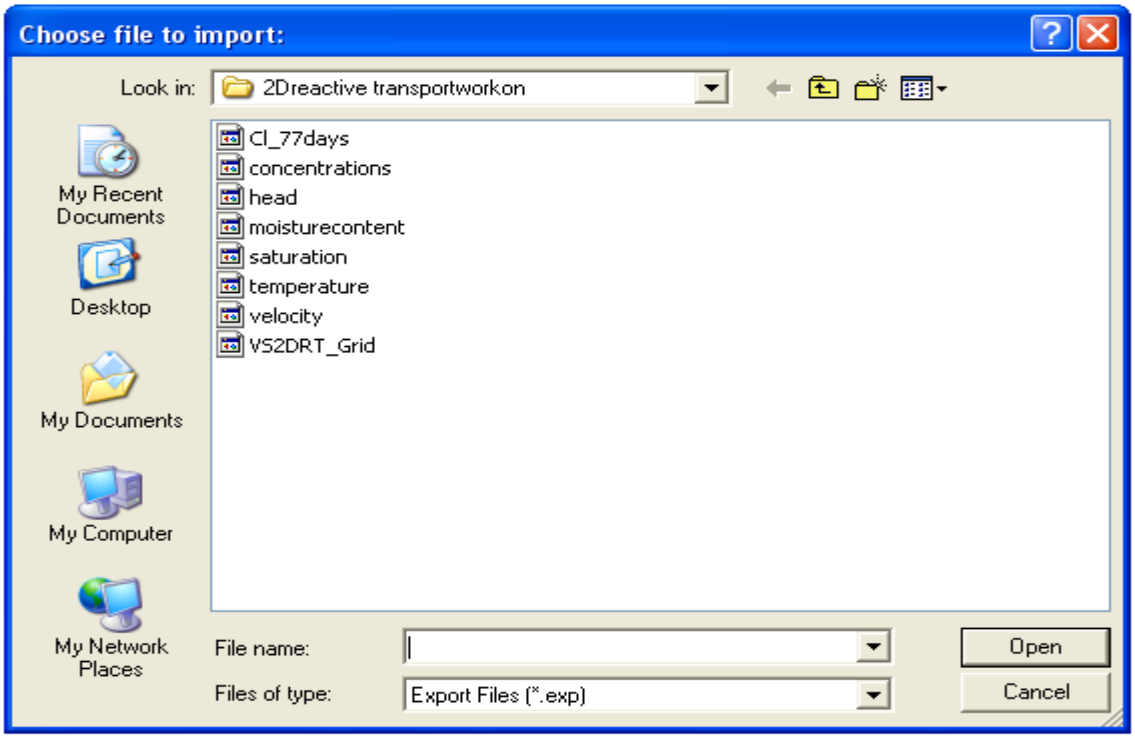

Figure 8.3.2e Schematic representation of choosing file to be imported to Data layer

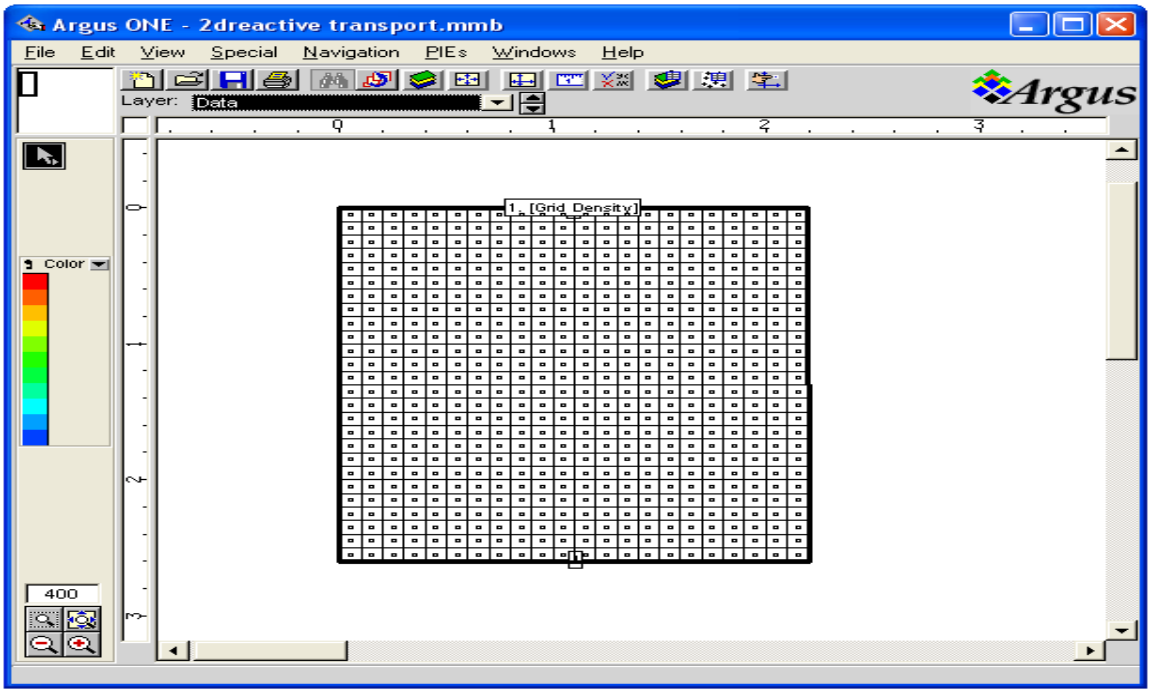

Figure 8.3.2f Schematic representation of imported data to the Data layer

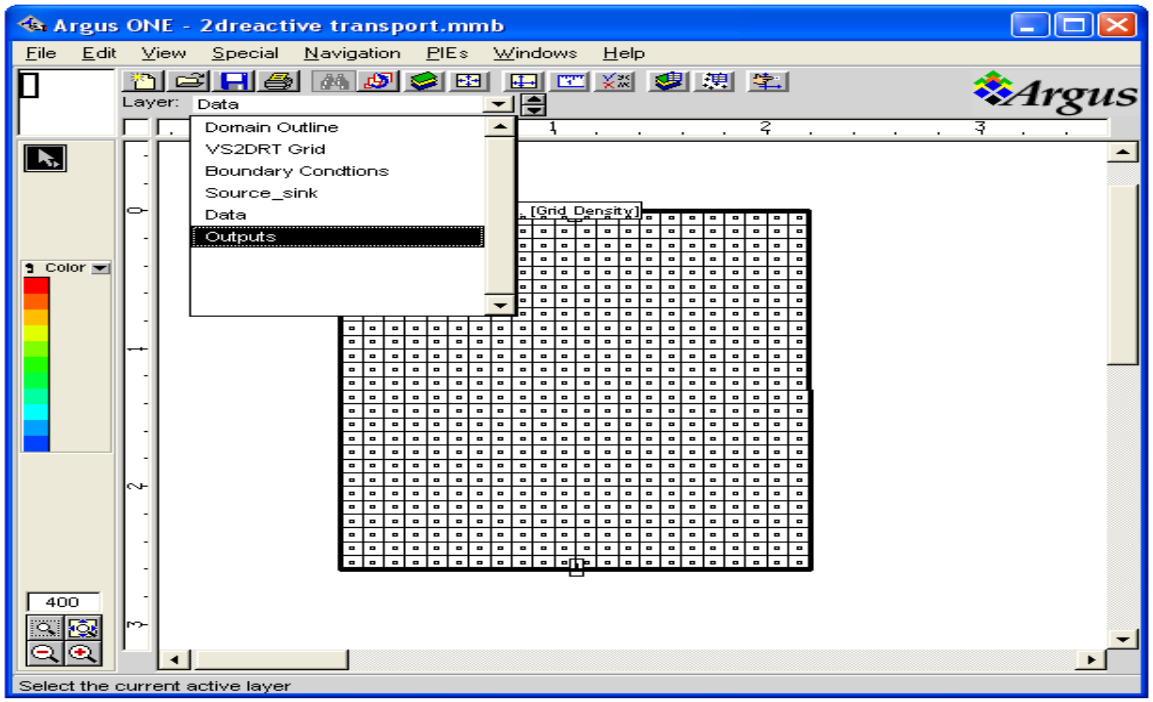

Figure 8.3.2g Schematic representation of selecting Output layer to plot the outputs of the simulation

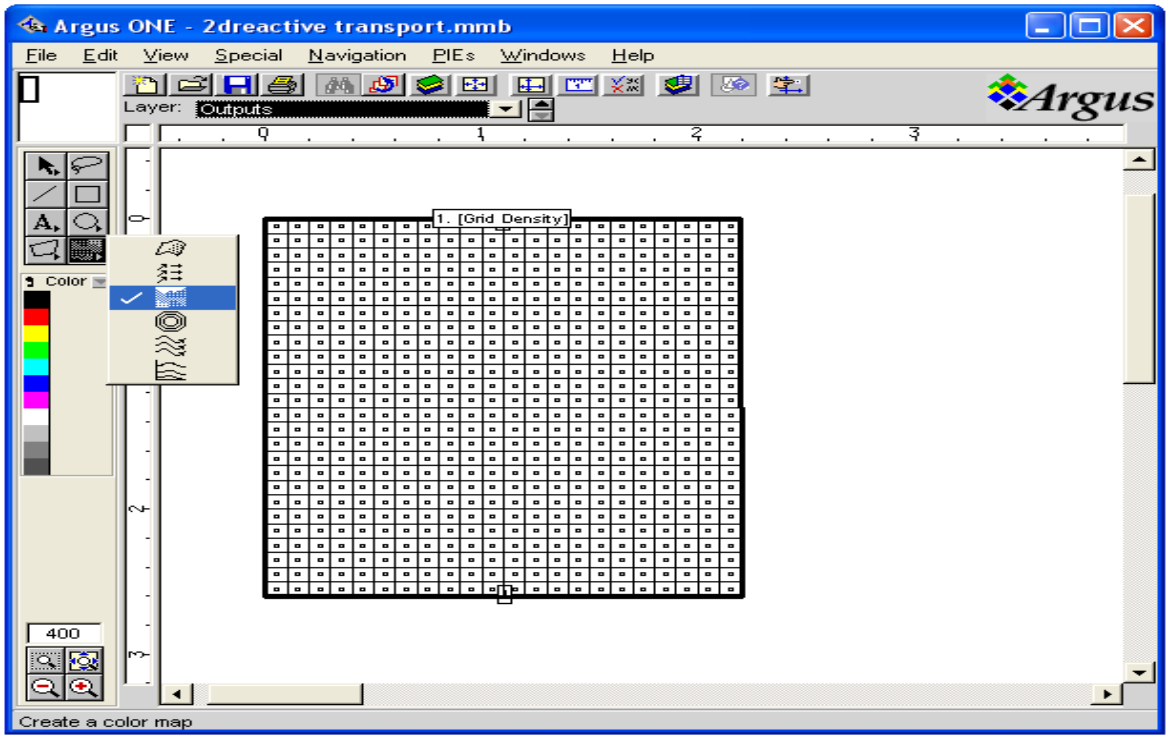

Figure 8.3.2h Schematic representation of selecting Argus ONE Post processing tools popup menu

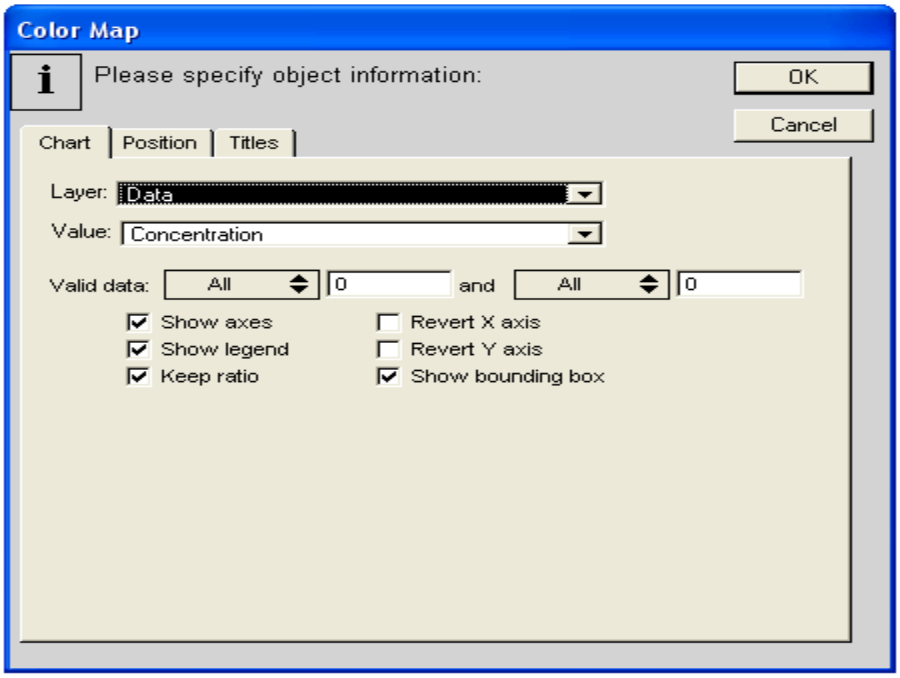

Figure 8.3.2i Schematic representation of setting Color Map parameters to create color map

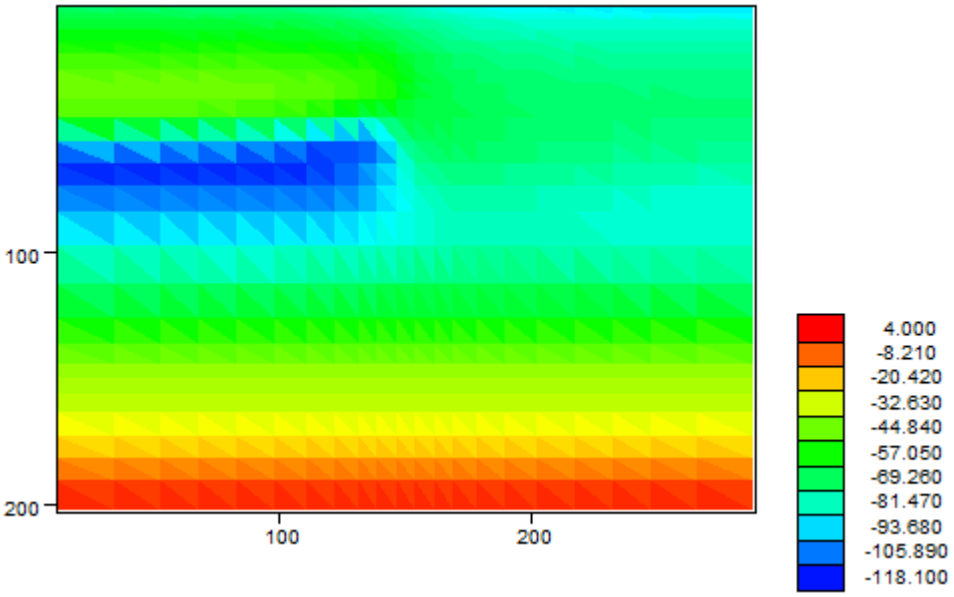

Figure 8.3.2j Example color map showing spatial distribution of pressure head plotted using Argus ONE Post-processing Color Diagram tool

Chapter Nine: Model verification

Model verification involves testing coupled VS2DRT model with various reactive transport problems from literature to check whether the model is working properly. For verification proposes seven cases are taken from literature involving simple 1D conservative single component transport, cation exchange, surface complexation, dissolution of calcite and gypsum, heat and conservative chemical transport, 2D reactive transport involving cation exchange and 2D multi-solute reactive transport. VS2DRT simulation results were compared with other reactive transport models like VS2DT, PHREEQC, HP1, VS2DH and HP2. Since VS2DH, VS2DT and PHREEQC are independently well tested programs the verification problems here are more focused on the testing the coupling of this programs.

9.1 1D Conservative single component transport in vadose zone

The problem is taken and modified from USGS Water-Resources Investigations Report 90-4025 (p. 45) (Healy, 1990). It deals with chloride transport in 40 cm sandy loam column. The simulation is conducted for half an hour and the column is divided in to 40 grids of 1cm length and 0.005 hour time step is used. Van Genuchten parameters for sandy loam soil are used as column's hydrologic properties. Longitudinal dispersivity assumed to be 10 cm. Initial pressured head of -120 cm and zero chloride initial concentration in column was assumed. Flux of 5.5 cm/h applied at the top of the column with 1 gm/kgw of Cl. This problem was simulated by both VS2DT and VS2DRT in order to check the link between PHREEQC and VS2DRT. The result of the simulation is presented in figure 9.1 and shows that both VS2DT and VS2DRT give identical result.

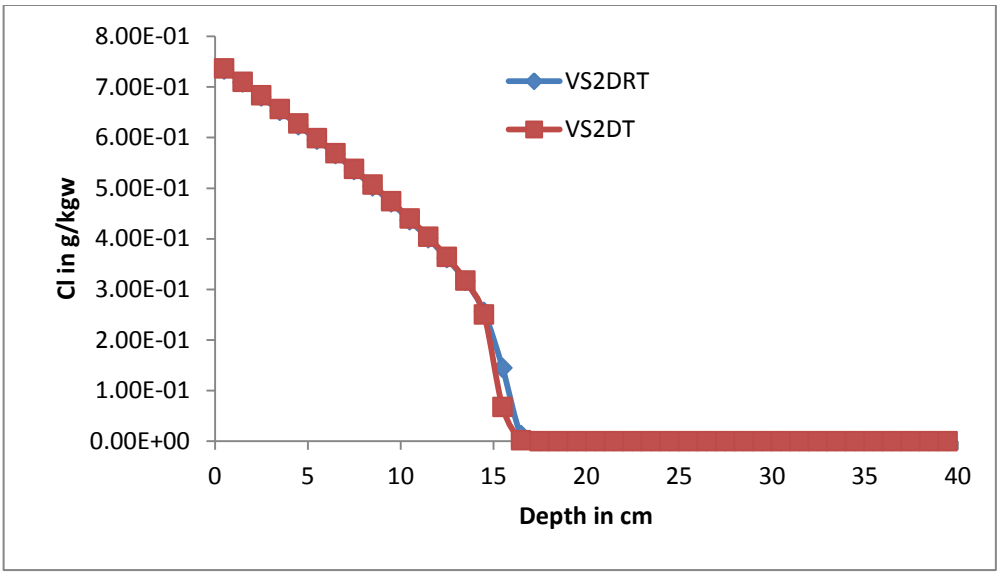

Figure 9.1 Comparisons of conservative Cl transport simulation using VS2DRT and VS2DT

9.2 Surface complexation and equilibrium phase

This problem is taken from (Wissmeier & Barry, 2008) to demonstrate the capabilities of VS2DRT to simulate surface complexation. 5 cm column of loamy sand was discretized in to 50 cells of 0.1 cm length and simulated for 200 days with time step of 0.01 days. The hydraulic and geochemical properties of the loamy sand column along with initial and boundary conditions are given in table 9.1 below.

Table 9.1 Hydraulic and geochemical properties of the loamy sand column along with initial and boundary conditions modified from (Wissmeier & Barry, 2008)

Hydraulic properties of loamy sand in terms of van Genuchten parameters			
α_g	0. 124 cm^{-1}		
ng	2.28		
K_s	0.00405324 cm/day		
θ_s	0.41		
θ_r	0.057		
Geochemical properties (surface assembly and solid phase in equilibrium with initial solution) (mol/l soil)			
Equilibrium phases			
Calcite	0.01152		
Surface properties			
Weak adsorption sites (Hfow)	0.02		
Strong adsorption sites (Hfos)	0.0005		
Specific surface area	600 m^2/g		
Total mass of surface in each cell	0.03 g		
Thickness of the diffuse layer	10^{-8} m		
Initial solution (mol/kg water)		*Boundary condition solution (mol/kg water)*	
pH	7.126	pH	13.2
Ca	2.08 x 10^{-3}	Na	2.421 x 10^{-1}
Na	7.877 x 10^{-7}	Water content	0.4
C	4.779 x 10^{-3}		
Water content	0.1		

The results of VS2DRT simulation are presented in the figure 9.2a, 9.2c, 9.2d and 9.2e for water content, Na, Ca and C respectively at 40 and 200 days. These results were compared with that of HP1 results presented in figures 9.2b and figure 9.2f (L. Wissmeier and D.A. Barry, 2008).

The profile of water content, Na and C at 40 days show similar pattern for both VS2DRT and HP1 while Ca shows slight difference towards the top of the column. However at 200 days the distribution of water content is different where VS2DRT calculates full saturation while HP1 gives near full saturation result. The profiles of Na and C at 200 days are also similar to that of HP1 but Ca shows slightly different towards the top of the column. The profile of Ca in top 10 and 20 cm of simulation shows some peak values in HP1 simulation

for both 40 days and 200 days respectively which are not observed in VS2DRT simulation. This variation may be due the variation in value of longitudinal dispersivity used in HP1 which is not clearly stated on the original paper. For this simulation longitudinal dispersivity of 0.1 cm used and zero molecular dispersivity was assumed.

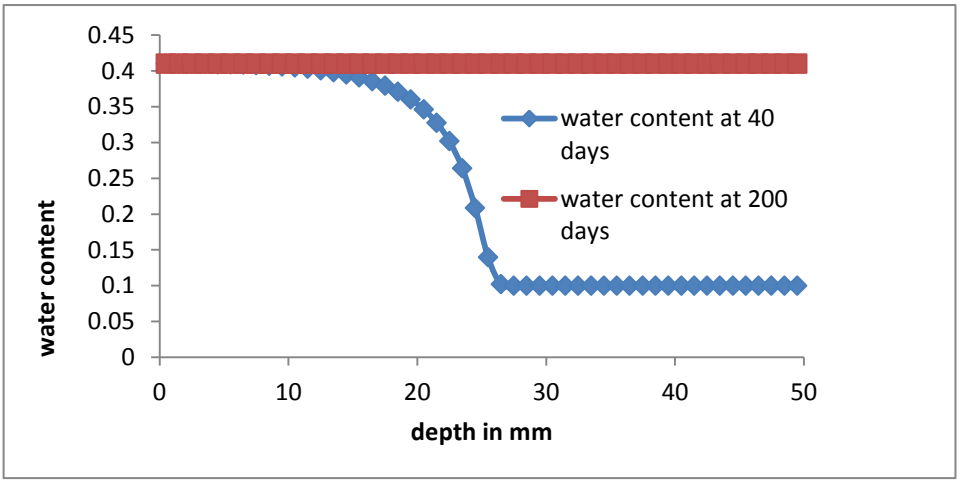

Figure 9.2a Distribution of moisture content at 40 and 200 days based on VS2DRT simulation

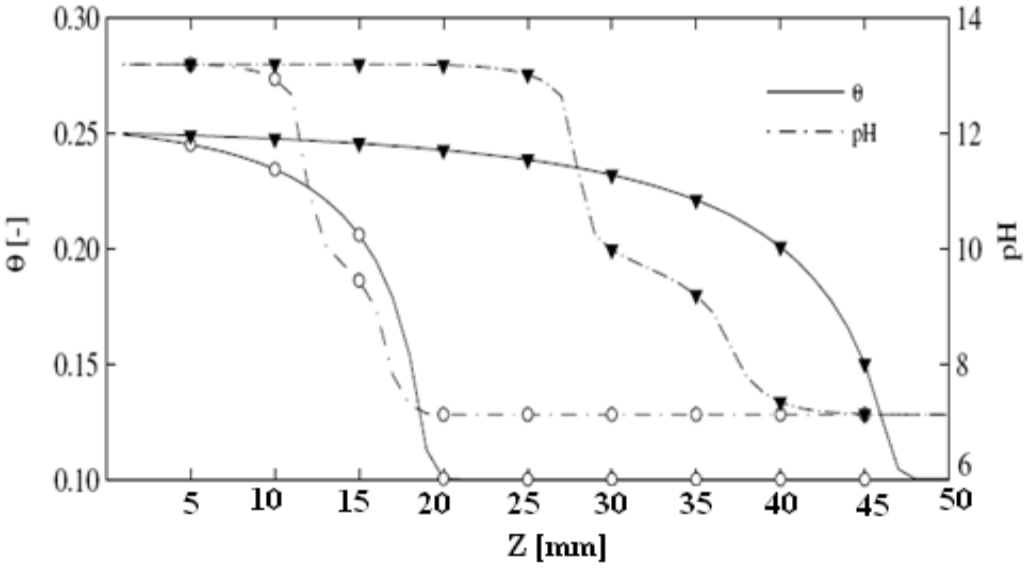

Figure 9.2b Distribution of water content and pH at 40 (circles) and 200 (triangles) days based on HP1 simulation respectively (Wissmeier & Barry, 2008)

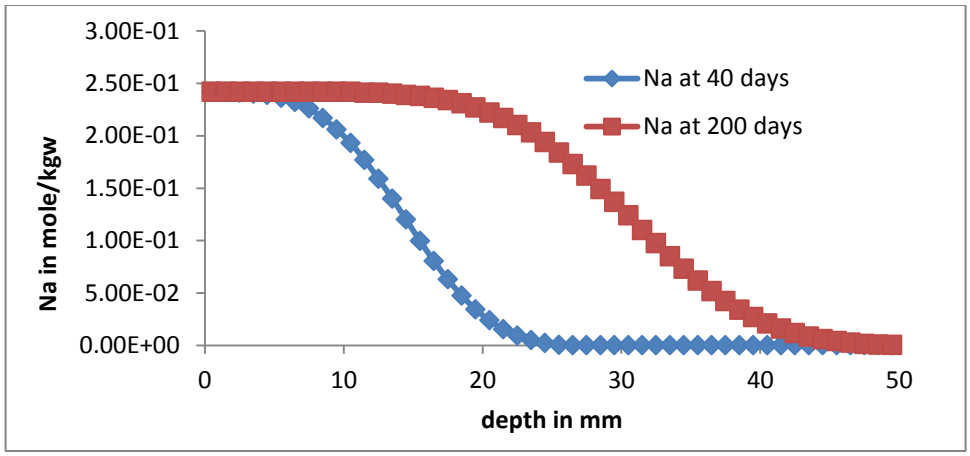

Figure 9.2c Distribution of Na at 40 and 200 days based on VS2DRT simulation

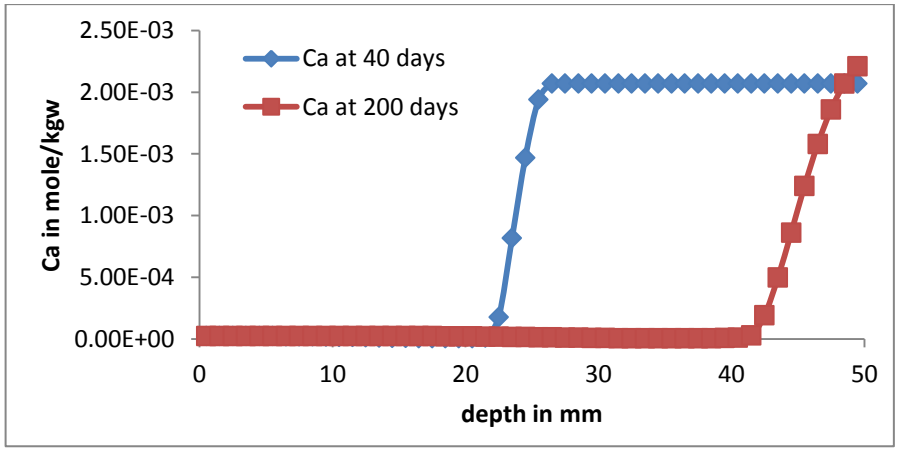

Figure 9.2d Distribution of Ca at 40 and 200 days based on VS2DRT simulation

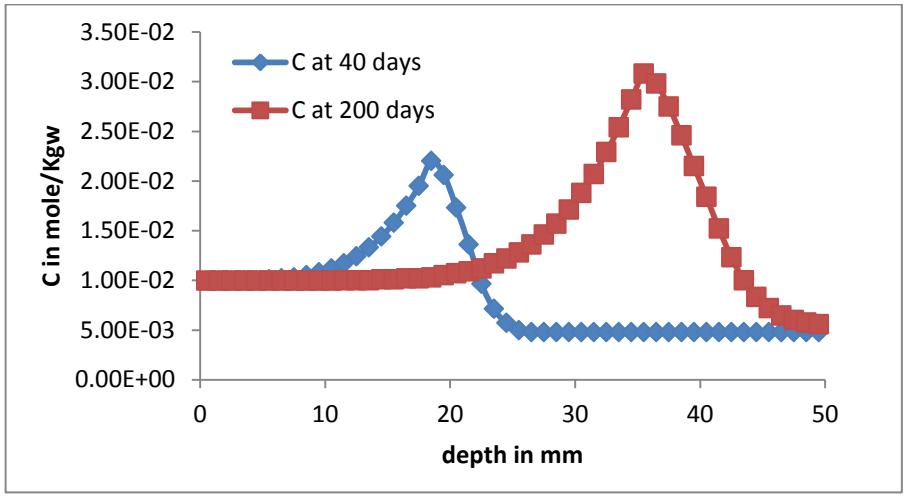

Figure 9.2e Distribution of C at 40 and 200 days based on VS2DRT simulation

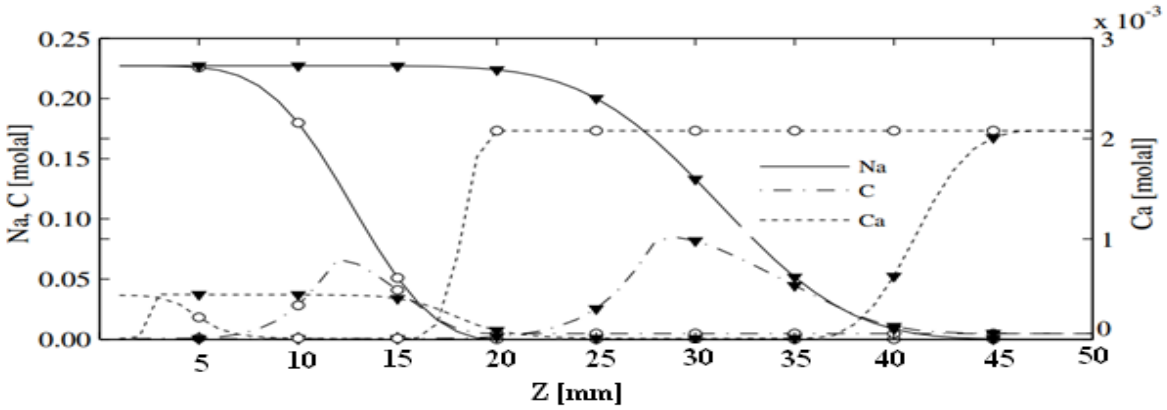

Figure 9.2f Distribution of Na, Ca and C at 40 (circles) and 200 (triangles) days based on HP1 simulation respectively (Wissmeier & Barry, 2008)

9.3 1D reactive transport involving cation exchange

A 1D reactive transport involving cation exchange was taken from PHREEQC (Parkhurst & Appelo, 1999) to be simulated using VS2DRT in 8 cm column of silt loam. Initially the column is filled with 1 mmol $NaNO_3$ and 0.2 mmol KNO_3 solution. Then the column was flushed with 3 pore volume of 0.6 mmol $CaCl_2$. The simulation was conducted for 24 hours at a time step of 0. 05 hour and grid size of 0.1 cm. The hydraulic and geochemical properties of the silt loam soil along with initial and boundary conditions are given in table 9.2.

The results of VS2DRT and PHREEQC simulation at the outlet of the column are presented in figure 9.3a and 9.3b respectively. The cell length, time step and longitudinal dispersivity used in PHREEQC simulation are 0.2 cm, 720 seconds and 0.2cm respectively. Due to lack information regarding hydraulic properties of the column medium used in the initial PHREEQC problem it was not possible to get exact result as PHREEQC in VS2DRT. However, the simulation results from VS2DRT are more or less shows similar pattern as that of PHREEQC. For example Na and Cl give same result for both simulations. For the cases of

Ca and K in case of PHREEQC Ca and K have maximum values is as high as 0.6 mmol/ kgw and 1.1 mmol/kgw respectively. However, VS2DRT results of Ca and K have maximum value is as high as 0.511 mmol/kgw and 0.86 mmol/kgw respectively.

Table 9.2 Hydraulic and geochemical properties of the silt loam column along with initial and boundary conditions

Hydraulic properties of silt loam soil in terms of van Genuchten parameters	
αg	0.00505 cm^{-1}
ng	7
Ks	2.7777E-04 cm/seconds
θs	0.43
θr	0.17
Geochemical properties	
Cation exchanger 1.1 mmol/l of pore water	
Longitudinal dispersivity 0.02 cm	
Initial solution (mmol/kg water)	*Boundary condition solution (mmol/kg water)*
temp 25.0	temp 25.0
pH 7.0 charge	pH 7.0 charge
pe 12.5 $O_2(g)$ -0.68	pe 12.5 $O_2(g)$ -0.68
Na 1.0	Ca 0.6
K 0.2	Cl 1.2
N(5) 1.2	

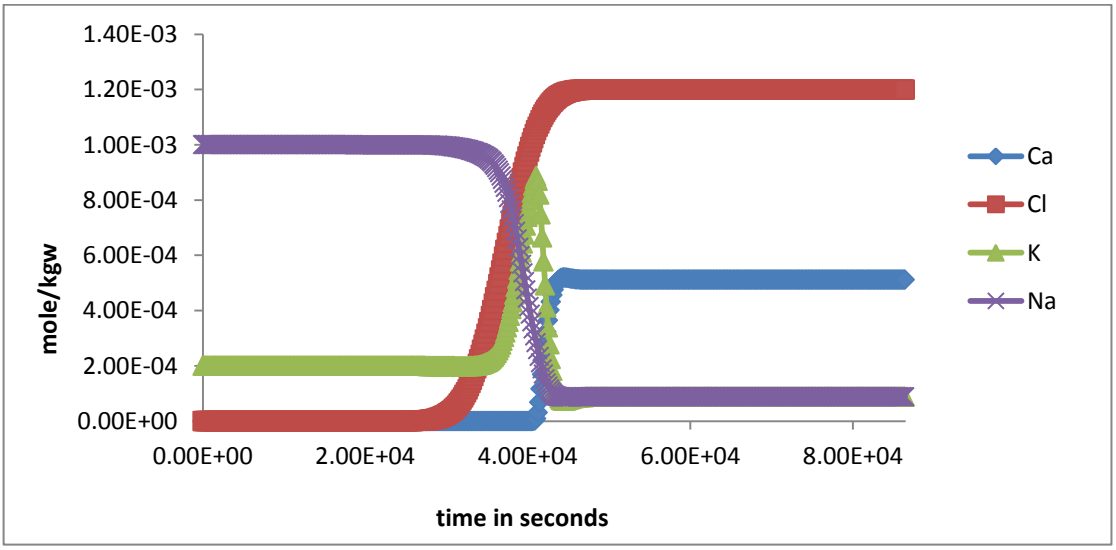

Figure 9.3a Simulation of cation exchange using VS2DRT

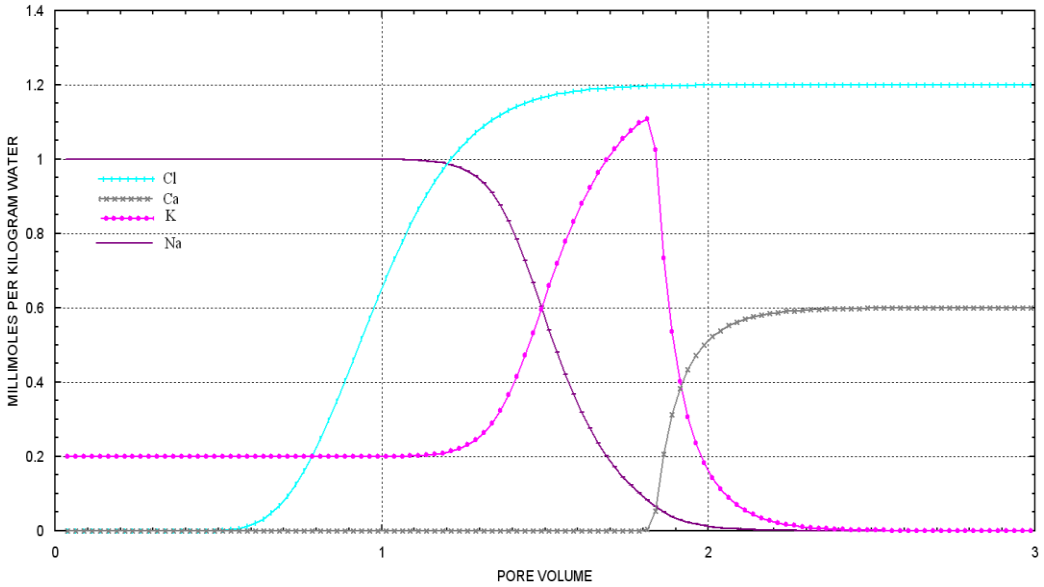

Figure 9.3b PHREEQC simulation of cation exchange in involving advection and dispersion transport.

9.4 1D reactive transport involving dissolution of calcite and gypsum

Reactive transport involving dissolution of gypsum and calcite was simulated with HP1 and is used here to show that VS2DRT capabilities to simulate dissolution of gypsum and calcite. In a 50 cm long column 1 mmol of $CaCl_2$ was infiltrated for 2.5 hour under steady-state saturated flow conditions. The infiltrating solution is in equilibrium with atmospheric partial pressure of oxygen and carbon dioxide. The soil column contains calcite ($CaCO_3$) and gypsum ($CaSO_4.2H_20$) minerals at 2.176 $x10^{-2}$ mmol/kg soil each. The initial solution in the soil column is in equilibrium with calcite, gypsum and atmospheric partial pressure of oxygen. Hydrologic and geochemical properties of the soil column and initial and boundary solutions are presented in table 9.3.

The results of gypsum and calcite dissolution reactive transport simulation using HP1 and VS2DRT are presented in figures 9.4a and 9.4b respectively. The results of the simulation

are identical except a slight difference at the bottom of the column due to difference in solute boundary condition used.

Table 9.3 Hydraulic and geochemical properties of soil column along with initial and boundary solutions

van Genuchten hydraulic properties of silt soil	
αg 0.036 cm^{-1}	
ng 1.56	
Ks 10 cm/day	
θs 0.35	
θr 0.078	
bulk density 1.8g/cm^3	
Geochemical properties	
Calcite 2.176 x 10^{-5} mol/kg soil	
Gypsum 2.176 x 10^{-5} mol/kg soil	
Longitudinal dispersivity 1 cm	
Transverse dispersivity 0.0 cm	
Molecular diffusion 0 cm^2/day	
Initial solution (mmol/kg water)	*Boundary solution (mmol/kg water)*
Gypsum	pH 7.0 charge
Calcite	Cl 2
O2(g) -0.68	Ca 1
	O(0) 1 O2(g) -0.68
	C(4) 1 CO2(g) -3.5

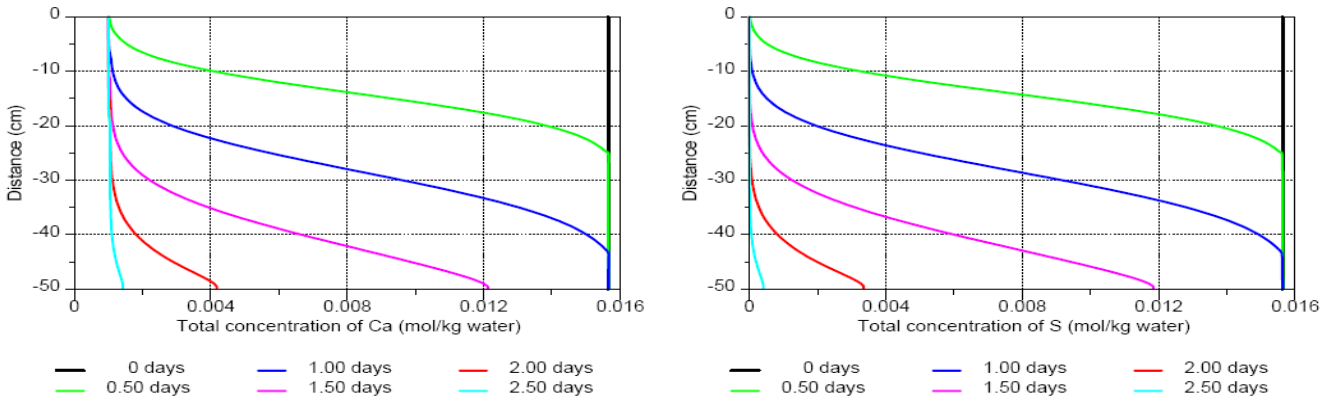

Figure 9.4a Ca and S profile at 0, 0.5, 1, 1.5, 2 and 2.5 days according to HP1 simulation (Jacques & Simunek, 2009)

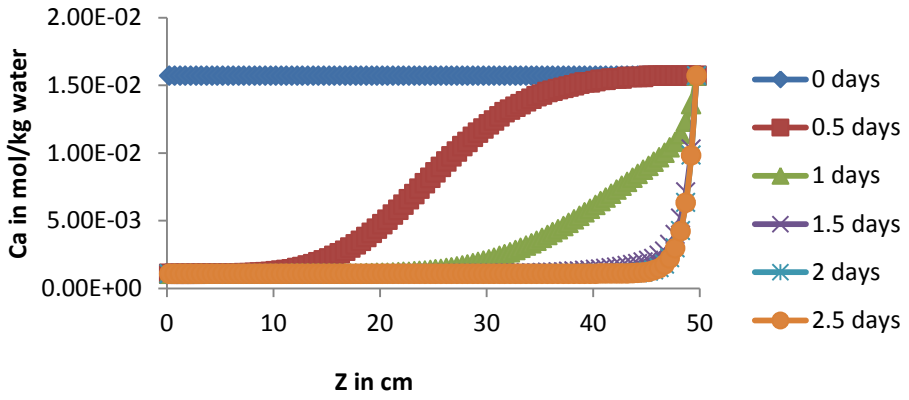

(a)

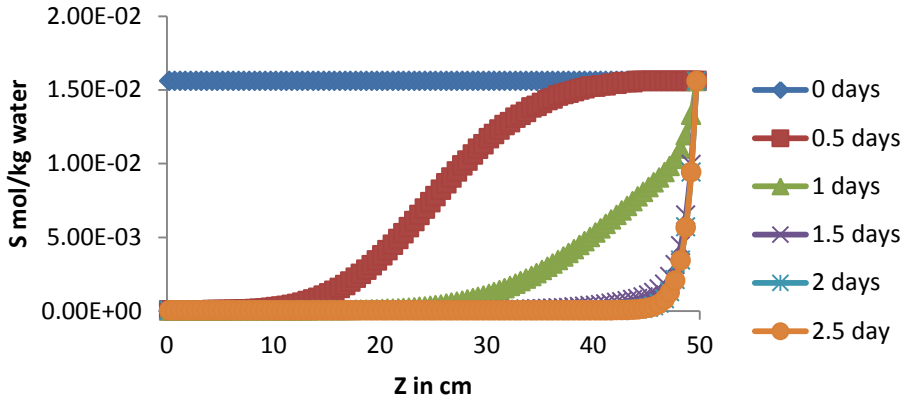

(b)

Figure 9.4b Ca and S profile at 0, 0.5, 1, 1.5, 2 and 2.5 days according to VS2DRT simulation

9.5 1D Heat and solute transport

The problem was taken from USGS Water-Resources Investigations Report 96-4230 (p. 5) (Healy & Ronan, 1996) with modification to simulate heat and chloride transport. A 60 m column soil with vertical spacing of 1.0 m and simulation time of 10765 s was used. Hydraulic, thermal and chemical properties of the medium along with initial and boundary conditions for flow, heat and reactive transport is given in table 9.4.

Table 9.4 Hydraulic, thermal and geochemical properties soil column along with initial and boundary conditions for heat and reactive transport

Hydraulic properties in terms of van Genuchten parameters	
α_g	0. 05 cm^{-1}
ng	3
K_s	0.0001389 m/second
θ_s	0.5
θ_r	0
Thermal properties of the medium	
α_L	10 m
α_T	10 m
C_s	2.08E+06
C_w	4.2E+06
K_{tr}	1.8
K_{ts}	1.8
Geochemical properties	
α_L	10 m
molecular diffusion	1.E-06
Initial solution (g/kg water)	*Boundary condition solution (g/kg water)*
Cl 0.0	Cl 1.
Initial Temperature	Boundary temperature (top)
T 20 °C	T 21 °C
Initial pressure head 1 m	Boundary pressure head 1m

Figure 9.5a shows that the spatial distribution of temperature based on VS2DRT and VS2DH simulation. The VS2DRT simulation result is same as that of VS2DH which show that the heat transport is properly coupled to the reactive transport. Figure 9.5b show spatial distribution of chloride based on VS2DRT model.

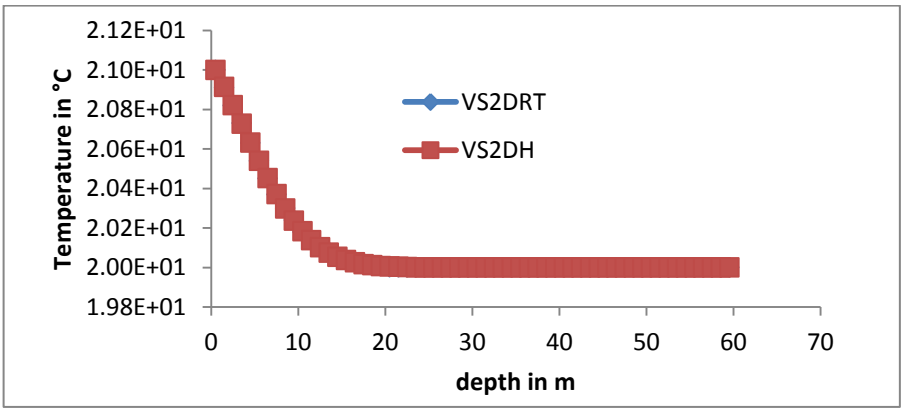

Figure 9.5a Comparison of heat simulation of VS2DRT with that of VS2DH

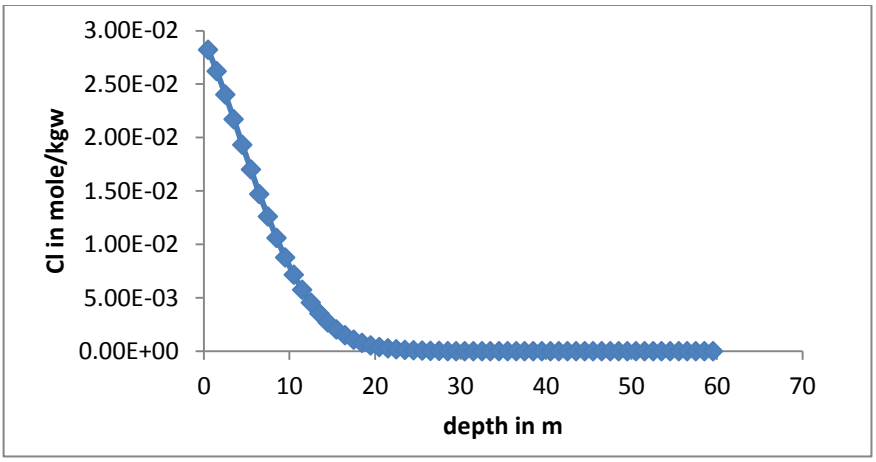

Figure 9.5b conservative Cl transport simulated with heat transport using VS2DRT

9.6 2D reactive transport involving cation exchange

A furrow irrigation problem presented in UNSATCHEM and HP2 (Simunek, Jacques, Sejna, & van Genuchten, 2012) manuals is used to simulate two dimensional infiltration of gypsum saturated water in to sodic soil. The schematic representation of the domain of simulation is presented in figure 9.6a along with the finite difference grid used. Initial pressure head condition of -200 cm is used. Soil hydraulic and chemical properties along with chemical initial and boundary conditions are presented in table 9.5. It is assumed that furrow is flooded with water and the water level in the furrow was kept at constant 6 cm. Due to symmetry, the simulation was carried out only for the domain between the axis the two neighboring furrows. The bottom boundary considered as free drainage and zero flux is considered for the rest of the boundaries. The simulation was carried out for 5 days with initial, maximum and minimum time steps of 0.001, 0.001 and 0.00001 days respectively and time multiplication factor of 1.3.

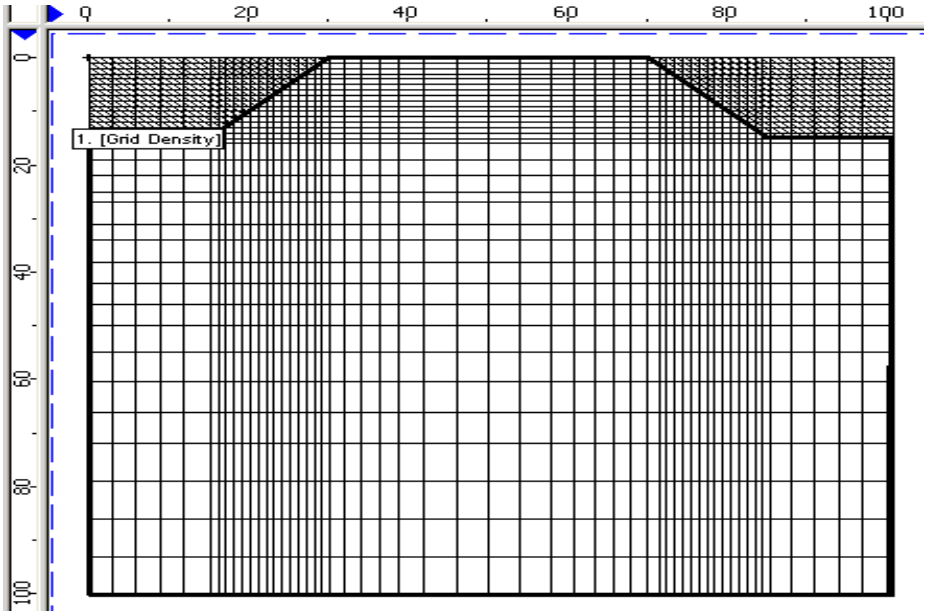

Figure 9.6a Schematic representation of furrow irrigation simulation domain along with finite difference grid.

Table 9.5 Hydraulic and geochemical properties of simulation domain along with initial and boundary solutions for furrow irrigation problem

van Genuchten hydraulic properties of silt soil			
αg	0.016 cm^{-1}		
ng	1.37		
Ks	6 cm/day		
θs	0.46		
θr	0.034		
bulk density	1.4g/cm^3		
Geochemical properties			
Cation exchanger	0.01 mol/L of soil		
Longitudinal dispersivity	2 cm		
Transverse dispersivity	0.2 cm		
Molecular diffusion	2 cm^2/day		
Initial solution (mmol/kg water)		*Boundary solution (mmol/kg water)*	
temp	25.0	temp	25.0
pH	7.0 charge	pH	7.0 charge
Na	5	Na	4.4
Ca	1	Ca	16.3
Cl	0.0	Cl	5.0
S(6)	3.5	S(6)	16.0
O(0)	1 O_2(g) -0.68	O(0)	1 O_2(g) -0.68

The results of VS2DRT simulation are presented in figures 9.6b, 9.6d, and 9.6f for pressure head, chloride and sodium profiles at various times respectively. The results of HP2 simulation are also presented in figures 9.6c, 9.6e and 9.6g for pressure head, chloride and sodium respectively.

Pressure head profile at 0.1, 0.5, 1 and 2 days based on VS2DRT simulation shows that pressure head ranges from -207.6 to 6 cm which is also similar to HP2 simulation result which shows pressure head ranges from -209.9 to 6 cm.

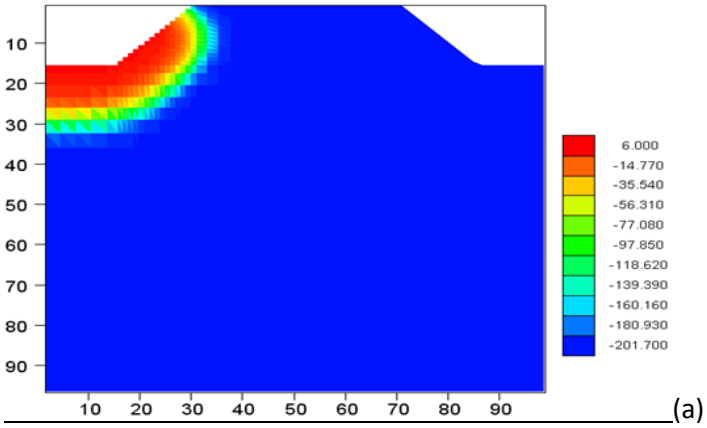

(a)

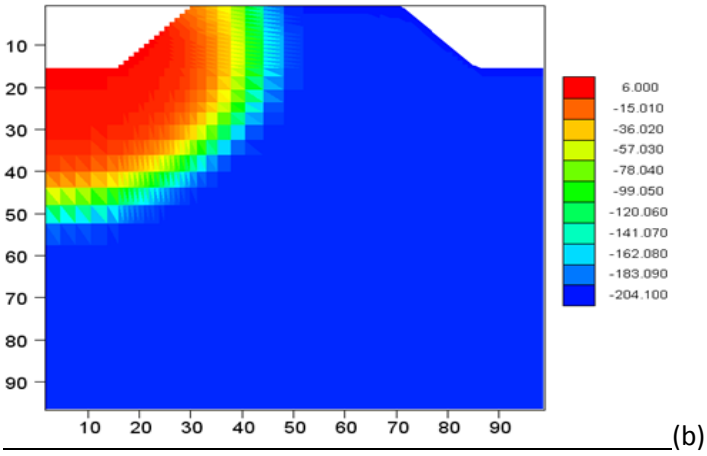

(b)

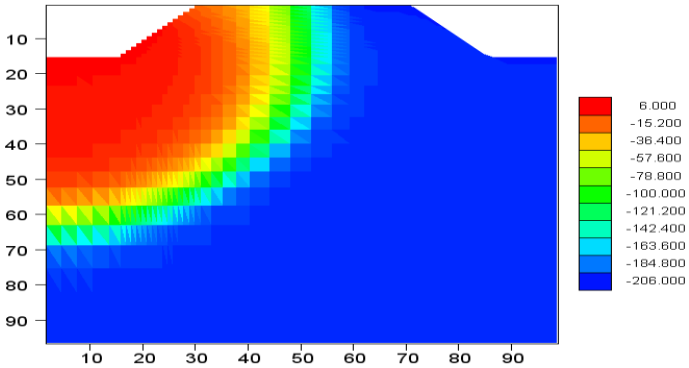

(c)

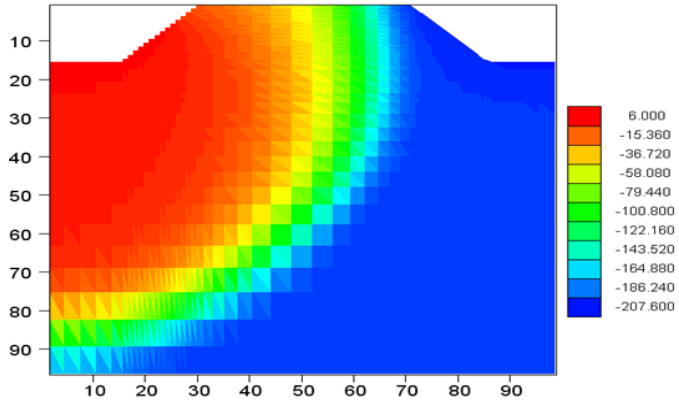

(d)

Figure 9.6b Pressure head profile at times a) 0.1, b) 0.5, c) 1 and d) 2 days using VS2DRT simulation

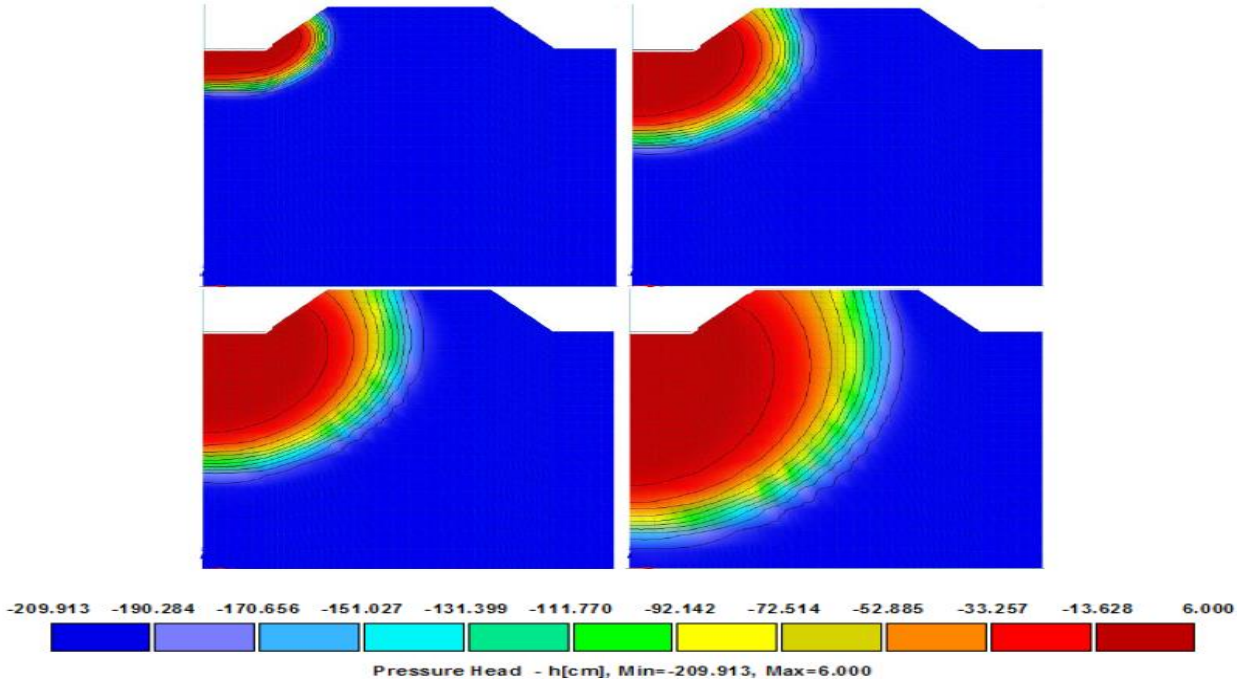

Figure 9.6c Pressure head profile at times a) 0.1, b) 0.5, c) 1 and d) 2 days using HP2 simulation (Simunek, Jacques, Sejna, & van Genuchten, 2012)

Chloride profile at 0.1, 1, 3 and 5 days based on VS2DRT simulation shows that concentration of Cl ranges from 0.005 to 0 mol/l. High concentration of Cl is observed near the furrow and concentration of Cl is zero towards the bottom and left side of the profile. Chloride profile at 0.1, 1, 3 and 5 days based on HP2 simulation also show same result.

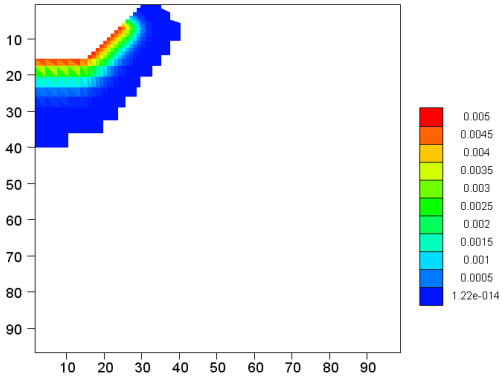

(a)

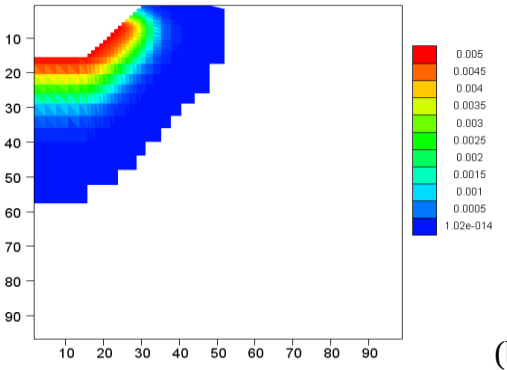

(b)

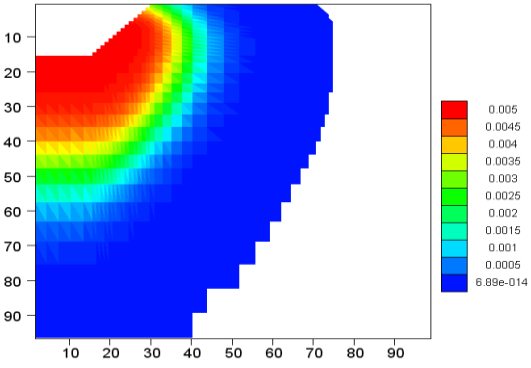

(c)

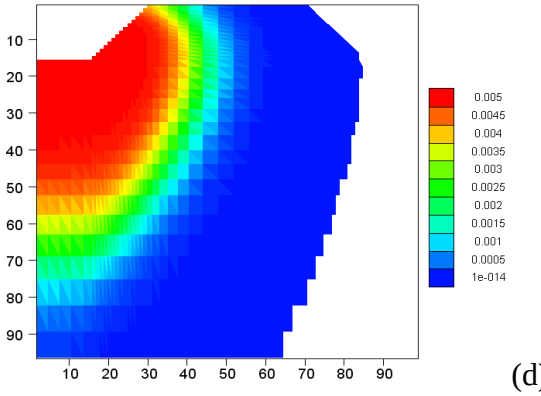

(d)

Figure 9.6d Chloride in mol/l profile at times a) 0.1, b) 1, c) 3 and d) 5 days using VS2DRT simulation

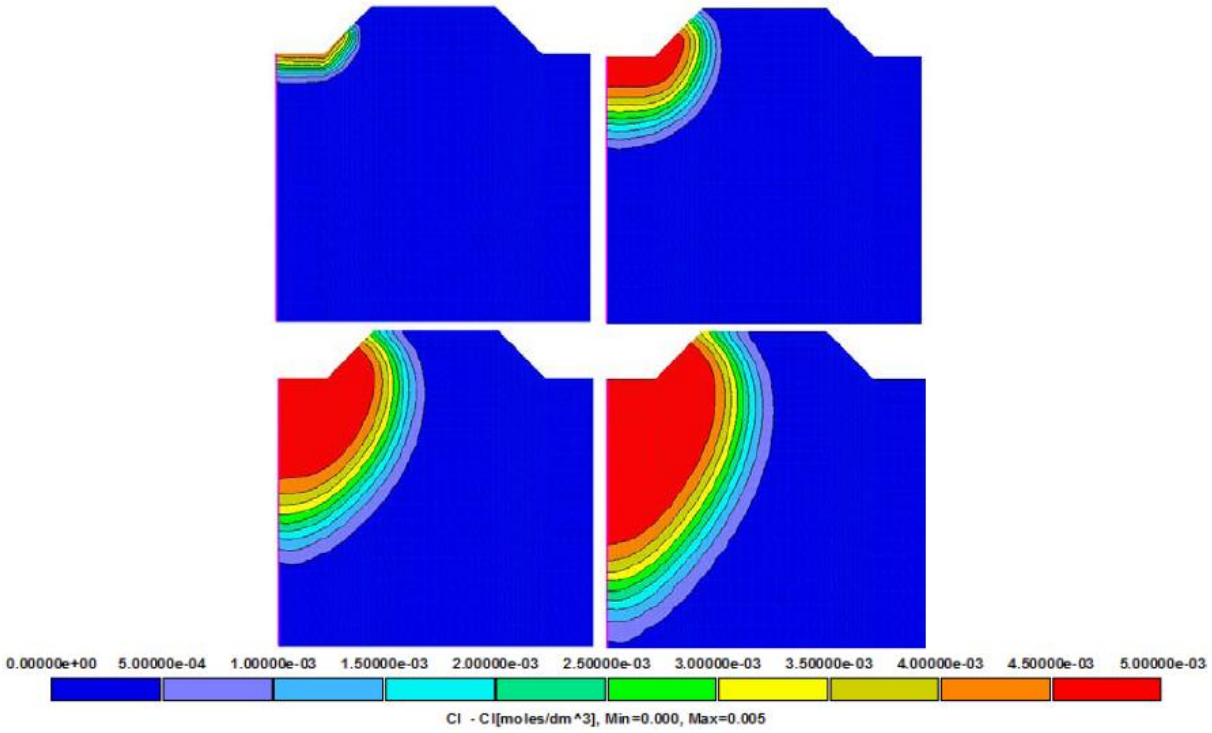

Figure 9.6e Chloride in mol/l profile at times a) 0.1, b) 1, c) 3 and d) 5 days using HP2 simulation (Simunek, Jacques, Sejna, & van Genuchten, 2012)

Sodium profile at 0.1, 1, 3 and 5 days based on VS2DRT simulation shows that concentration of Na ranges from 0.00581 to 0.0049 mol/l. High concentration of Na is observed water

flow front and concentration of Na is lower towards the furrow and left side of the profile. Chloride profile at 0.1, 1, 3 and 5 days based on HP2 simulation also show same result with Na range of 0.0044 to 0.0067 mol/l.

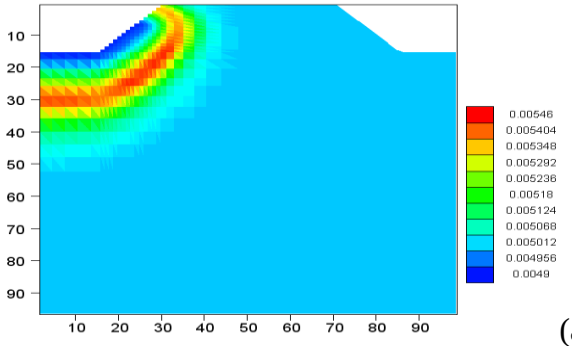

(a)

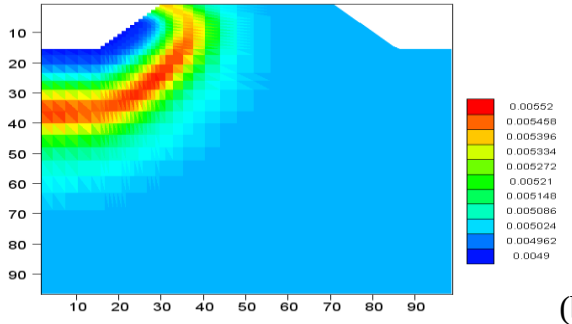

(b)

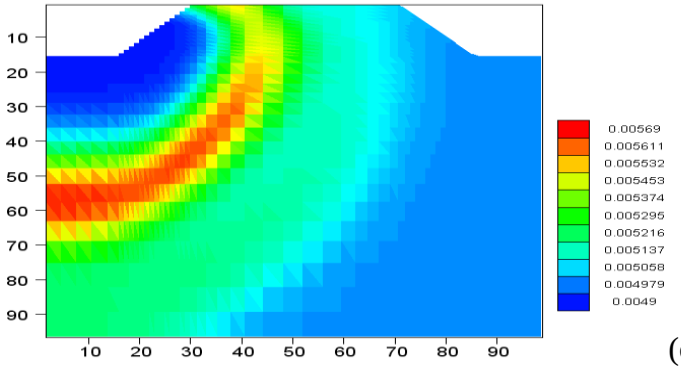

(c)

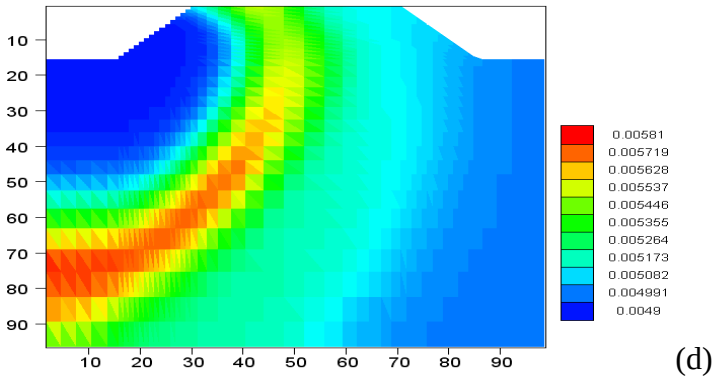

(d)

Figure 9.6f Na in mol/l profile at times a) 0.1, b) 1, c) 3 and d) 5 days using VS2DRT simulation

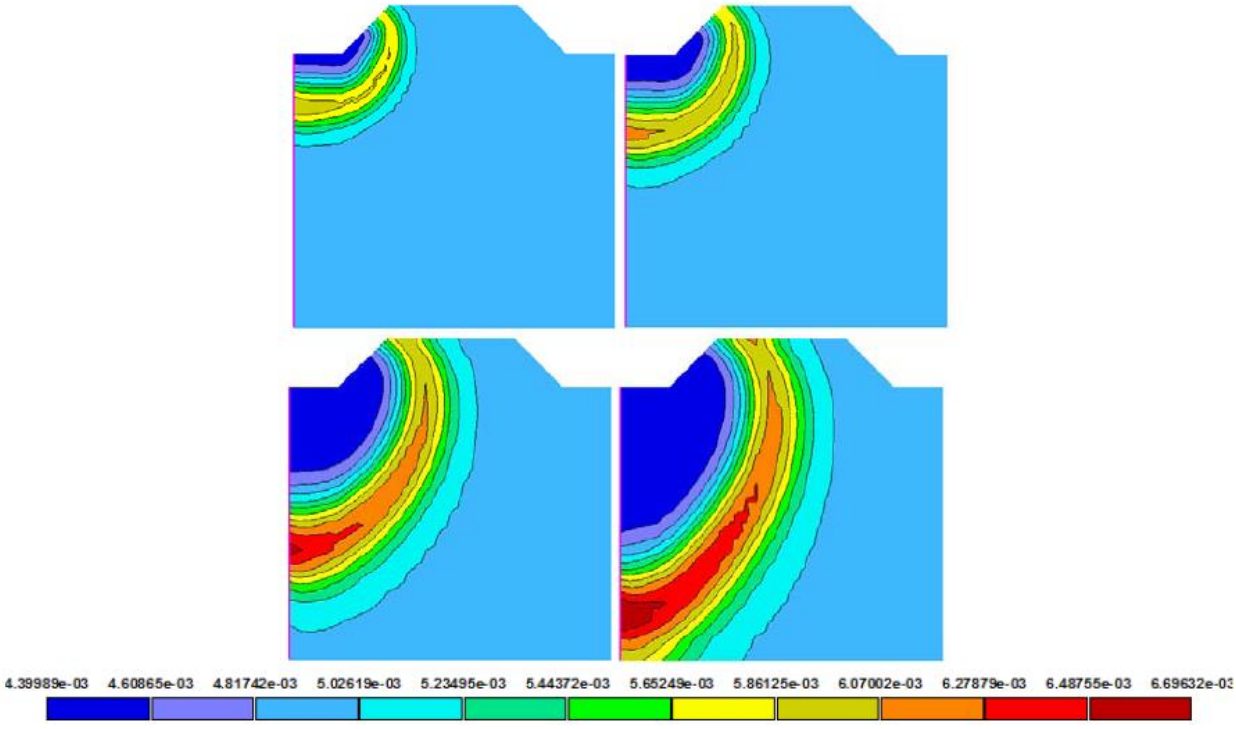

Figure 9.6g Na in mol/l profile at times a) 0.1, b) 1, c) 3 and d) 5 days using HP2 simulation (Simunek, Jacques, Sejna, & van Genuchten, 2012)

9.7 2D reactive transport

The problem was taken from USGS Water-Resources Investigations Report 83-4099 (p. 93) (Healy & Ronan, 1996) and modified to include reactive transport. It involves 2D infiltration and evaporation along with reactive transport. The simulation domain has 3 m width and 2.1 m height and contains clay, sand and gravel textural classes as presented in figure 9.7a. A gravel of 0.6m thick is overlaid by 1.5m thick clay which embeds 0.3m thick and 1.5m wide sand at depth of 0.4 m.

The Brooks & Corey hydraulic parameters of clay, sand and gravel soils, chemical properties along with the initial flow condition and initial solution in the domain of simulation is given in table 9.6. The simulation was conducted for 77 days with four recharge periods and the recharge period parameters are presented in table 9.7. Evaporation and evapotranspiration related parameters were given in table 9.8. The results of the simulation are presented in figures 9.7b, 9.7d to 9.7g for pressure head, Ca, Cl and Na at 1, 16, 33 and 77 respectively. Figure 9.5b and 9.5c depict temporal variation of evaporation and evapotranspiration rate simulated by VS2DRT and VS2D respectively and shows that VS2DRT simulation of evaporation and evapotranspiration are rather consistent with that of VS2D.

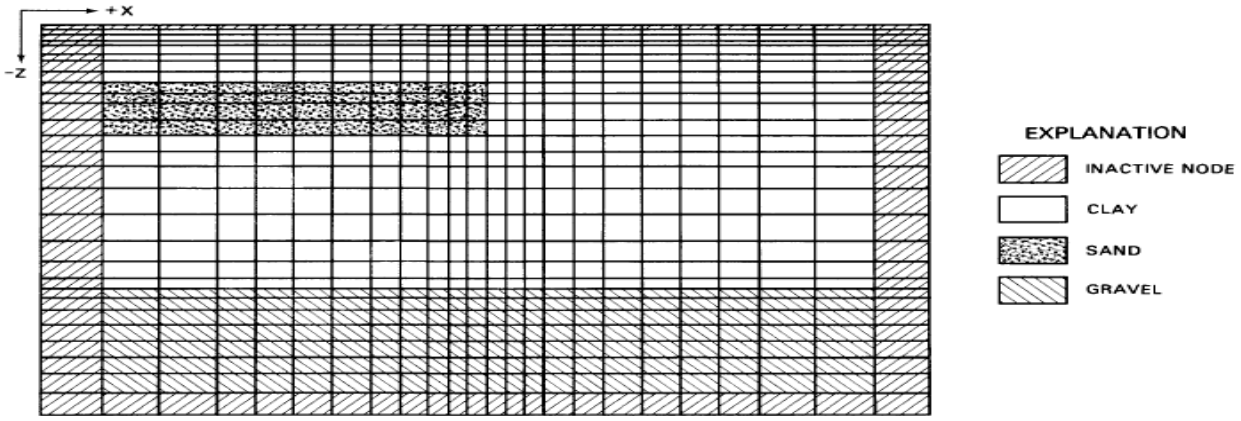

Figure 9.7a vertical section of simulation domain (Lappala, Healy, & Weeks, 1987)

Table 9.6 Hydraulic and geochemical properties, initial and boundary conditions for 2D reactive transport

Hydraulic properties in terms of Brooks & Corey parameters			
	Clay	*Sand*	*Gravel*
K_z/K_x	1	1	1
K_s	5 cm/day	100 cm/day	300 cm/day
Specific storage	1e-6	1e-6	1.e-6
θ	0.45	0.40	0.42
θ_r	0.15	0.08	0.05
h_b	- 50 cm	-15	-8
λ	0.6	1	1.2
Geochemical properties			
α_L	1 m		
α_T	1 m		
molecular diffusion	1.E-06		
Initial solution (mmol/kg water)		*Boundary condition solution (mmol/kg water)*	
Ca 1		Na 1	
C 1		Cl 1	
Initial equilibrium head profile			
Water table depth at 2 m			
Minimum pressure head of -1 m			

Table 9.7 Recharge period parameters used for 2D reactive transport

Recharge Period	*Duration (days)*	*Type of boundary at the top*
1	1	Infiltration at 75mm/day rate and Pressure head of 4 m at the bottom
2	30	Evaporation
3	1	Infiltration at 75mm/day rate
4	45	Evaporation and Evapotranspiration

Table 9.8 Evaporation and evapotranspiration parameters used for 2D reactive transport simulation

Evaporation periods	*PEVAL*	*SRS*	*HA*		
1	0.2	0.6	-100000		
2	0.2	0.6	-100000		
3	0.2	0.6	-100000		
4	0.2	0.6	-100000		
Evapotranspiration periods	*PTVAL*	*Root depth*	*RA Bottom*	*RA Top*	*P.Head at Root*
1	0.0	0.0	0.2	0.9	-8000
2	0.0	35	0.2	0.9	-8000
3	0.45	35	0.2	0.9	-12000
4	0.6	35	0.2	0.9	-15000

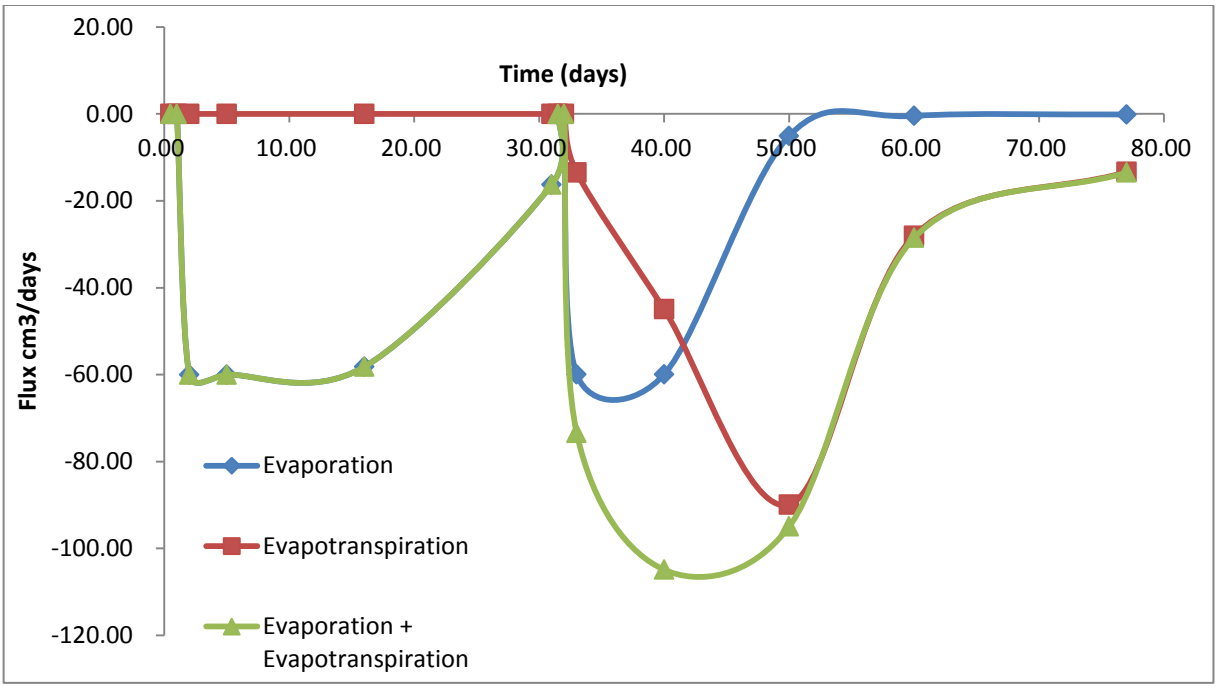

Figure 9.7b VS2DRT simulation of evaporation and evapotranspiration rates

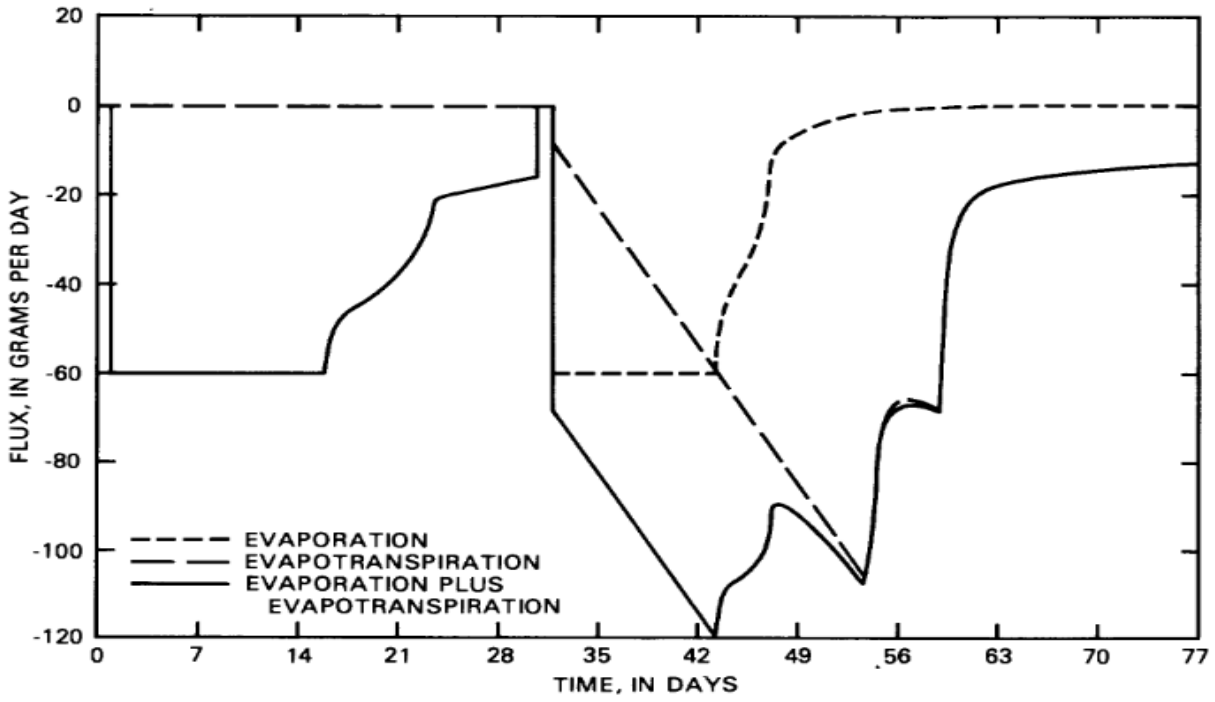

Figure 9.7c VS2D simulation of evaporation and evapotranspiration rates (Lappala, Healy, & Weeks, 1987)

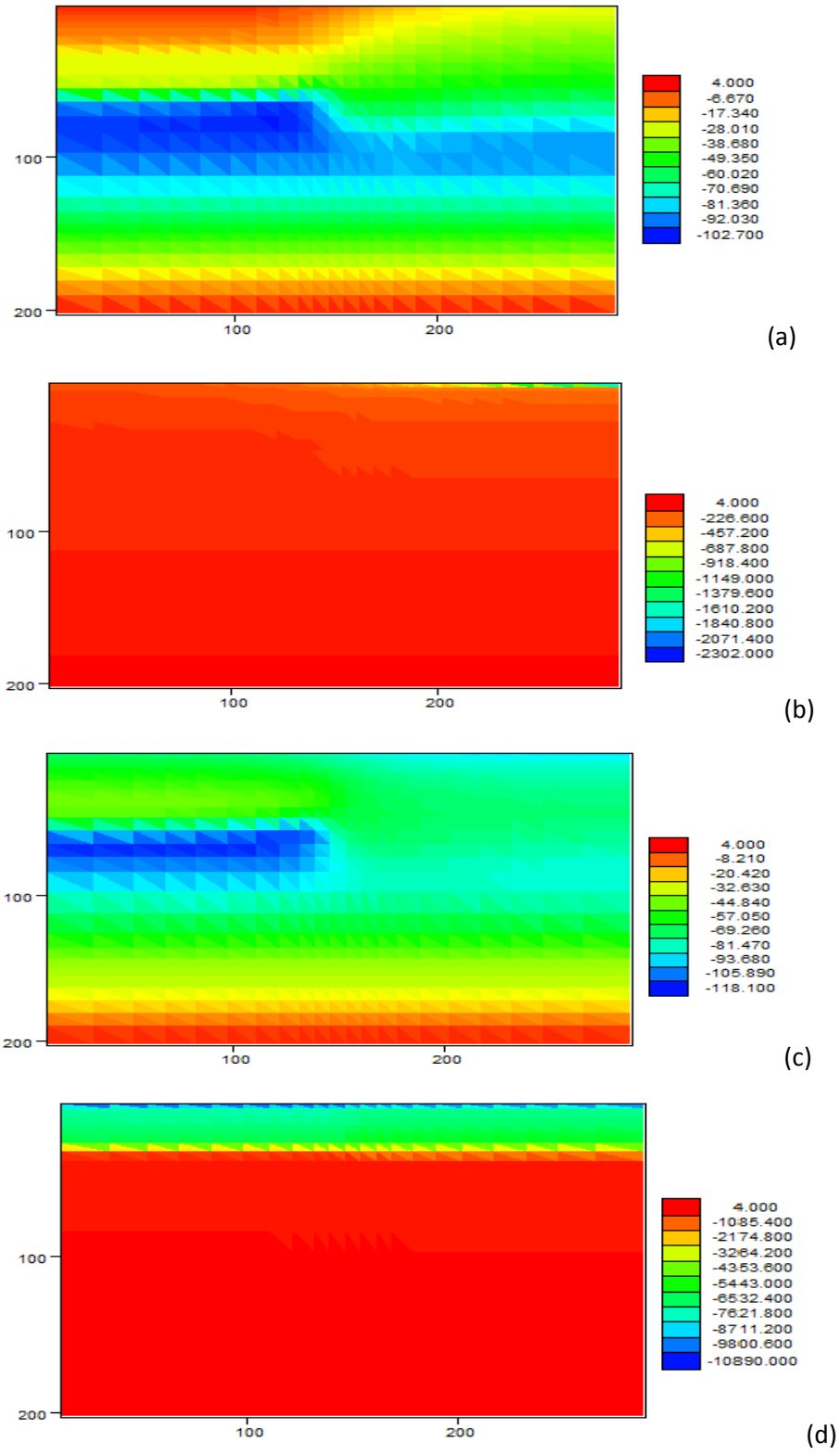

Figure 9.7d Pressure head profile based on VS2DRT at a) 1, b) 16, c) 33 and d) 77days respectively

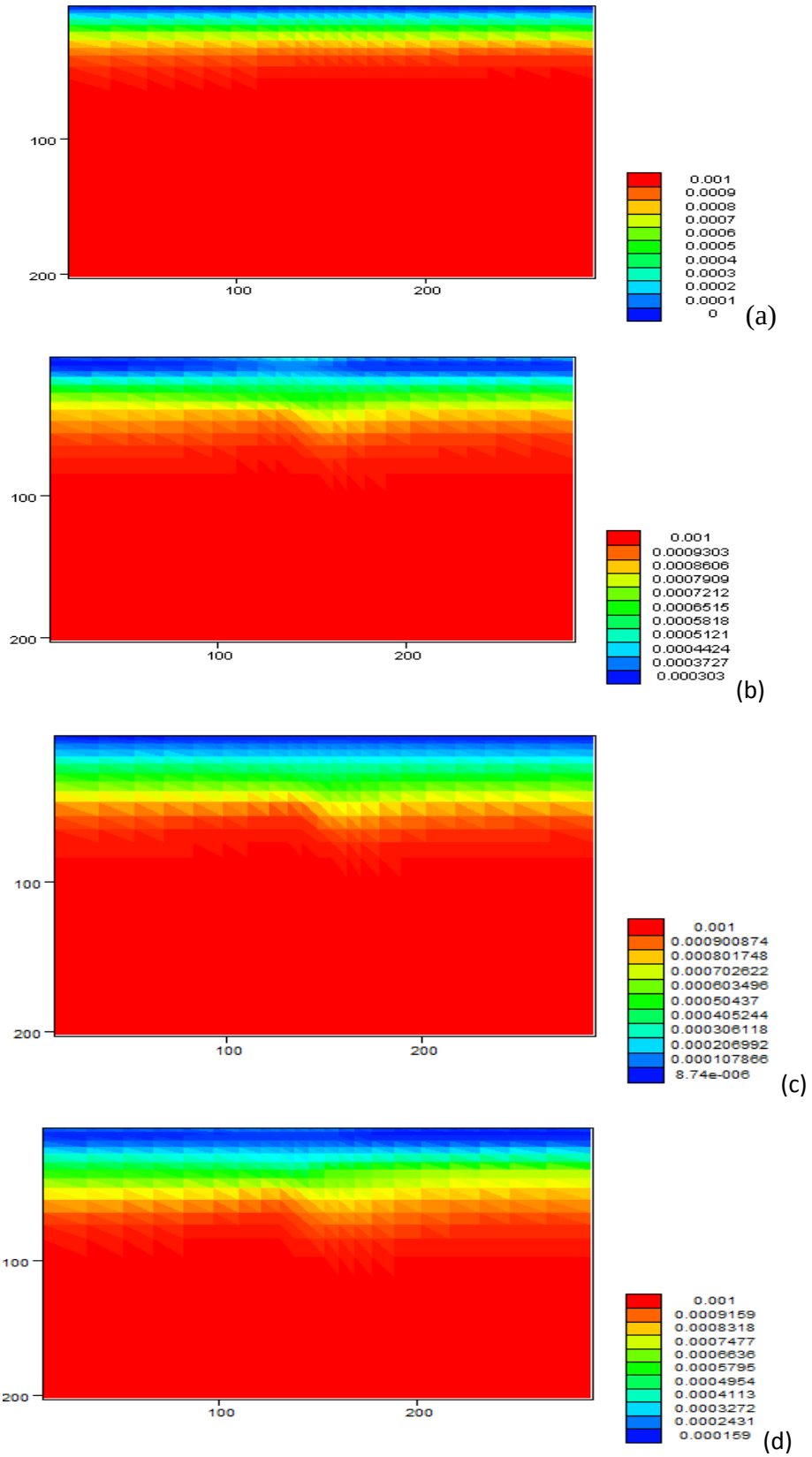

Figure 9.7e Ca profile based on VS2DRT at a) 1, b) 16, c) 33 and d) 77days respectively

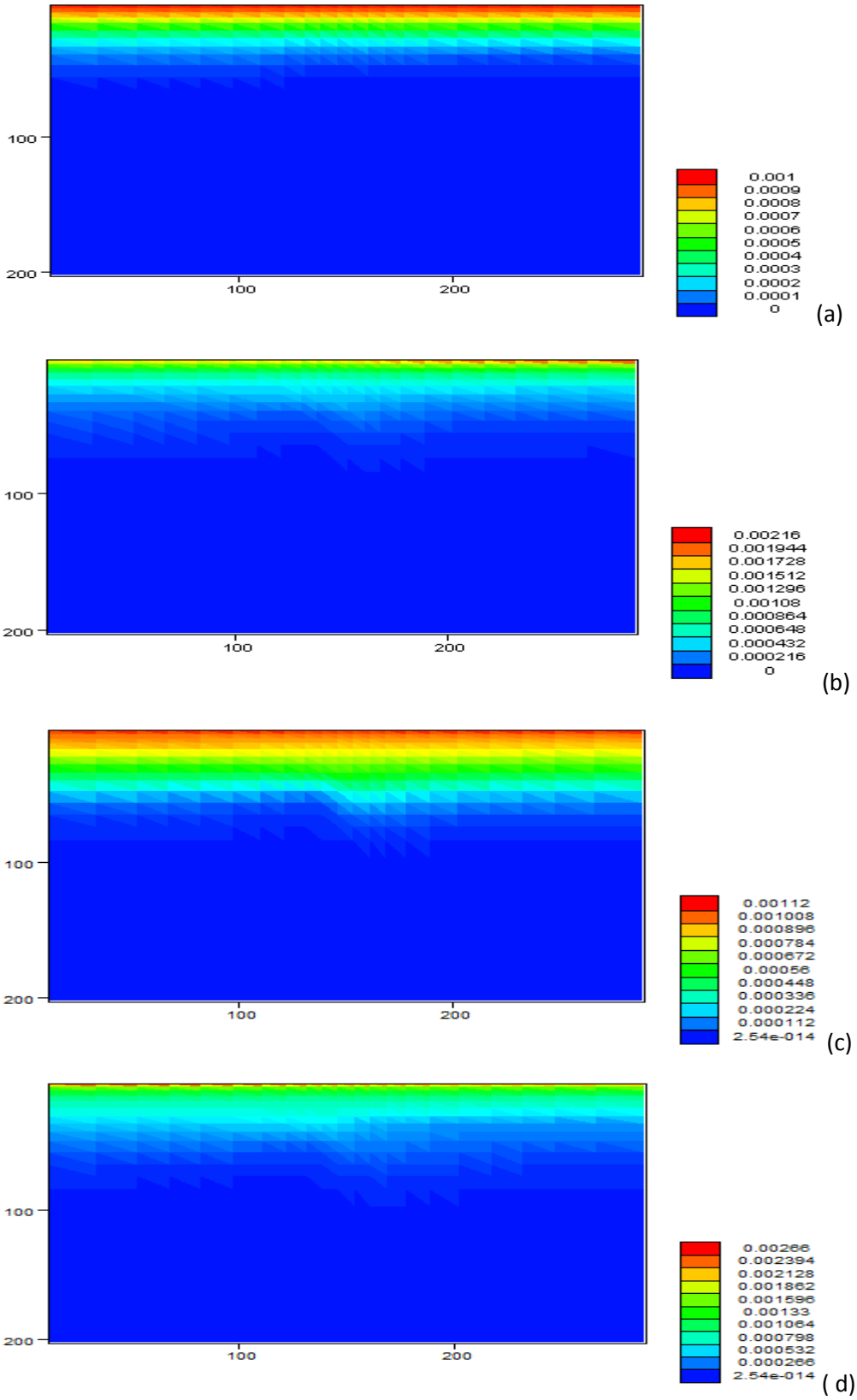

Figure 9.7f Cl profile based on VS2DRT at a) 1, b) 16, c) 33 and d) 77days respectively

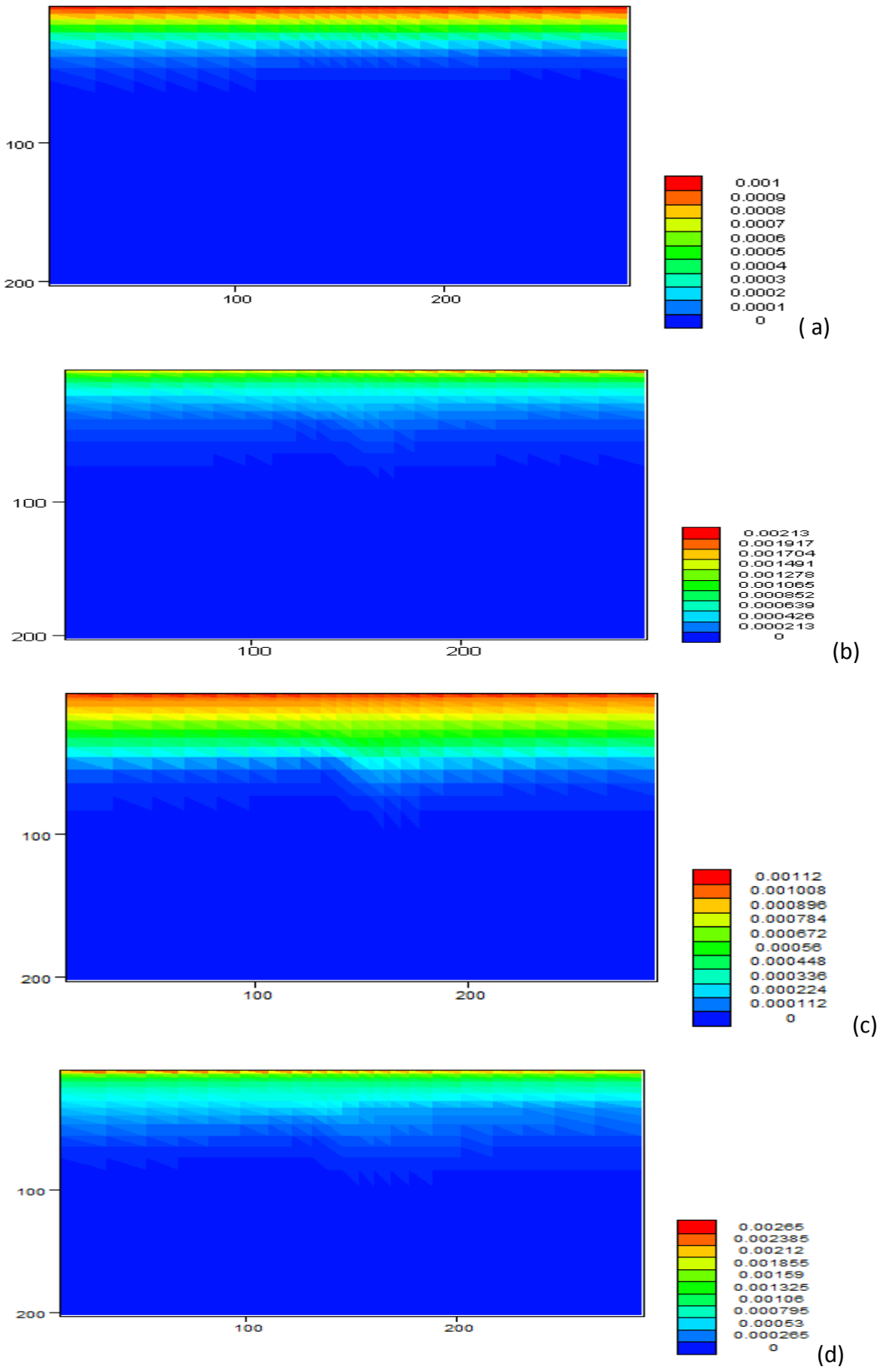

Figure 9.7g Na profile based on VS2DRT at a) 1, b) 16, c) 33 and d) 77days respectively

Chapter Ten: Conclusion and recommendations

10.1 Conclusion

VS2DRT couples VS2DT and VS2DH with PHREEQC using sequential non-iterative operator splitting techniques where unsaturated flow, heat and multi-solute transports are computed by VS2DT and VS2DH followed by equilibrium and kinetic chemical reaction computations done by PHREEQC. The coupling physical properties are flow velocity, saturated hydraulic conductivity and chemical constitute of the medium. The VS2DRT model does not take into considerations the variation of density, porosity, hydraulic conductivity due to chemical reaction and consider only liquid phase flow. Additionally, in case of heat transport and reactive transport simulation the effect of chemical reaction on temperature is not considered however the effect of temperature on hydraulic conductivity is considered.

The FORTRAN based flow, heat and solute transport and C/C++ based PHREEQC codes were compiled using MinGW compiler with the help of tools like Autotools and Automake and libraries like zlib and Boost. Graphical user interface was also prepared using Qt creator and Argus ONE development tools.

VS2DRT has successfully coupled VS2DT, VS2DH with PHREEQC and can be used to simulate reactive transport in variably saturated media. VS2DRT has been tested with published data for non-reactive, cation exchange, surface complexation transport cases and works well. Since VS2DT, VS2TH and PHREEQC are well tested programs the verification case for chloride transport, cation exchange, surface complexation, dissolution of calcite and gypsum and heat transport was focused on testing the coupled processes. The VS2DRT simulation results for the verification cases give similar result for 1D chloride and heat transport

as that of VS2DT and VS2DH. In the cases of 1D cation exchange, surface complexation and dissolution of calcite and gypsum show same pattern but slightly different. However the reliably of the result depends highly on the inputs provided. It is always advisable to compare reactive transport models with other available reactive transport models to get more reliable solutions in cases of decision making. VS2DRT can be used to simulate cation exchange, sorption, dissolution and precipitation and various kinetic reactive transport and heat transport in the vadose zone. It can be used to predict the fate of contaminate transport in vadose zone as well to design proper remedial measures for contaminated sites.

10.2 Recommendations

The obtain a reliable result all the necessary hydraulic, thermal and geochemical properties should be representative of the simulation domain and boundary and initial conditions should be properly assigned. Moreover, grid size and time step should be careful chosen to obtain more reliable results as well as to reduce numerical errors. Initial and boundary solutions as well as cation exchange, surface complexation, equilibrium phase as well as kinetic reaction should be properly set. Comparing results of the simulation with other relevant reactive transport models results as well as measured data would be helpful in making decisions.

The capabilities of VS2DRT could be improved by incorporating gas phase transport and CO_2 production which is common for the vadose zone. Moreover, the impact of geochemical reactions on hydraulic properties of medium could be incorporated as well. Additionally, computational speed could be improved using parallel programing techniques.

Future area of research could be a further development of the graphical user interface and parallelized versions for existing numerical models, development and implementation of spatial and temporal error estimators and adaptive local grid and time-step refinement algorithms to automatically minimize these errors (Šimůnek and Bradford, 2008). However, future advances in vadose zone modeling will also be limited by our understanding of the fundamental physical, chemistry and biology that occurs in subsurface environments (Šimůnek and Bradford, 2008). Moreover, future developments in vadose zone modeling will impacted by new numerical techniques , linear and nonlinear solvers, grid generation, parallel computing techniques, visualizations and optimization techniques and others (U.S. Department of Energy, 2001).

Reference

Abrahamsen, P., & Hansen, S. (2000). Daisy: an open soil-crop-atmosphere system model. *Environmental Modelling & Software*, 313-330.

Appelo, C., & Rolle, M. (2010). PHT3D: A reactive Multicomponent Transport Model for Saturated Porous Media. *National Ground Water Association*.

Bear, J. (1979). *Hydraulics of Groundwater.* McGraw-Hill Publishing Company.

Brooks, R., & Corey, A. (1964). *Hydraulic properties of porous media.* Colorado State University.

Carrayrou, J., Mose, R., & Behra, P. (2004). Operator-Splitting procedures for reactive transport and comparison of mass balance errors. *Journal of Contaminant Hydrology*, 239-268.

Constantz, J., Tyler, S., & Kwiccklis. (2003). Temperature-profile methods for estimating percolation rates in arid environments. *Vadose Zone Journal*, 12-24.

Corapcioglu, M. (1994). *Advances in porous media, Volume 2.* Elsevier.

Fayer, M. J. (2000). *UNSAT-H Version 3. Unsaturated Soil Water and Heat Flow Model , Theory, User Manual and Examples.* U.S. Department of Energy.

Flerchinger, G. N. (2000). *The Simultaneous Heat and Water (SHAW) Model User's Manual.* Boise, Idaho: Northwest Watershed Research Center USAD Agricultural Research Service.

Gwo, J., D' Azevedo, E., Frenzel, H., Mayes, M., Yeh, G., Salvage, K., & Hoffman, F. (2001). HBGC123D: a high-performance computer model for coupled hydrogeological and biogeochemical processes. *Computers and Geosciences*, 1231-1242.

Healy, R. (1990). *Simulation of solute transport in variably saturated porous media with supplemental information on modifications to U.S. Geological Survey's Computer Program VS2D.* Denver, Colorado: U.S. Geological Survey.

Healy, R., & Ronan, A. (1996). *Documentation of Computer Program VS2DH for simulation of energy transport in Variably saturated porous media--modification of the US Geological Survey's computer program VS2DT.* Denver, Colorado: US Geological Survey.

Jacques, D., & Simunek, J. (2005). *User Manual of the Multicomponent variably-saturated Flow and Transport model HP1.* Boeretang, Belgium: Belgian Nuclear Research Center.

Jacques, D., & Simunek, J. (2009). *HP1 Tutorials II (HYDRUS-1D + PHREEQC).* Prague: Pc- progress engineering software developer.

Källvenius, G., & Ekberg, C. (2003). TACK- a program coupling chemical kinetics with a two-dimensional transport model in geochemical systems. *Computers and Geosciences*, 511-521.

Kipp, K. (1987). *HST3D: A computer code for simulation of heat and solute transport in three-dimensional ground-water flow systems.* Denver,Colorado: U.S. Geological Survey.

Kroes, J., van Dam, J., Huygen, J., & Vervoort, R. (1999). *User's Guide of SWAP Version 2.0.* Wageningen Agricultural University, Department of Water Resources.

Lappala, E., Healy, R., & Weeks, E. (1987). *Documentation of computer program VS2D to solve the equations of fluid flow in variably saturated porpous media.* Denver, Colorado: U.S. Geological survey.

Larsbo, M. a. (2003). *MACRO 5.0 A model of water and solute transport in macroporous soil, Technical description.* Swedisch University of Agricultural Sciences Department of soil sciences.

Leij, F., & Bradford, S. (1994). *3DADE: A Computer Program for Evaluating Three-Dimensional Equilibrium Solute Transport in Porous Media.* Riverside, California: U.S. Salinity Laboratory.

Leij, F., & Toride, N. (1997). *N3DADE: A Computer Program for Evaluating Nonequilibrium three-dimensional Solute Transport in Porous Media.* Riverside, California: U.S. Salinity Laboratory.

Lichtner, P. (1996). Continuum formulation of multicomponent-multiphase reactive transport. In P. S. Lichtner, *Reactive transport in porous media* (pp. 1-79). Washington, DC: The Mineralogical society of America.

Mao, X., Prommer, H., Barry, D., Langevin, C., Panteleit, B., & Li, L. (2006). Three-dimensional model for multi-component reactive transport with variably density groundwater flow. *Environmental Modelling & Software*, 615-628.

Nielsen, D., van Genuchten, M., & Biggar, J. (1986). Water flow and Solute transport Processes in the unsaturated Zone. *Water Resources Research*, 89S-108S.

Nimmo, J., & Landa, E. (2005). The soil physics contributions of Edgar Buckingham. *Soil Science Society of America*, 328-342.

Parkhurst, D. L., Kipp, K., Engesgaard, P., & Charlton, S. (2004). *PHAST-A Program for Simulating Ground-Water Flow, Solute Transport, und Multicomponet Geochemical Reactions.* Denver, Colorado: U.S. Geological Survey.

Parkhurst, D., & Appelo, C. (1999). *User's guide to PHREEQC (version-2) a computer program for speciation, batch-reaction, one-dimensional transport, and inverse geochemical calculations.* Denver, Colorado: U.S. Geological survey.

Philip, J. (1974). Fifty years progress in soil physics. *Geoderma*, 265-280.

Pruess, K., Oldenburg, C., & Moridis, G. (1999). *TOUGH2 USER'S GUIDE , VERSION2.* Berkeley, California: Lawrence Berkeley National Laboratory, University of California.

Raats, P., & van Genuchten, M. (2006). Milestones in soil physics. *Soil Science,* S21-S28.

Rolston, D. (2007). Historical development of soil-water physics and solute transport in porous media. *Water Science & Technology: Water supply*, 59-66.

Ronen, D., & Sorek, S. (2005). The unsaturated zone-a negelected component of nature. In P. V. Gunnar Nützmann, *Reactive transport in soils and groundwater , processes and models* (pp. 3-15). Springer.

Rossi, C., & Nimmo, J. (1994). Modeling of soil water retention from saturation to oven dryness. *Water Resources Research*, 701-708.

Schwartz, F., & Zhang, H. (2003). *Fundamentals of ground water.* John Wiley & Sons, Inc.

Sejna, M., Simunek, J., & and van Genuchten, M. (2011). *The HYDRUS Software Package for Simulating the Two and Three-Dimensional Movement of water, Heat and Multiple Solutes in Variably-Saturated Media Version 2.* Prague: Pc-progress engineering software developer.

Selker, J., Keller, C., & McCord, J. (1999). *Vadose zone processes.* Lewis Publishers.

Simunek, J., & Bradford, S. (2008). Vadose Zone Modeling: Introduction and importance. *Vadose Zone Journal*, 581-586.

Simunek, J., & Suarez, D. (1994). Two-dimensional transport model for variably saturated porous media with major ion chemistry. *Water Resources Research*, 1115-1133.

Simunek, J., Jacques, D., Sejna, M., & van Genuchten, M. (2012). *The HP2 Program for HYDRUS(2D/3D) A coupled code for simulating two dimensional variably saturated water flow,heat transport,solute transport and biogeochemistry in porous media (HYDRUS + PHREEQC + 2D).* PC-PROGRESS Engineering software developer.

Simunek, J., Sejna, M., Saito, H., Sakai, M., & van Genuchten, M. (2009). *The HYDRUS-1D Software Package for simulating the One-Dimensional Movement of Water, Heat and Multiple Solutes in Variably-Saturated Media.* Riverside, California: Department of environmetal sciences , University of California Riverside.

Simunek, J., van Genuchten, M., Sejna, M., Toride, N., & Leij, F. (1999). *The STANMOD Computer Software for Evaluating Solute Transport in Porous Media Using Analytical Solutions of Convection-Dispersion Equation.* Golden, Colorado: International Groundwater Modeling Center, Colorado School of Mines.

Steefel, C. (2009). *CrunchFlow Software for modeling multicomponent reactive flow and transport user's manual.* Berkeley, CA: Lawrence Berkeley National Laboratory.

Steefel, C., & Yabusaki, S. (1996). *OS3D/GIMRT Software for Modeling Multicomponent-Multidimensional Reactive Transport User Manual and Programer's Guide.* Richland, Washington: Pacific Northwest National Laboratory.

Suarez, D., & Simunek, J. (1996). Solute transport modeling under variably saturated water flow conditions. In C. S. P.C. Lichtner, *Reactive transport in Porous media* (pp. 229-268). Washington ,USA: The Mineralogical Society of America.

Tindall, J., & Kunkel, J. (1999). *Unsaturated zoneHydrology.* New Jersey: Prentice-Hall, Inc.

U.S. Department of Energy. (2001). *A national roadmap for vadose zone science and technology,understanding,monitoring and predicting contaminant fate and transport in the unsaturated zone.* U.S. Department of energy.

van Genuchten, M. (1980). A closed-form equation for predicting the hydraulic conductivity of unsaturated soils. *Soil Science Society of America*, 892-898.

van Genuchten, M. (1980). *Determining Transport Parameters from Solute Displacement experiments.* Riverside, California: U.S Salinity Laboratory.

van Genuchten, M. (1981). *Non-equilibrium Transport Parameters from Miscible displacement Experiments.* Riverside, California: U.S. Salinity Laboratory.

van Genuchten, M. (1985). Convective-Dispersive Transport of Solutes Involved in Sequential First-order Decay Reactions. *Computers and Geosciences*, 129-147.

Wissmeier, L., & Barry, D. (2008). Reactive transport in unsaturated soil: Comprehensive modelling of the dynamic spatial and temporal mass balance of water and chemical components. *Advances in Water Resources*, 858-875.

Xu, T., E.I., S., Spycher, N., & Pruess, K. (2004). *TOUGHREACT User's Guide: A simulation Program for Non_isothermal Multiphase Reactive Geochemical Transport in variably saturated Geological Media.* Berkeley: Lawrence Berkeley National Laboratory , University of Califorina.

Yeh, G., & Cheng, H. (1999). *3DHYDROGEOCHEM: A 3-Dimensional model of density-dependent subsurface flow and thermal multispecies-multicomponent HYDROGEOCHEMical Transport.* US Environmetal Protection Agency.

Yeh, G., & Tripathi, V. (1990). *HYDROGEOCHEM:A Coupled Model of Hydrological Transport and Geochemical Equilibria in Reactive Multicomponent Systems.* Oak Ridge, Tennessee: OAK, RIDGE, NATIONAL LABORATORY.

Zhang, F., Zhang, R., & Kang, S. (2003). Estimating temperature effects on water flow in variably saturated soil using activation energy. *Soil Sciences Society of America*, 1327-1333.